GEORGIA DOT RESEARCH PROJECT 18-25

FINAL REPORT

EVALUATION OF FACTORS INFLUENCING ROUNDABOUT PERFORMANCE

OFFICE OF PERFORMANCE-BASED MANAGEMENT AND RESEARCH

600 WEST PEACHTREE NW
ATLANTA, GA 30308

1. Report No. FHWA-GA-21-1825	2. Government Accession No. N/A	3. Recipient's Catalog No. N/A
4. Title and Subtitle Evaluation of Factors Influencing Roundabout Performance		**5. Report Date** June 2021
		6. Performing Organization Code N/A
7. Author(s) Michael O. Rodgers, Ph.D. (https://orcid.org/0000-0001-6608-9333); Franklin Gbologah, Ph.D. (https://orcid.org/0000-0003-0235-4278); Anqi Wei (https://orcid.org/0000-0003-1041-1754)		**8. Performing Organization Report No.** N/A
9. Performing Organization Name and Address Georgia Tech Research Corporation School of Civil and Environmental Engineering 790 Atlantic Dr. NW, Atlanta, GA 30332 Phone: (404) 385-0569 Email: michael.rodgers@ce.gatech.edu		**10. Work Unit No.** N/A
		11. Contract or Grant No. RP18-25
12. Sponsoring Agency Name and Address Georgia Department of Transportation Office of Performance-based Management and Research 600 West Peachtree St. NW Atlanta, GA 30308		**13. Type of Report and Period Covered** Final Report (March 2018 – June 2021)
		14. Sponsoring Agency Code N/A

15. Supplementary Notes
Prepared in cooperation with the U.S. Department of Transportation, Federal Highway Administration.

16. Abstract
This project focused on determining the potential impacts of various geometric and operational parameters on gap-acceptance behavior for approaches to roundabouts in the metro-Atlanta area. Twelve roundabouts were selected to provide a range of different conditions in terms of number of legs, number of circulating lanes, conflicting volumes, presence of pedestrian crossings, etc. Observational data were collected at these roundabouts using a remotely operated drone equipped with a stabilized high-resolution (4k) video camera operating at a sufficient altitude (just less than 400 ft/120 m) to encompass the complete facility within a single frame.

The resulting videos were processed using commercial machine vision analysis (DataFromSky™) supplemented by additional computer-assisted analysis to determine vehicle trajectories, spacings, and potential conflicts on frame-by-frame (0.033 s) basis. These data, in turn, were used to establish gap-acceptance behavior of each roundabout approach and, through the use of logistic regression on the data, to establish observed critical headways (defined as the logistic inflection point [t_{50}]).

The variability of observed headways was compared against known parameters of both the roundabout and of the specific approach to develop a predictive model as to how critical headways and gap-acceptance behavior were impacted by variations in these parameters. Several factors were observed to have significant impacts on critical headways, including geometric (size category of the roundabout, number of legs and visual angle to the upstream approach), environmental (presence of a state route on the upstream approach, presence of additional conflicting lanes, presence of a pedestrian crosswalk on the approach), and operational (approach speeds) factors.

A spreadsheet tool for evaluating individual roundabouts based on these findings has been provided in the supplemental materials for this project.

17. Keywords	18. Distribution Statement		
Intersections; Roundabouts; Capacity; Drones	No Restriction		
19. Security Classification (of this report) Unclassified	**20. Security Classification (of this page)** Unclassified	**21. No. of Pages** 148	**22. Price** Free

GDOT Research Project No. 18-25

Final Report

EVALUATION OF FACTORS INFLUENCING ROUNDABOUT PERFORMANCE

By

Michael O. Rodgers, Ph.D.
Regents' Researcher and Adjunct Regents' Professor

Franklin Gbologah, Ph.D.
Research Engineer II

Anqi Wei
Graduate Research Assistant

School of Civil and Environmental Engineering
Georgia Institute of Technology
Atlanta, GA 30332

Contract with
Georgia Department of Transportation

In cooperation with
U.S. Department of Transportation
Federal Highway Administration

June 2021

TABLE OF CONTENTS

LIST OF FIGURES

LIST OF TABLES

LIST OF ABBREVIATIONS

(aa)SIDRA	(Akçelik & Associates) Signalized Intersection Design and Research Aid (Australia)
ACF	Additive Conflict Flow
AGL	Above Ground Level
ARCADY	Assessment of Roundabout Capacity and Delay
ARRB	Australian Road Research Board
BIC	Bayesian Information Criteria
CERTU	Center for Studies on Urban Planning, Transport, Utilities, and Public Construction (France)
COVID-19	Coronavirus Disease 2019
FAA	Federal Aviation Administration
FHWA	Federal Highway Administration
GDOT	Georgia Department of Transportation
HCM	Highway Capacity Manual
ISO	International Organization for Standardization
MLM	Maximum Likelihood Method
MPH	Miles Per Hour
NCHRP	National Cooperative Highway Research Program
NOTAM	Notice to Airmen

OAT	One-at-a-Time
OD	Origin–Destination
PCE	Passenger Car Equivalents
PEM	Probability Equilibrium Method
R^2	Coefficient of Determination
Rd	Road
RMSE	Root Mean Square Error
SIDRA	Signalized Intersection Design and Research Aid (Australia)
St	Street
TRB	Transportation Research Board
TRL	Transport Research Laboratory (UK)

EXECUTIVE SUMMARY

This project focused on determining the potential impacts of various geometric and operational parameters on gap-acceptance behavior for approaches to roundabouts in the metro-Atlanta area. Twelve roundabouts were selected to provide a range of different conditions in terms of number of legs, number of circulating lanes, conflicting volumes, presence of pedestrian crossings, etc. The primary data collection method employed in the project was use of a remotely operated drone equipped with video stabilization controls to provide the high-resolution (4k) videos shot at sufficient altitude (just less than 400 ft) to encompass the complete facility within a single frame.

The resulting videos were processed using commercial machine vision systems (DataFromSky™) supplemented by additional computer-assisted analysis to determine vehicle trajectories, spacings, and potential conflicts on a frame-by-frame (0.033 s) basis. These data, in turn, were used to establish gap-acceptance behavior of each roundabout approach and, through the use of logistic regression on the data, to establish observed critical headways (defined as the logistic inflection point [t_{50}]).

The variability of observed headways was then modeled against known parameters of both the roundabout and the specific approach to develop a predictive model as to how critical headways and gap-acceptance behavior were impacted by these parameters. The major findings of this model were that several factors were observed to have significant impacts on critical headways, including geometric (size category of the roundabout,

number of legs and visual angle to the upstream approach), environmental (presence of a state route on the upstream approach, presence of additional conflicting lanes, presence of a pedestrian crosswalk on the approach), and operational (approach speeds) factors. The model parameters for the prediction of critical headways (in seconds) are given in the table below:

Parameter Estimates and Summary of Fit for Model LR 4B

Term	Estimate	Standard Error	Prob>|t|
1) Intercept (added to all other parameters)	1.40	0.165	<0.0001
2) Angle to Upstream Approach – 90 degrees	−0.008/deg	0.002	0.0008
3) Number of Roundabout Legs – 4	−0.425	0.098	<0.0001
4) Additional Crossing Lanes at Approach	0.934	0.141	<0.0001
5) Upstream Approach on a State Route?	0.895	0.117	<0.0001
6) Pedestrian Crossing on Approach	0.288	0.129	0.0275
7) Approach Speed – 20 miles-per-hour	−0.061	0.015	<0.0001
8) Small Roundabout (≤ 125 ft)	1.07	0.120	<0.0001
9) Large Roundabout (≥ 145 ft)	0.329	0.111	0.0037

The modeled versus observed values of critical headway are shown below:

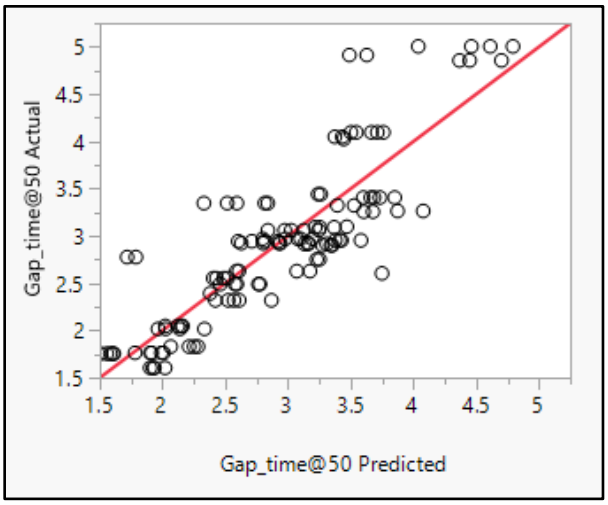

Conclusions Regarding Data Collection

The superior field of view and near-Nadir camera orientation greatly reduced the required labor, time, and complexity of the data collection and analysis process compared to former methods. While a direct comparison with earlier methods is difficult to make, it is likely that data collection and analysis at a roundabout or a similar intersection for the parameters measured in this study using older methods would cost at least five times as much as the drone approach. ***Given the results from this project, it would be difficult to recommend that fixed near-surface cameras be used for any analytical work that can be achieved with drone systems.*** This recommendation obviously does not apply to continuous monitoring for which fixed-camera systems excel but rather for the short-term types of studies represented by this project.

Conclusions Regarding Data Analysis

Similar to the conclusions regarding data collection, the rapidity by which the field data could be reduced to usable vehicle trajectories and the volume of information that could be achieved by the simultaneous tracking of all vehicles in the field of view greatly exceeded that which could be achieved by traditional methods. Although the need for experienced and qualified data analysts is similar for both the current and more traditional approaches, the time and labor spent by support personnel (e.g., those involved in manual or semi-automated data extraction from videos) is greatly reduced. Perhaps more importantly, ***the data collected by the trajectory analysis approach represent a resource that could be of enormous value in the future. These georeferenced vehicle trajectories represent a resource that can be used in the future to examine how subtle***

changes in the operations of facilities can occur over extended periods. The Georgia Department of Transportation (GDOT) should consider standards for the archival of vehicle trajectory data for use in future operational, safety, and evaluation studies.

Conclusions Regarding Factors that Influence Gap Acceptance at Roundabouts

Despite the small number of roundabouts involved in the study (i.e., 12), the resulting data were remarkably consistent and many of the conclusions were significant at a very high statistical level. That, of course, does not imply that these conclusions are universal or that our interpretations of their underlying roots are correct, but they do provide a first glimpse into some important factors.

First, it appears that many of the factors are related to the ***visual complexity*** of the roundabout scene. For example, the presence of a pedestrian crossing in the approach, along with the presence of a second circulating lane conflicting with the approach in a large (>145-ft inscribed circle) roundabout is predicted to add more than 2 seconds to the critical gap time for a typical driver relative to a simpler roundabout.

Second, some of the variables imply that drivers increase their desired gap-acceptance times when confronted with conditions that they may view as representing ***elevated risk***. For example, the presence of a state route on the upstream approach, a visual angle to that approach of less than 90 degrees, and smaller (<125-ft diameter) roundabouts were all shown to increase critical headway time.

These are, obviously, conclusions based on a limited sample of observations, but they do represent the result of observing driver behavior over a wide range of conditions. ***These***

results should help designers and planners to evaluate how these factors may impact "real world" performance of an individual roundabout rather than using national or Georgia-specific conditions. To assist in this effort, a spreadsheet tool for evaluating individual roundabouts has been provided in the supplemental materials for this project.

CHAPTER 1. INTRODUCTION

PROJECT PURPOSE

Roundabouts have become a popular alternative to conventional stop-controlled or signalized intersections due to their significant safety and operational advantages. However, operational analysis of roundabouts is generally more complex than that of more traditional intersections and, in some cases, the full impact of various design alternatives may not be fully understood. Consequently, roundabout capacity models must incorporate simplifying assumptions into their analytical frameworks. While these assumptions may be valid for most conditions, they may not fully account for unusual or challenging conditions or specific features of an individual roundabout. As the use of roundabouts continues to expand, there is a need to develop additional tools to help assess the operational and safety impacts of various roundabout design alternatives. This project aims to evaluate the potential impacts of several common roundabout design features on observed approach capacity.

The principal goal of this project was to develop a decision-based (gap-acceptance) model for the evaluation of roundabout capacity and safety. This model focuses on the impact that a range of geometric and environmental factors have on drivers' gap-acceptance behavior regarding entering a roundabout. This modeling approach offers the potential to evaluate both the operational (accepted gap distribution) and safety (unsafe gap acceptance) impacts that these factors have on roundabout performance and, thus, can help guide design decisions.

BACKGROUND

The roundabout capacity model currently used most frequently in the United States is that described in the *2016 Highway Capacity Manual* (HCM) (Transportation Research Board [TRB] 2016). This model is largely based on the analysis of data collected from earlier National Cooperative Highway Research Program (NCHRP) observational studies by Rodegerdts et al. (2007a,b; 2010, 2015) and the theoretical framework established earlier by Troutbeck and Brilon (1997) and Siegloch (1973). The HCM model uses a simple conflict-based approach based on ratios of transit to conflict time to estimate capacity. While being both simple and direct, the HCM model does not incorporate any additional information (e.g., the trajectory of another vehicle through the roundabout) that may alter and/or influence a driver's decision as to when to enter the roundabout. These additional factors may, in fact, strongly impact the operations of individual roundabouts. Such effects were noted in a previous Georgia Department of Transportation (GDOT) study (RP11-14) used to calibrate the HCM single-lane roundabout model for Georgia conditions (Barry 2012, Schmitt 2013). Some empirically based roundabout capacity models do account for some of these effects, but their empirical basis limits their ability to fully evaluate the potential impacts of new design alternatives. Several of these models are discussed more fully in chapter 2.

GAP ACCEPTANCE

Safe navigation of a roundabout in traffic requires that a driver estimate the available gap between an approaching vehicle and his or her location and, based on this estimate, decide whether to enter the roundabout or remain at the approach. These gap-

acceptance/rejection decisions, along with the physical capability of the vehicles, largely control both the operational capacity and the multi-vehicle crash safety of roundabouts. For maximum capacity, the gap-acceptance probability for drivers should closely follow the "Ideal" Gap Curve illustrated in figure 1. That is, virtually all gaps greater than the "minimum safe distance" are accepted and all gaps less than the "minimum safe distance" are rejected.

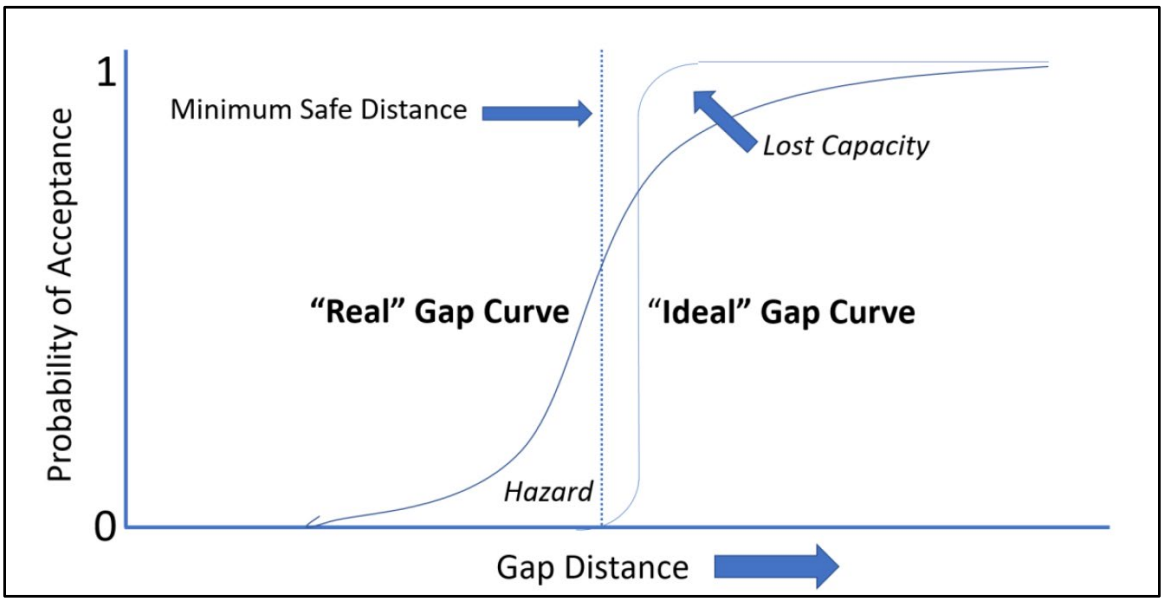

Figure 1. Illustration. Gap-acceptance behavior in roundabouts.

In practice, real drivers tend to follow a shallower logistical curve in their gap acceptance, as illustrated by the "Real" Gap Curve in Figure 1. The shape and characteristics of the actual gap-acceptance curve have a profound influence on both intersection capacity and crash safety. Driver rejection of safe gaps lowers the operational capacity of the roundabout and acceptance of potentially unsafe gaps introduces additional crash safety risk. Thus, the principal task in determining the influence of various factors on roundabout safety and operational capacity is to determine how

geometric, environmental, and operational factors influence the location and shape of the roundabout gap-acceptance curve. This study's approach to determining these "gap-acceptance" functions is described in chapter 3 of this report. Chapter 4 discusses the methods used for the collection of the "real world" observations of driver/vehicle behavior from several modern roundabouts in the metro-Atlanta, Georgia, area used for model development in the project. The procedures used for the determination of the vehicle trajectories necessary for evaluation of gap acceptance are described in chapter 5, and the methods for using these trajectories in determining accepted and rejected gaps are discussed in both chapter 5 and chapter 6. The gap-acceptance model developed using these data is presented in chapter 7 and the results from application of this model are discussed in chapter 8. Chapter 9 provides a summary of project conclusions and recommendations for additional study.

CHAPTER 2. ROUNDABOUT CAPACITY MODELS

Capacity is a key determinant of a roundabouts' operational performance. The Federal Highway Administration (FHWA) roundabout guide (Robinson et al. 2000) defines roundabout capacity as the maximum rate at which vehicles from an approach can be expected to enter the roundabout under the traffic and roadway (geometric) conditions prevailing at a given time. As capacity is influenced by various geometric and operational factors, many countries and other jurisdictions have developed their own capacity models based on local observations. Current methods used for developing these roundabout capacity models may be categorized into three main groups: (1) empirical methods, (2) gap-acceptance methods, and 3) microscopic simulation methods. In addition, models based on conflict techniques are also considered as an alternative for roundabout capacity estimation. Each of these approaches is discussed in the following sections.

EMPIRICAL MODELS

Models using empirical methods are usually developed through regression-based analysis of observed field data on roundabout operations to determine the relationships between roundabout entry capacity and its influential factors, including geometric variables. The first empirical model to find wide use was the United Kingdom (UK) Transportation Research Laboratory (TRL) model (also known as the LR942 linear regression model) developed by Kimber (1980), which was later used as the basis of the ARCADY™ and RODEL™ software packages. The TRL model was derived from about 3 hours of recorded observations collected at 86 roundabout approaches in the UK. This model

found that under saturated conditions the entry capacity is linearly dependent on the circulating flow rate, which can be expressed as:

$$Q_e = k(F - f_c \cdot Q_c) \quad (1)$$

Where, Q_e is the entry flow and Q_c is the circulating flow, both in units of passenger car equivalents per hour (pce/h). The other parameters in the equation are given by:

$$k = 1 - 0.00347(\phi - 30) - 0.978(1/r - 0.05) \quad (2)$$

$$F = 303(v + \frac{e - v}{1 + 2S}) \quad (3)$$

$$f_c = 0.21\, t_D(1 + 0.2(v + \frac{e - v}{1 + 2S})) \quad (4)$$

Where, ϕ is the entry angle (degrees); r is the entry radius in meters (m); e is the entry width (m); v is the approach half-width (m); $S = 1.6(e - v)/l'$ is the measure of the degree of flaring and l' is the effective flare length (m), and $t_D = 1 + 0.5/(1 + e^{(D-60)/10})$ where D is the inscribed circle diameter (m).

Based on this UK model, early investigators in France (Alphand et al. 1991), the United States (Robinson et al. 2000) and Jordan (Al-Omari et al. 2004) also developed linear regression models that accounted for the influence of operational factors, including circulating and exiting flow rates, as well as geometric factors such as entry width, circulating lane width, the splitter island width, and the number of entry lanes.

Continuing this line of research, the French national transport research agency CERTU-CETE West developed an exponential regression model with critical-gap and follow-up headway as additional influential factors (Guichet 1997). This later model formed the core of the GIRABASE™ software implementation. The detailed equation is shown in equation 5:

$$Q_e = \left[\frac{3600}{t_f}\left(\frac{e}{3.5}\right)^{0.8}\right] e^{-C_b Q_d} \quad (5)$$

Where, t_f is the follow-up headway (seconds), e is the entry width (m), C_b is an adjustment factor between urban and rural areas, and Q_d is a function of circulating flow and exiting flow leaving at the same arm as the approach being evaluated and geometric parameters.

Since many studies have observed that empirical capacity models are sensitive to the variations in geometric features and driver behavior within a roundabout, Wei et al. (2011) proposed a streamlined process to develop new capacity models based on local roundabout conditions. The process consists of three steps: video data collection, data processing and verification, and model development and comparison. Following this approach, Patnaik et al. (2018, 2021), Patnaik, Rao et al. (2017), and Patnaik, Krishna et al. (2017) employed different regression techniques to model roundabout capacity under heterogeneous traffic conditions in India. All the models have identified the same set of variables as used in the earlier studies, with the addition of variables for weaving width and weaving length that were found to significantly influence roundabout capacity. The model created by Patnaik, Rao et al. (2017) was also compared with the UK TRL

model (Kimber 1980) and Jordan model (Al-Omari et al. 2004) and found that both of these earlier models underestimated actual capacity.

As empirical models are typically developed based on roundabout field data under saturated conditions, a lack of available congested roundabout entries could easily constrain model development in terms of statistical significance (Rodegerdts et al. 2007b). Additionally, as discussed by Yap et al. (2013), since the regression-based models are purely derived from empirical data, the models' coefficients and intercepts can sometimes be difficult for engineers to interpret and, thus, limit the model's utility for design purposes.

GAP-ACCEPTANCE MODELS

Gap-acceptance theory, applied in the analysis of unsignalized intersections, is based on the concept of defining the extent drivers will be able to utilize a gap of a particular size or duration (Troutbeck and Brilon 1997). Derived from this theory, the gap-acceptance models mainly depend on three key variables representing driver behavior: critical headway, follow-up headway, and headway distribution of circulating vehicles.

Driver-behavior Parameters

Critical Headway

Critical headway (or critical gap) is defined as the minimum gap that all drivers in the minor stream are assumed to accept at all similar locations, where the gap refers to the headway between two subsequent vehicles on the major road (Troutbeck and Brilon

1997). In gap-acceptance models, the critical headway is a threshold for drivers in the minor stream to decide whether to accept the gap to enter the roundabout or not.

For saturated conditions when there is a continuous queue on the minor approach, Siegloch (1973) evaluated the critical headway values $t_c = t_0 + t_f/2$ based on the regression analysis of the average gap size against the number of vehicles that can enter during this average gap size, where t_f is the slope of the regression equation and t_0 is the intercept.

Although for undersaturated conditions, as driver behavior in the minor approach could vary with time and geometric features of roundabouts, it is more reasonable to presume that the critical headway is randomly distributed rather than being constant (Patnaik, Krishna et al. (2017)). A range of methods has been developed to estimate this critical headway, t_c. These methods include Raff's method (Raff 1950) that computes t_c based on the cumulative distribution functions of both the accepted and rejected gaps; Ashworth's method (Ashworth 1968) that estimates t_c based on the mean and variance of the accepted gap distributions; Hewitt's method (Brilon et al. 1999) that iteratively computes the expected number of accepted and rejected lags and gaps to estimate the probability of t_c being within a particular time interval; and Troutbeck's Maximum Likelihood Method (MLM) (Troutbeck and Brilon 1997) that estimates $\mathrm{t_c}$ by iteratively computing its distribution mean and variance to maximize the sum of log likelihoods. All of these approaches have been used to evaluate critical headways.

To evaluate the performance of these estimation methods, Brilon et al. (1999) conducted a simulation study and found that MLM and Hewitt's method gave the best results in terms of consistency, robustness, and compatibility. Later, Wu (2006) developed the Probability Equilibrium Method (PEM) that directly yields the probability distribution function of the critical headways without iteration. Unlike MLM, which assumes a log-normal distribution for the critical headways and only uses accepted gaps and maximum rejected gaps, PEM considers all available gaps (Wu 2006). Similarly, Vasconcelos et al. (2013) compared the performance of several estimation methods at six roundabouts in Portugal. Results suggested that Raff's method, PEM, and MLM are more reliable than the other alternatives but did not identify a clear advantage for using any one of these three. Following these efforts, Troutbeck (2014) used a simulation method to review the prediction ability of MLM and PEM again and found that, although both methods were reasonably consistent, PEM had a significant bias compared to MLM that was dependent on the flow in the priority (circulating) stream.

Follow-up Headway

Follow-up headway (also referred to as the queue discharging headway) is defined as the time gap between two consecutive entering vehicles from the minor stream utilizing the same gap in the circulating stream (Rodegerdts et al. 2007a,b). Follow-up headway can be directly measured based on field data. In earlier studies, (Brilon 1988) reported that a constant ratio of 0.6 exists between follow-up time and critical headway, Tian et al. (2000) further investigated their relationship and observed that the ratios of the follow-up time and the critical headway ranged between 0.4 and 0.9 with the majority being around 0.6.

Because several studies (e.g., Tian et al. 2000) found that critical headway and follow-up time were impacted by intersection geometry, vehicle type, approach grade, and traffic movements, Vasconcelos et al. (2013) recommended a dedicated data-collection and estimation process for these parameters for local applications. For example, SIDRA™ (software) uses a linear regression equation with roundabout geometric parameters and environmental factors to calculate the follow-up headway (Akçelik 2006).

Arrival Headway Distributions

The distribution of arrival headways in the circulating roadway is fundamental to gap-acceptance models, as many studies have shown that critical headway at roundabout approaches depends strongly on that distribution (Rossi et al. 2018). Akçelik (2007) reviewed a class of exponential distribution models known as negative exponential (M1), shifted negative exponential (M2), and bunched exponential (M3) to describe arrival headway distributions. Since the M1 and M2 models can be viewed as special cases of the M3 model through the simplifying assumption that no bunching (platooning) vehicles exist in the circulating stream, most studies use the more realistic M3 model to describe the headway distribution. These distributions were first proposed by Cowan (1975) by assuming that a proportion of $(1-\varphi_m)$ vehicles are tracking their predecessor at headway Δ_m whilst a proportion of φ_m are traveling freely at some headway greater than Δ_m. The cumulative distribution equation for the circulating headway is as follows:

$$F(t) = \begin{cases} 1 - \varphi_m \cdot \exp[-\lambda(t-\Delta_m)], & t \geq \Delta_m \\ 0, & otherwise \end{cases} \quad (6)$$

Where, $\lambda = \frac{\varphi_m \, q_m}{1-\Delta_m \, q_m}$ is the decay rate that is related to the arrival flow rate q_m (veh/s) and subject to the condition that $q_m \leq 0.98/\Delta_m$.

The intra-bunch headway Δ is the minimum (average) headway in the circulating headway distribution model. In the SIDRA INTERSECTION™ software, the default values of Δ_m are set to 2.0 s, 1.0 s, and 0.8 s for single-lane, two-lane, and more-than-two-lane circulating flows, respectively (Akçelik 2006). In addition, as discussed by Akçelik (2007), the intra-bunch headway could also be treated as the average headway at capacity flow, which is calculated as $\Delta_m = 3600/q_m$, where q_m is the circulating flow rate in vehicles/hour (veh/h).

The proportion of free vehicles φ_m represents the unbunched vehicles with randomly distributed headways, and it depends on the selected value of the intra-bunch headway as well as the circulating flow rates (Akçelik 2006). Previous popular estimation models include a linear model developed by Tanner (1962) and an exponential model proposed by Akçelik (1994). In SIDRA™ 2.1, Akçelik (2003) then introduced another model, which includes a traffic delay parameter k_d for roundabout analysis to replace the previous exponential one (suggested value $k_d = 2.2$ for roundabout circulating stream). It can be noted that Tanner's earlier linear model (Tanner 1962) is a special case of this approach when setting the delay parameter $k_d = 1.0$. The detailed equation is as follows:

$$\varphi_m = \frac{(1 - \Delta_m \, q_m)}{[1 - (1 - k_d) \, \Delta_m \, q_m]}, \text{ subject to } \varphi_m \geq 0.001 \qquad (7)$$

Where, q_m is the circulating (or exiting) flow rate (pce/s), and Δ_m is the average intra-bunch headway (s).

Models with M1 Headway Distribution Assumptions

Conventional gap-acceptance models, such as the one developed by Tanner (1962), consider the major stream as imposing 'blocks' and 'anti-blocks' on the minor stream, where a block could contain one or more consecutive gaps less than the critical gap. The classic method of estimating capacity is to determine the distribution of gaps in the major stream and the number of vehicles that can depart during a gap within the major stream (Yap et al. 2013). Early capacity models like Siegloch (1973), which is used in the German national guidelines, assumed a negative exponential distribution of circulating headways (M1) and the corresponding equation is as follows:

$$Q_g = \frac{3600}{t_f} e^{-q_m(t_c - 0.5t_f)} \quad (8)$$

The critical gap and follow-up headways were regressed from measurements in saturated conditions. This model is the basis for the HCM 2010 model (Yap et al. 2013).

HCM 2010 Model

Rodegerdts et al. (2007b) conducted research that evaluated the implementations of worldwide roundabout capacity models (i.e., Australian, UK, German, French, Swiss, HCM 2000, and FHWA models) as well as the two major software implementations (RODEL™ and aaSIDRA™) in the U.S. based on field data collected in 2003. The results of their research were published in NCHRP Report 572 (Rodegerdts et al. 2007a,b), and

the evaluation results indicated that, except for the HCM 2000, all models and their software implementations overestimated the entry capacity. Additionally, these researchers found that the impacts of the geometric parameters on the roundabout capacity appear to be less significant than those of the driver-behavior parameters. Thus, for accurate capacity estimation, they recommended the calibration of models to account for local driver behavior (Rodegerdts et al. 2007b).

Based on the model evaluation results, their study further compared the capacity estimated by the HCM 2000 model with average field values for the gap parameters and exponential regression of the data. The simplified HCM 2000 model can be expressed as:

$$c = A \cdot \exp(-B \cdot q_m) \tag{9}$$

Where, $A = 3600/t_f$; $B = \left(t_c - 0.5\ t_f\right)/3600$; the field-measured weighted average critical headway t_c is set to 5.19 s, 4.11 s, and 4.29 s for a single-lane roundabout, and the critical (right) lane and left lane of multi-lane roundabouts, respectively; and follow-up headway t_f is set to be a constant 3.19 s (Rodegerdts et al. 2007b).

Those researchers found that the intercept and slope of both models were consistent, whereas the exponential regression model was slightly better with lower root mean square error (RMSE; Rodegerdts et al. 2007b). Therefore, based on the results of NCHRP Report 572, in HCM 2010, the recommended form for the entry-capacity estimation for single-lane roundabouts was:

$$c = 1130\exp(-0.0010 \cdot v_c) \quad (10)$$

For multi-lane roundabouts, the recommended capacity model for the critical lane (right lane) was:

$$c_{crit} = 1130\exp(-0.0007 \cdot v_c) \quad (11)$$

For the left lane of multi-lane roundabout the capacity model was given as:

$$c_{left} = 1130\exp(-0.00075 \cdot v_c) \quad (12)$$

Where, $c = q_{e,max}$ is the entry capacity (pce/h), c_{crit} is the capacity of the critical lane (pcu/h), and $v_c = q_m$ is the conflicting circulating traffic volume (pce/h).

HCM Edition 6 Model (2016)

The latest HCM Edition 6 model (TRB 2016) has the same basic form of the roundabout capacity equation as the HCM 2010 model, but it has significantly different parameter values. The changes were based on the research carried out by Rodegerdts et al. (2015) to assess the fit of the HCM 2010 models to a new set of roundabout capacity data collected in 2012. As the new data confirmed that HCM 2010 generally underestimated capacity, a recalibration in terms of the model intercept and slope based on regression of the data was conducted. For the HCM 6 model, the field-measured weighted average critical headway t_c and follow-up headway t_f were determined to be:

- 4.98 s and 2.61 s, respectively, for the single-lane roundabout.
- 4.54 s and 2.54 s for multi-lane roundabouts with a single circulating lane.

- 4.33 s and 2.54 s for the right lane of multi-lane roundabouts.
- 4.65 s and 2.67 s for the left lane of multi-lane roundabouts (Akçelik 2011, Akçelik 2017).

By applying these gap parameters into the general HCM model, the recommended entry-capacity estimation of single-lane roundabouts is:

$$c = 1380\exp(-0.00102 \cdot v_c) \tag{13}$$

For the multi-lane roundabout with one circulatory lane, the capacity equation is:

$$c = 1420\exp(-0.00091 \cdot v_c) \tag{14}$$

For the multi-lane roundabout with two circulatory lanes, the approach capacities of the right lane and left lane are computed by:

$$c_R = 1420\exp(-0.00085 \cdot v_c) \tag{15}$$

$$c_L = 1350\exp(-0.00092 \cdot v_c) \tag{16}$$

Where, c is the lane capacity in pce/h, and v_c is the circulating flow rate (pce/h).

In order to better apply the HCM Edition 6 model into the SIDRA INTERSECTION™ software, Akçelik (2017) further compared the capacity estimated by three models (i.e.,

HCM 2010, HCM Edition 6, and SIDRA™ Standard model) using a multi-lane roundabout example. Since the SIDRA™ Standard model was developed based on research on Australia roundabouts, to match the estimates from the HCM 6 model, the default value of the Environmental (local calibration) Factor in the SIDRA™ Standard model was set to 1.05 for one-lane roundabouts and 1.2 for two-lane roundabouts. Results showed that the HCM 6 and the SIDRA™ Standard model calibrated using the Environmental Factor parameter gave similar capacity and performance results with subtle differences, while the HCM 2010 model estimated lower capacity and gave poorer performance results (Akçelik 2017).

Local Calibration

As recommended by NCHRP Report 572 (Rodegerdts et al. 2007b), for more accurate capacity estimation in terms of the local roundabouts, the general model described above should be recalibrated by applying locally observed values of the gap parameters (i.e., critical headway and follow-up headways) to account for differences in driver behavior. Many states have conducted their own studies to analyze local gap parameters. The results from these measurements of critical and follow-up headways are listed in table 1 and table 2, along with the national averages from Rodegerdts et al. (2015).

Table 1. Critical headway and follow-up headways for single-lane roundabouts.

Study Sites within U.S.		Critical Headway (s)	Follow-up Headway(s)
HCM 2010 Model (Rodegerdts et al. 2010)		4.2 – 5.9 (avg 5.1)	2.6 – 4.3 (avg 3.2)
HCM 6 Model (Akçelik 2017)		4.98	2.61
California (Xu and Tian 2008)		4.5 – 5.3 (avg 4.8)	2.3 – 2.8 (avg 2.5)
Bend, OR (Kittelson & Associates, Inc. 2010)		4.1	2.7
Maryland (Mensah et al. 2010)		2.5 – 2.6	Not studied
Wisconsin (Zheng, et al. 2012)	Exiting vehicle excluded	5.5	2.6
	Exiting vehicle included	4.6	2.3
Carmel, Indiana (Wei et al. 2012)		3.19 – 3.75 (avg 3.47)	2.1 – 2.43 (avg 2.2)
Georgia (Barry 2012)	Exiting vehicle excluded	3.47 – 4.91 (avg 4.17)	3.03 – 3.75 (avg 3.46)
	Exiting vehicle included	2.9 – 4.18 (avg 3.34)	2.6 – 2.98 (avg 2.8)
Georgia (Schmitt 2013)	Exiting vehicle excluded	3.46 – 7.73 (avg 4.75)	2.52 – 3.69 (avg 3.27)
	Exiting vehicle included	3.34 – 6.03 (avg 4.19)	2.32 – 3.11 (avg 2.79)
Florida (Ruhazwe et al. 2019)	1 approaching, 1 circulating	4.71– 6.81 (avg 5.46)	2.77 – 3.26 (avg 2.86)
	1 approaching, 2 circulating	4.19 – 6.08 (avg 4.79)	2.71 – 3.22 (avg 2.90)
Louisiana (Codjoe et al. 2021)		3.94 – 6.89 (avg 4.76)	2.46 – 3.76 (avg 3.36)

Table 2. Critical headway and follow-up headways for multi-lane roundabouts

Study Sites within U.S.		Right Critical Headway (s)	Left Critical Headway (s)	Right Follow-up Headway (s)	Left Follow-up Headway (s)
HCM 2010 Model (Rodegerdts et al. 2010)		3.4 – 4.9 (avg 4.2)	4.2 – 5.5 (avg 4.5)	2.7 – 4.4 (avg 3.1)	3.1 – 4.7 (avg 3.4)
HCM 6 Model (Akçelik 2017)		4.33	4.65	2.536	2.667
California (Xu and Tian 2008)		4.0 – 4.8 (avg 4.4)	4.4 – 5.1 (avg 4.7)	2.1 – 2.3 (avg 2.2)	1.8 – 2.7 (avg 2.2)
Wisconsin (Zheng et al. 2012)	Exiting vehicle excluded	4.2 – 5.0 (avg 4.32)	3.4 – 4.4 (avg 3.56)	2.8 – 4.4 (avg 3.24)	2.8 – 4.9 (avg 2.92)
	Exiting vehicle included	3.3 – 3.9 (avg 3.5)	3.1 – 4.0 (avg 3.28)	2.2 – 3.7 (avg 2.85)	2.2 – 3.9 (avg 2.40)
Minnesota (Chen 2018)		3.992	4.428	2.964	3.049
Florida (Ruhazwe et al. 2019)	2 approaching, 1 circulating	4.86 – 5.84 (avg 4.82)	4.94 – 5.93 (avg 5.18)	2.57 – 3.64 (avg 2.72)	2.61 – 3.11 (avg 2.74)
	2 approaching, 2 circulating	4.42 – 4.63 (avg 4.47)	4.51 – 6.97 (avg 5.01)	2.37 – 2.6 (avg 2.37)	2.2 – 2.78 (avg 2.63)

Models with M3 Headway Distribution Assumptions

Since the assumption of randomly distributed arrival headways without bunching (M1 distribution) is often considered to be unrealistic, by replacing the headway distribution in Siegloch's (1973) formula with the bunched exponential (M3) distribution model proposed by Cowan (1975), a more general form of the roundabout capacity model can be obtained:

$$Q_g = \frac{3600\varphi_m q_m e^{-\lambda(t_c-\Delta_m)}}{1-e^{-\lambda t_f}} \quad (17)$$

Where, $\lambda = \frac{\varphi_m\, q_m}{(1-\Delta_m\, q_m)}$, Q_g is the gap-acceptance capacity (veh/h), q_m is the opposing (circulating) flow rate (pce/s), and φ_m is the proportion of free (unbunched) vehicles.

This form is also found similar to many capacity models reported in the current literature (Tanner 1967, Troutbeck 1986, etc.). If the proportion of free vehicles in the circulating stream is estimated using the linear model $\varphi_m = (1 - \Delta_m\, q_m)$, then the general capacity equation could be reduced to that of Tanner's model (1962), which was used in the older AUSTROADS (1988) capacity guide with the intra-bunch headway $\Delta_m =$ 2.0 s for single-lane and $\Delta_m =$ 0 for multi-lane circulating flow. By applying a different linear model $\varphi_m = 0.75(1 - \Delta_m\, q_m)$, the adjusted general form would be the same as the model used in the AUSTROADS (1993) roundabout guide (Akçelik 2007).

Models Based on Traffic Signal Analogy

Under the same assumption that circulating headways follow a bunched exponential (M3) distribution, Akçelik (1994) first introduced the traffic signal analogy concept to the capacity analysis of unsignalized intersections. This type of model treats the blocked and unblocked periods defined in the traditional gap-acceptance models as equivalent to the "red" and "green" periods in a traditional signal-controlled traffic stream. The capacity Q_g (veh/h) can be expressed as:

$$Q_g = su = \left(3600/t_f\right)u = \left(3600/t_f\right)\left(1 - \Delta_m q_m + 0.5\varphi_m q_m t_f\right)e^{-\lambda(t_c-\Delta_m)} \tag{18}$$

Where, $s = 3600/t_f$ is the saturation flow rate (veh/h); $u = g/c$ is the unblocked time ratio, where g is the average unblocked time (s), and c is the average gap-acceptance

cycle time (s), and the subscript m stands for the major stream, which for a roundabout is the conflicting circulating stream.

The model parameters for this model were first estimated using a microscopic simulation program (MODELC) (Akçelik 1994) and field observations of 55 roundabout entry lanes reported in the Australian Road Research Board (ARRB) Special Report SR45 (Troutbeck 1989). The model was later recalibrated and incorporated into the SIDRA™ software. To analyze the model's compatibility, Macioszek and Akçelik (2017) calibrated it using data from both one- and two-lane roundabouts in Poland and compared it with Macioszek's model which was developed based on local research. The average difference in the capacity estimates obtained from both models was only 0.2 percent, which implied that the calibration of the SIDRA™ Standard model through the Environmental Factor could well match driving conditions in Poland.

Later, this model was further refined by including factors, including an origin–destination (OD) factor, to allow for the effects of priority sharing under heavy circulating flow rates and a general environmental factor to match the local roundabout environment (Akçelik 2006). This approach will be discussed in the subsequent Model Improvement section.

Comparison Between Traditional and Traffic-signal-analogy-based Models

Akçelik (2007) reviewed some early gap-acceptance models, including those by Siegloch (1973), which assumed a negative exponential (M1) headway distribution; Armitage and McDonald (1974), which assumed a bunched exponential (M3) headway distribution; and Jacobs (1979), which assumed a shifted negative exponential (M2) headway

distribution. By applying each of these headway distributions into Akçelik's (1994) capacity model that was based on the traffic signal analogy, the author found that the adjusted model would have quite similar forms as the early models, assuming the same headway distributions. Since these earlier models would also predict capacity values close to those of the corresponding adjusted Akçelik (1994) model, they could all be considered as similar to that based on traffic signal analogy (Akçelik 2007).

Model Improvement

In addition to the driver-behavior parameters—including circulating flow rate, the critical headway, and follow-up headway—previous case studies have observed that unbalanced circulating flow, the fraction of potentially conflicting vehicles exiting on the same leg as entering vehicles, and the presence of pedestrians were also important factors influencing the entry capacity of roundabouts.

Priority Sharing and Priority Emphasis

The gap-acceptance theory assumes that vehicles in the circulating roadway would have absolute priority over the entry vehicles in the minor approach. However, this may not hold true in reality, especially under the conditions of high circulating flow rates. *Priority sharing* occurs when circulating vehicles are forced to adjust the gaps to allow entry vehicles to merge into the circulating stream. Troutbeck and Kako (1999) have observed in a field study a significant effect of limited priority merge on the entry capacity at two-lane roundabouts. To account for the influences, they developed a new gap-acceptance model based on limited priority for the major stream and applied it to the roundabouts in a simulation.

Contrary to priority sharing, *priority emphasis* occurs when a major stream restricts the flow of entering traffic from a particular approach due to a continuous flow from an upstream approach that can enter the roundabout unimpeded due to a low circulating flow against them (Akçelik 2004). The follow-up headways within this upstream vehicle flow can be larger than the intra-bunch headways, thereby forming a "forced flow" condition that further reduces the downstream entry capacity. Akçelik (2004) introduced an OD factor to the capacity model used in aaSIDRA™ to allow for both situations of reduced capacity due to priority sharing and reduced unblock times due to priority emphasis. Based on the Australian capacity model discussed previously (SIDRA™), the calculation of the unblock time ratio was changed to the form below:

$$u = \max\{Q_m/s, f_{od}(1 - \Delta_c q_c + 0.5\beta\varphi_c q_c)e^{-\lambda(\alpha-\Delta_c)}\} \quad (19)$$

Where, Q_m is the minimum capacity per lane (veh/h) and $\lambda = \varphi_c q_c/(1 - \Delta_c q_c)$, subject to the constraint that $q_c \leq 0.98/\Delta_c$.

This adjusted model was then compared with other existing models, such as the UK model, in several case studies to conclude that any method based on gap-acceptance modeling or empirical analysis without allowance for priority emphasis would fail to provide satisfactory estimates of roundabout capacity with unbalanced flow near capacity (Akçelik 2004, Akçelik and Besley 2005).

Exiting Vehicles

The influences of exiting vehicles on roundabout entry capacity have also been reported by many studies; for example, Mereszczak et al. (2005) discovered that the capacity of a

given approach will increase when the proportion of exiting vehicles increases even when the major street flow remains the same. They also compared the capacity estimated by models with and without the incorporation of exiting vehicles to the measured field data and found that capacity estimates with exiting vehicles result in improved prediction of the actual capacity (Mereszczak et al. 2005). To further understand potential model improvements by considering exiting vehicles, Rodegerdts et al. (2015) discussed two methods of adding exiting flows into the capacity model, and the factor k_{ex} was introduced to represent the proportion of exiting vehicles that are added to the conflicting flow. However, results indicated that neither method significantly improves the fit of the model as well as that achieved by calibrating the model based on measured local follow-up times. Other countries have also proposed some methods to deal with the exiting vehicle issue. For example, the German highway capacity manual recommends reducing the circulating traffic by 0.15 times the volume of the exiting traffic based on their investigations on mini roundabouts (Brilon and Vandehey 1998).

Pedestrians

Other than circulating flows, vehicles at the roundabout entry may also have conflicts with crossing pedestrian flows. As pedestrians usually have priority over entering vehicles, an increase in pedestrian volume tends to cause significant entry- and/or exit-capacity reduction, especially under low vehicular circulating flow conditions. Stuwe and Springer (1991) observed in Germany three roundabouts with a heavy pedestrian flow and developed an empirical entry-capacity equation for one-lane and two-lane roundabouts. They employed a factor “M” to account for the influence of pedestrians, which was determined through regression analysis, and the method was included in the

FHWA Roundabout Guide (Robinson et al. 2000). While the HCM 2010 model does not consider the impacts of pedestrians on the entry flow, it uses capacity models for a yielding bypass lane to approximate its influences (Rodegerdts et al. 2010). Most of the existing methods also consider using adjustment factors to represent pedestrian impact. For example, Kang and Nakamura (2015) used gap-acceptance theory to the include effects of a splitter island and the far-side pedestrian yield rates. Simulation analysis and theoretical models were both used to estimate the capacity, and the findings implied that the estimated capacities were higher for the theoretical model and the HCM model than for the simulation analysis.

MODELS BASED ON CONFLICT TECHNIQUES

While most of the available models for roundabout capacity estimation are either based on empirical regression analysis or gap-acceptance theory, Brilon and Wu (2001) argued that these approaches treat specific conflicts at roundabouts with different and incoherent methods, and these methods do not consider any interactions between adjacent conflict areas within the roundabouts. As a short-term overload at one of the conflict points within a roundabout could easily impede movements at other conflict points, the lack of consideration regarding these interactions could result in biased capacity-estimation results. Thus, based on the concept of additive conflict flows (ACFs), Wu and Brilon (2018) proposed a new model that estimates the capacity of the roundabout as a whole to account for the mutual interdependence of the different conflict points within a roundabout.

The ACFs concept was first developed by Gleue (1972) for signalized intersection analysis. It treats each conflict point as one queuing system with a simplified queuing mechanism, while also considering the interactions between the consecutive queuing systems according to the theory of chains-of-queues (Brilon and Wu 2001). Following this idea, Wu and Brilon's capacity model was derived from the general formula for the capacity of a single-lane entry to a roundabout (Wu 2001):

$$C = T_1 \cdot (1 - T_2) \cdot exp(-T_3 \cdot (t_0 - \tau)) \tag{20}$$

Where, $T_1 = 3600/t_f$, $T_2 = q_c\tau/3600$ represents the portion of time of no vehicle platooning in the major stream, and $T_3 = q_c/3600$ represents the portion of time of no impedance caused by a vehicle arriving from upstream in the major stream.

Through simplification and further incorporating the impacts of limited priority, pedestrian crossing, and considering the stochastic property of a queuing system, the total capacity of a two-stage queuing system with n_w waiting places can be expressed by four significant parameters (Wu and Brilon 2018):

$$C_T = f(C_a, C_b, C_{0,ab}, n_w) \tag{21}$$

Where, $C_a = C_{0,a} \cdot p_{0,a}$ is the capacity of the first stage "a" (veh/h); $C_b = C_{0,b} \cdot p_{0,b}$ is the capacity of second stage "b" (veh/h); and $p_{0,a}$, $p_{0,b}$ are the probabilities that the queuing at stage a or b is not impeded by vehicles from the conflicting stream.

For a multi-lane roundabout, the capacities of the individual lanes at the entry cannot be fully used as calculated. To determine the capacity of shared lanes, Wu extended the

formula that was first developed by Harders (1968) considering the volumes of both left (q_L) and right (q_R) entry lanes and the distance of the double-lane area (n_d) upstream from the pedestrian crossing. The total capacity of the double-lane entry ($C_{E,d}$) can then be estimated (Wu and Brilon 2018) using:

$$C_{E,d} = \frac{q_L + q_R}{\sqrt[n_d+1]{(\frac{q_L}{C_{L,T}})^{n_d+1} + (\frac{q_R}{C_{R,T}})^{n_d+1}}} \quad (22)$$

Where $C_{L,T}$ and $C_{R,T}$ are the total capacity for the left and right entry, respectively.

For practical application, the above model derivation process can be summarized into four steps:

1. Obtain the demand volumes of circular, entry, and exit flows at the subject entry and exit.
2. Determine the distribution of demand volumes by lanes based on applicable assumptions.
3. Estimate the two-stage capacities at the downstream exit lanes to analyze their impedance influences.
4. Estimate the two-stage capacities at the upstream entry lanes by considering the downstream impedance impacts on the second-stage capacities (Wu and Brilon 2018).

This model was evaluated for the case of a single-lane roundabout. Results suggested that the conventional roundabout capacity models may lead to a significant overestimation of

the total capacity, and the interference of potential queuing processes between conflicts on the circular lanes cannot be neglected (Wu and Brilon 2018).

MICROSCOPIC SIMULATION MODELS

Microscopic simulation models simulate the movement and interactions of individual vehicles based on car-following and lane-changing theories. These models are effective in evaluating heavily congested conditions, complex geometric configurations, and system-level impacts of transportation systems (FHWA 2020). Because of these distinct advantages of microscopic simulation models, many studies have used them to analyze the roundabout operational performances. Some of the most widely used microsimulation models include VISSIM™, PARAMICS™ and SimTraffic®, although many others are also used.

As simulation models typically require a variety of input parameters, Vaiana et al. (2013) evaluated the effect of geometric and behavioral parameters in the simulation of roundabouts using VISSIM™ by an analysis of variance (ANOVA). These results indicated that traffic flow, time gap, and width of circulating roadway have the most significant impacts. Oketch et al. (2004) compared the performance of a roundabout with a traffic signal alternative using the PARAMICS™ model. Their findings implied that the roundabout approach delay was affected by characteristics of the conflicting flow within the circulatory area, and the model is sensitive to both traffic and geometric features of a roundabout.

Bared and Edara (2005) also used VISSIM™ to model urban single- and dual-lane roundabouts and set the minimum time gaps as 2.5 s and 3 s, respectively. The simulation results were compared with field data and capacity estimates obtained from RODEL™ (empirical model) and aaSIDRA™ (analytical model). They observed that the VISSIM™ capacity values were closer to the real data and less than both the RODEL and aaSIDRA™ capacity predictions. Stanek and Milam (2005) compared the capacity analysis suggested in the FHWA roundabout guidelines with the results of analysis software RODEL™, aaSIDRA™, VISSIM™, and Paramics™. They found that microsimulation models were able to provide more accurate and reasonable results due to their sensitivity about the effects of roadway geometry and gap acceptance, particularly for roundabouts with unique geometric features under the oversaturated conditions.

While previous research has rarely considered roundabout capacity by lane, Bared and Afshar (2009) proposed capacity models for two-lane and three-lane roundabouts by separate entry-lane and separate circulatory-lane traffic volumes through VISSIM™. For the two-lane roundabouts, 130 different traffic scenarios were simulated by randomly selecting the turning ratio level and circulating traffic volumes. From these results, the resulting capacity equations were determined to be:

$$E_L = e^{(7.2079 - \frac{1.3008 c_1}{1000} - \frac{1.2940 c_2}{1000})} \quad (23)$$

$$E_R = e^{(7.2079 - \frac{0.9259c_1}{1000} - \frac{1.0120c_2}{1000})} \quad (24)$$

Where, E_L, E_R is the entry capacity for left, right lane in veh/h, and c_1, c_2 is the circulating flow of inner, outer lane in veh/h.

For the three-lane roundabout, these authors found that the capacity equations also have similar forms, whereas in terms of the right lane, the capacity model was also a function of percentage of right-turning vehicles of this shared lane (Bared and Afshar 2009). Their simulation results were then compared with those estimated by the NCHRP models, as well as the Australian (SIDRA™) and German (Tanner–Wu) models. The findings revealed the importance of considering circulatory lanes separately as opposed to a combined effect of total circulating volumes (Bared and Afshar 2009).

CHAPTER 3. PROJECT APPROACH

THEORETICAL APPROACH

As discussed in chapter 2, a variety of theoretical frameworks have been used to develop and calibrate roundabout capacity models. As the major objective of this project was to evaluate the influence of several potential geometric and operational factors on roundabout performance, it was necessary to adopt an approach based on physically observable effects. As discussed in chapter 1, this study focuses on the gap-acceptance behavior of drivers in the metro-Atlanta area and how these observed gap-acceptance behaviors are influenced by the geometric and operational characteristics of the roundabout.

EXPERIMENTAL AND ANALYTICAL APPROACH

Drone Data Collection

In the previous GDOT local calibration study (Barry 2012, Schmitt 2013), the investigators adopted a variation on the procedures used in the NCHRP 572 and 672 studies (Rodegerdts et al. 2007a,b, 2010) for field data collection and analysis. This approach involved the use of video data collection from both "permanent" (pole-mounted) and "temporary" (tripod-mounted) cameras. The fields of view of these cameras were adjusted to show both the circulating flow and the approach of interest. The resulting videos were analyzed using specialized software (developed for the study) and manual data entry to record both accepted and rejected gaps. In this approach, each video

was screened by an analyst who recorded the time when vehicles reached a pre-determined "queued" position, the positions of potential conflicting vehicles at this time, and the times in which the vehicles entered the roundabout. From these data, subsequent analysis determined the distribution of accepted and rejected gaps from which critical and follow-up headways were determined.

While effective, the process was slow and labor-intensive and was subject to potential analyst effects as the determination of the precise times that a vehicle reached either the queue point or began to enter the intersection were somewhat subjective. As a consequence, significant additional quality-control and quality-assurance activities were necessary to ensure the integrity and usability of the final data.

During the intervening decade since that prior study, there have been significant advances in video data collection. Specifically, higher resolution (e.g., "4k-type" cameras) have become commonplace as have stabilized airborne "drone" platforms capable of carrying these cameras to significant elevations and maintaining stable positioning for the duration of a flight.

These drone video platforms offer a number of significant advantages over earlier methods. Most notably, the near-nadir (i.e., almost vertical) view from the camera significantly improves the field of view and dramatically reduces data-processing requirements to correct for foreshortening effects associated with the angle of the camera relative to the vehicles being recorded. Likewise, the higher resolution of these modern cameras also allows a broader field of view that enables observations of vehicles within the entire roundabout, as well as along the approaches near the roundabout. This larger

field of view thus enables evaluation of behaviors on all roundabout approaches simultaneously rather than sequentially.

Concurrent with the increased availability of drone video equipment were improvements in computer image processing. Improvements in machine vision systems for use in industrial, commercial, and security applications have been adapted for use in the transportation sector, particularly in the area of vehicle trajectory analysis. These systems, originally developed for defense applications, can continuously track and record the position of a moving vehicle across a fixed background (e.g., vehicles moving along a fixed highway). The time-dependent changes of position for each vehicle produce individual vehicle trajectories from which position, speed, acceleration, and other parameters (e.g., gaps between vehicles or position relative to other objects) can be determined by postprocessing of these data. Notably, several companies (e.g., DataFromSky™) are now providing these video processing services commercially. Based on the availability of these services, drone video data collection was selected in this study for collection of field observations of gap-acceptance behavior. Specific information on the equipment and procedures used in the study are provided in subsequent chapters.

Roundabout Selection

The roundabouts used in this project were all modern roundabouts, with most coming into service during the last decade. As mentioned previously, the primary emphasis of this study was on how gap-acceptance behavior was influenced by a variety of geometric and operational parameters, and thus the roundabouts for field data collection were selected to provide a range of geometric configurations. These parameters included the

number of legs (three to five), presence/absence of bypass lanes, variation in inscribed circle and lane widths, etc. to ensure that opportunities existed for the influences of these characteristics to be evaluated. In contrast to earlier studies, there was no specific effort to collect data from roundabouts under saturated conditions, as the study was aimed at observing the influence of various factors on observed gap-acceptance behavior rather than ultimate capacity. These impacts are discussed in detail in chapter 6, chapter 7, and chapter 8.

CHAPTER 4. FIELD DATA COLLECTION

DATA COLLECTION APPROACH

One of the main shortfalls of the roundabout capacity model in the 2016 *Highway Capacity Manual* (TRB 2016) is that it fails to account for additional information (e.g., the trajectory of another vehicle through the roundabout) that may alter a driver's decision as to when to enter the roundabout. Also, the more versatile models that have since been developed (e.g., the algorithms used in the SIDRA™ model) are often based on empirical results that may or may not be applicable to Georgia conditions. Therefore, the data collection approach adopted in this study was to collect "real-world information" on operations of several Georgia roundabouts. Specifically, the data-collection approach was as follows:

1. Record drone-based aerial videos of roundabout operations in the metro-Atlanta area.
2. Analyze these videos to determine vehicle trajectories within and near the roundabouts.
3. Use these trajectories to quantitatively establish gap-acceptance behavior at these roundabouts.

In turn, these gap-acceptance data were used to: (1) evaluate how specific geometric, operational, and environmental factors present in the roundabout influence the gap-acceptance behavior of drivers entering a roundabout; and (2) predict how these factors would influence roundabout operations, including the capacity of a particular approach.

A “quadcopter-type” drone was selected for the data collection both due to the stability of this platform and its ability to position the camera in a location where the field of view of the resulting video provides a complete view of the entire geometry of the roundabout, including its upstream approaches. Such a wide view allows the analyst to see all angles and screen lines at once and to accurately determine when they were crossed by vehicles. The use of a drone eliminates the need to erect a video camera pole and to seek special permission from local jurisdictions. Furthermore, with on-board video recording, the need to provide network infrastructure to transmit video back to a central data repository for recording was also eliminated.

SELECTED ROUNDABOUTS

During the data collection portion of this project, the Georgia Institute of Technology was in “research lockdown” due to the coronavirus disease 2019 (COVID-19) pandemic and research travels were limited to a 50-mile radius of its Atlanta, Georgia, campus. Most of the roundabouts within this 50-mile radius were located in the northern portions of metropolitan Atlanta and roundabout selection was limited to these areas and to the vicinity of campus to minimize overall travel.

From all of the roundabouts available in these locations, a list of 18 candidate roundabouts was selected in consultation with GDOT personnel. These selections were designed to provide a broad array of roundabout configurations, including various sizes (inscribed circle/lane widths/center island diameters); number of legs (3 to 5); number of circulating lanes; presence/absence of bypass lanes; presence on/off the State highway

network, etc. From these, 13 roundabouts were selected for final data collection. The data collected from one of the 13 locations (Holly Springs Rd / Davis Drive) proved to be unusable for analysis due to unstable video imaging and was not included in the final data analysis. Figure 2 and table 3 provide information on the location of the 12 roundabouts that were ultimately used for data collection in this study. These 12 roundabouts included seven 4-legged roundabouts, three 3-legged roundabouts, and two 5-legged roundabouts. More detailed information (e.g., opening year, inscribed circle diameter, number of circulating lanes, etc.) on each roundabout is provided in appendix A.

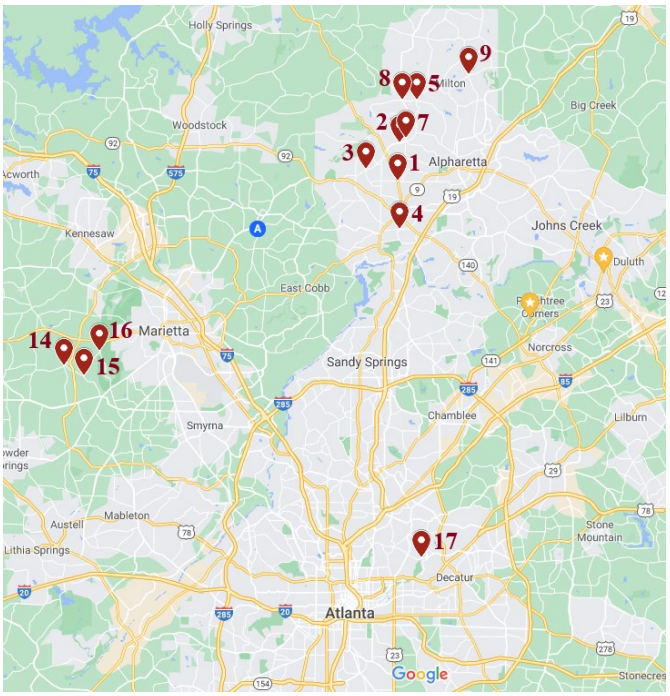

Original Photo: © 2021 Google®

Figure 2. Photo. Final 12 roundabouts used in the study shown with their ID numbers.

Table 3. List of final roundabouts.

ID	Latitude	Longitude	No. of Legs	City	Crossroad Names
1	34.06127	−84.346205	4	Roswell	Hembree Rd/Houze Rd
2	34.08884	−84.344491	4	Milton	Crabapple Rd/Crabapple Chase Dr/Heritage Walk
3	34.06921	−84.373888	3	Roswell	Hardscrabble Rd/Chaffin Rd
4	34.02621	−84.344737	5	Roswell	Norcross St/Warsaw/Grimes Bridge Rd/Melody Ln
5	34.11962	−84.330101	4	Milton	Providence Rd/Freemanville Rd
7	34.0918	−84.33949	4	Milton	Heritage Walk/SR 372
8	34.11946	−84.342467	4	Milton	New Providence Rd/ SR 372/Providence Rd
9	34.13777	−84.284486	4	Milton	Hopewell Rd/ Cogburn Rd/Francis Rd
14	33.92694	−84.637778	4	Cobb County	Villa Rica Rd/W Sandtown SW
15	33.91969	−84.620126	3	Cobb County	Irwin Rd/John Ward Rd SW
16	33.93735	−84.606286	3	Cobb County	John Ward Rd SW/ Cheatham Hill Rd
17	33.78833	−84.325833	5	Atlanta	Oxford Rd NE/N Decatur Rd/ Dowman Dr

FIELD DATA COLLECTION

Field data collection for this project consisted of aerial video recordings of traffic at the selected roundabouts. The recordings were made with a Zenmuse X5S™ camera attached to a DJI Inspire 2™ Quadcopter drone. The Zenmuse camera is a professional camera used for high-end aerial and ground imaging. The camera supports a 5.2k resolution at 30 frames per second (fps) video recording and up to 20.80 MP still photo capture. Table 4 presents a summary of the camera's technical specifications. Standard camera settings used for data collection are provided in appendix B.

Table 4. Summary technical specifications of Zenmuse X5S™ camera.

Item	Value
Lens	M4/3 Interchangeable lens
Sensors	4/3 CMOS
ISO Range	Photo: 100–25600 Video: 100–6400
Shutter Speed	Photo: 8 s – 1/8000 s Video: 1/24 s – 1/8000 s
Maximum Aperture	F1.7 – F16
Field of View	72°
Focus Distance	0.2 meters – ∞
Video Recording	H.264
Maximum Resolution	4096 × 2160

The camera was anchored to the drone via a detachable 3-axis DJI Gimbal Connector 2.0 that facilitates remote control of the camera's photographic settings as well as mechanical pan, tilt, and pitch. The mechanical range for pan is ± 320°, for pitch is −130° to +40°, and for tilt is ± 20°. Therefore, when the drone is hovering high above a roundabout, the gimbal can be remote-controlled to align the camera so that it looks almost directly down on the roundabout. In addition, the 3-axis control system provides stability even during rapid maneuvering of the drone. Figure 3 shows a picture of a DJI Inspire 2™ drone. Figure 4 gives a graphical representation of the gimbal's mechanical ranges.

@ 2019 DJI

Figure 3. Photo. An image of the DJI Inspire 2™ Quadcopter.

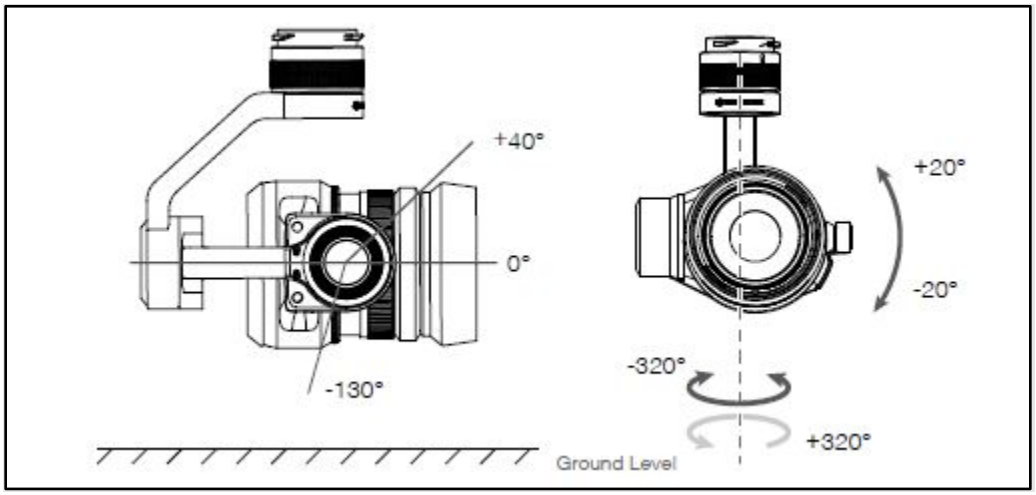

Figure 4. Photo. Mechanical range of the DJI Gimbal Connector 2.0.

For data collection, the drone was flown at an altitude of 390–395 ft above ground level (AGL), just shy of the maximum allowable height of 400 ft AGL, in order to ensure that the video captured both the circular path of the roundabout as well as a significant portion

of the approaches. This was necessary to develop vehicle trajectories that begin upstream of the roundabout along the approaches. Also, the camera was set at a minimum resolution of 1080P at 30 fps in order to obtain quality videos in which traffic is seen as a smooth rather than "glitchy" movement of vehicles. Figure 5 shows a typical high-resolution image from the Zenmuse X5S™ camera.

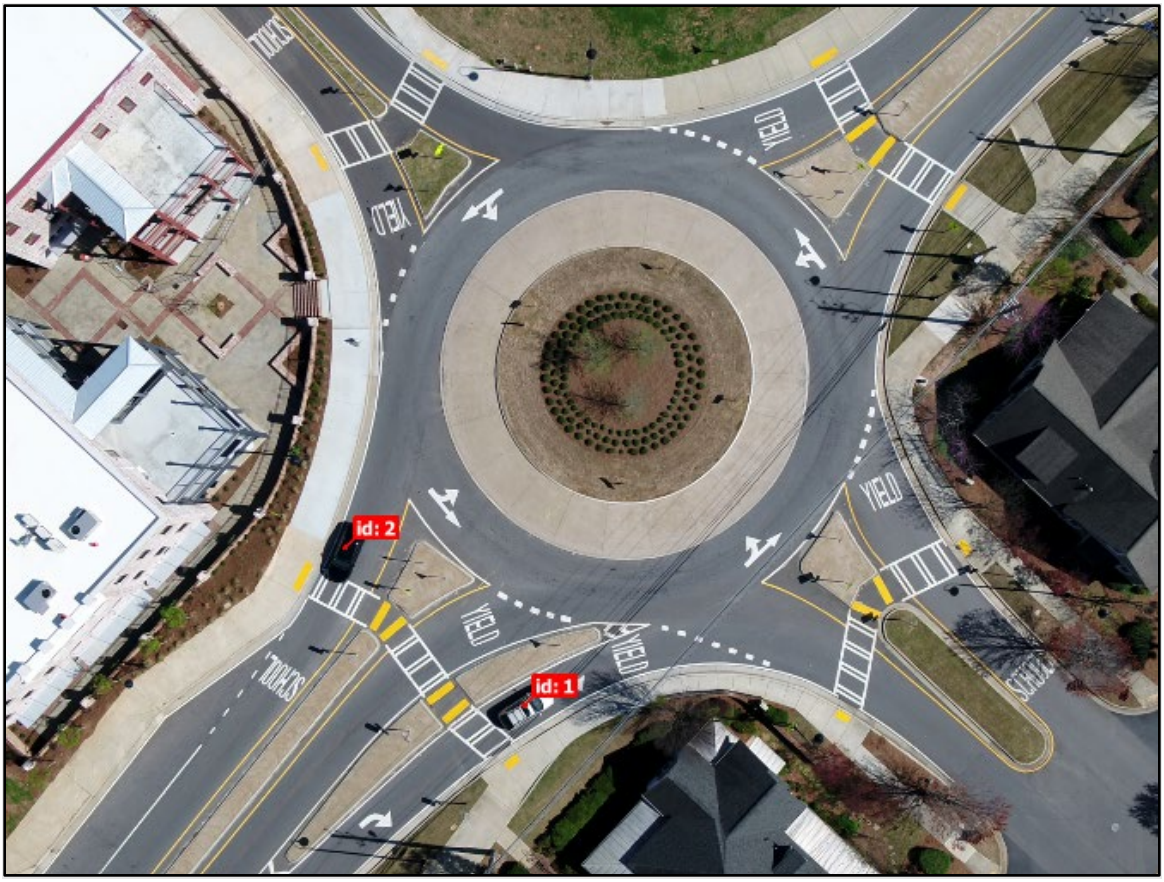

Figure 5. Photo. A typical high-quality image resolution from the drone.

All video recordings were made between 3 PM and sunset. For each roundabout location, two video recordings of about 10–15 minutes duration each were made. The duration of a video is influenced by how much battery power is needed by the drone to ascend to its data collection altitude, how much power is used to resist wind forces for the drone to

hold a stable position, and how much power the software estimates the drone will require to land safely from the takeoff point. These losses can be significant. For example, the drone was observed to typically use 12–18 percent of its available battery power in the ascent portion of the data collection flight.

Each flight requires two fully charged DJI Intelligent Flight Batteries. Therefore, for this project each roundabout site required two pairs of batteries. A pair of batteries takes about 1–2 hours to be fully recharged. Therefore, it is important to prepare as many pairs of fully charged batteries as possible in advance of deployment as otherwise significant field time will be spent waiting for batteries to recharge. The data collection teams on this project were typically equipped with 8–12 fully charged battery packs at the beginning of data collection.

Field data collection was performed by a two-member team, both of whom held a piloting license from the Federal Aviation Administration (FAA) for small unmanned aircraft. One team member was assigned to serve both as a lookout for any potential hazards and to communicate with any persons who may have questions as to why the team was flying a drone in the area. The other team member was dedicated to piloting the drone and to maintaining continuous visual contact and a clear line of sight to the drone.

All personnel were required to wear yellow and orange traffic safety vests at all times while in the field. In order to not distract drivers and/or influence driver behavior, the team was instructed to sets up at a significant distance from the roundabout but in a location such that the pilot would always have a clear line of sight to both the drone and the roundabout. Some field setup locations used in this study included adjacent parking

lots, right-of-way reservations around the roads, and driveways of residential buildings (with permission of the owners). Figure 6 shows a typical setup in a parking lot by the data collection team. Please note that this position is away from the roundabout and out of normal view of road users so the field team is unlikely to influence driver behavior. During the course of the study, a total of 24 flights were conducted at the 13 sites (including the rejected data from the Holly Springs/Davis Drive site). Chapter 5 will discuss how these videos were processed for further use.

Figure 6. Photo. Image showing typical setup position by data collection team in a parking lot.

CHAPTER 5. TRAJECTORY ANALYSIS

DATA PROCESSING

At the conclusion of each day of field data collection, the research team would download the recorded videos and initiate the data processing steps. A flowchart of this initial data processing is shown in figure 7. After downloading the videos and examining them to ensure that they properly showed the roundabout and its approaches, the video files were electronically transmitted to DataFromSky™—a traffic engineering company that analyzes drone footage for trajectory generation and analysis—for processing. The company has a 24-hour turnaround time to produce a video-based "tracking log" containing the vehicle trajectories that can then be analyzed using their proprietary DataFromSky™ Viewer. This "tracking log" file includes information on the frame-by-frame position of all vehicles within the video image in terms of pixel location within the image. If the image is fixed, these positions can be interpreted as the trajectory of the vehicle against the fixed roadway background.

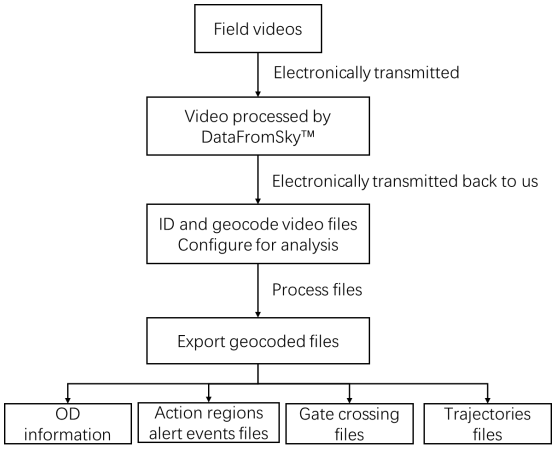

Figure 7. Diagram. Flowchart of initial video data processing steps.

The research team used tools in the DataFromSky™ Viewer to configure the trajectory file to export the data to be used in the gap-acceptance analysis. The main steps required to configure the trajectory file in the DataFromSky™ Viewer for data export are described below. A complete flow diagram of the entire data processing scheme is also provided in appendix H.

Quality Assurance

As mentioned previously, the process of accurate automatic extraction of vehicle trajectories by machine vision methods requires that the video image of the underlying pavement remains in a fixed location within the field of view of the camera over the period of analysis.

Modern video drones have sophisticated control systems designed to keep the cameras view fixed on a particular position as required for the extraction of vehicle trajectories. These systems control the camera view largely by maintaining the drone platform in a fixed location by continuously controlling the thrust of each of the drone's four propellers to rapidly compensate for any platform movement. Additional control of the camera view is achieved by adjustment of the camera's multi-axis (pan and tilt control) electronic gimbal mounting system.

These control systems, in general, work extremely well, but there are limits to their ability to maintain platform stability. The most common stability issue is associated with operation in high and variable wind conditions. The ideal condition to fly the drone for field data collection is under conditions of clear skies with light winds below 8 MPH.

High ambient wind speeds, e.g., in excess of 15 MPH, can cause the drone to dither in its position as it tries to stabilize and hold its position against these wind forces. Consequently, the image in the captured videos can shift as the drone moves. Without correction for this shift, the resulting apparent vehicle trajectories can appear to wander across the background image instead of remaining fixed on the roadway/pavement, making it difficult to analyze the data and, in some cases, render the resulting videos unusable for trajectory analysis.

The impact of operating the drone in high wind conditions is shown in figure 8, which shows results for a video image with distorted vehicle trajectories due to high winds affecting the drone's positioning. Figure 9 shows a video image of the same roundabout with generated vehicle trajectories well positioned in the lanes due to more favorable wind conditions.

Figure 8. Photo. Spreading of vehicle trajectories due to high wind speeds affecting drone's positioning.

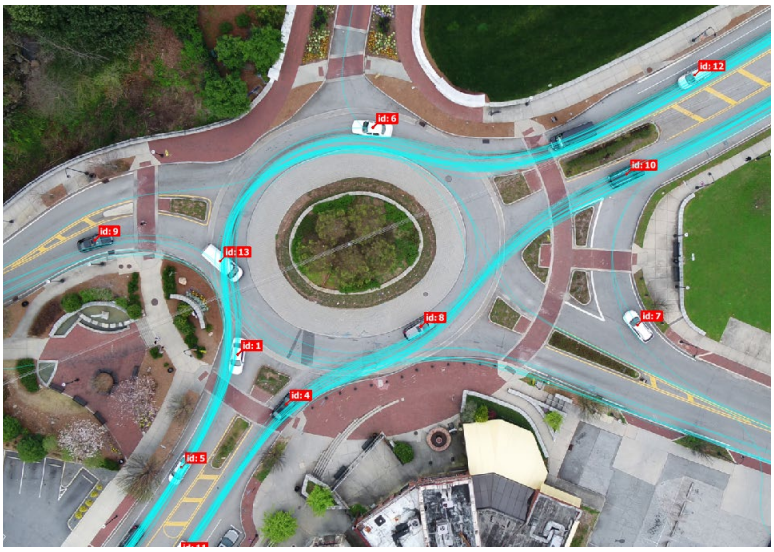

Figure 9. Photo. Well placed trajectories at low wind speeds.

Upon receipt back from DataFromSky™, all video trajectory files were examined by an analyst to ensure that the recorded trajectories were stable and well placed on the background image. If a video file was found to contain inaccurate trajectory placement, the analyst was asked to determine if the issue impacted only a portion of the video (e.g., before or after a particular time) or was prevalent throughout, and these videos were flagged for further analysis.

While there are quantitative methods for compensating for platform movement in evaluating trajectories, they are labor-intensive and complex and were not used in this study as it was more cost-effective to redeploy the field team to the same site under more favorable conditions.

Geocoding Roundabout Locations

The trajectory file produced by DataFromSky™ is not geocoded by default. Consequently, all distances within the file are based on pixels, e.g., speed values will read

as pixels per second. Therefore, the first step in configuring the file for data export is to geocode it to reference the pixel positions to their fixed positions in space. This process is based on known latitude and longitude information corresponding to at least four well-defined points within the image, (e.g., a corner of a splitter island or the location of a yield sign). In this study, the research team extracted the latitude and longitude of these selected reference locations from georeferenced images available from Google Maps®. Figure 10 shows a set of four geocoding points for a roundabout.

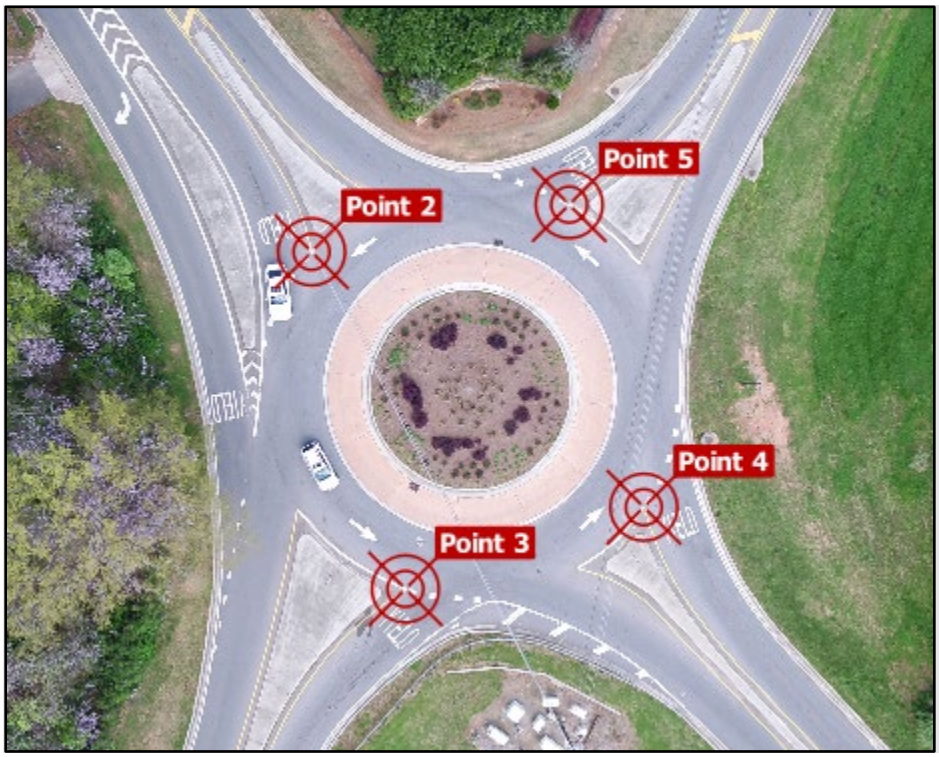

Figure 10. Photo. A set of geocoding points for a roundabout.

Annotation Configuration

Annotation configuration of the trajectory file allows the analyst to define certain "detectors" (e.g., screenlines) that record vehicle activity and generate time stamps when vehicles cross these positions that can later be exported for subsequent analysis. The

DataFromSky™ Viewer comes with many such options but, for these analyses, the research team used a combination of "gates" (line detectors) and "action regions" (area detectors) that detect the presence of vehicles over a defined portion of the pavement. Whenever a vehicle crosses a gate, certain attributes of the vehicle and its trajectories are recorded. These attributes include the vehicle ID, speed, acceleration, position (latitude and longitude), and the time it crossed the gate.

The first set of gates that were defined in each trajectory file were the entry and exit gates on the roundabout approaches. Apart from the vehicle and trajectory attribute data that are collected at these gates, the scripts use this information to generate an origin–destination matrix of traffic entering and leaving the roundabout. Gates can also be set to record vehicles crossing in either one direction or both directions. Figure 11 shows a typical setup of entry (green lines) and exit (red lines) gates at a roundabout.

Figure 11. Photo. Typical setup of entry and exit gates at a roundabout.

The second group of gates were “approach monitoring gates”. These gates consisted of a set of three gates on each approach between the circular path and the entry and exit gates. These gates record vehicle attributes as drivers modify their driving to enter the roundabout. These three gates were positioned as follows:

- The gate closest to the roundabout circle was positioned such that it begins at the top right corner of the splitter island and its direction is normal to the entry lane.
- The middle gate was positioned with the upstream end at the Yield Sign marking on the pavement. Where there is no Yield Sign marking on the pavement, the analyst estimated where it would have been placed if it had been present.
- The third gate was positioned near the pedestrian crosswalk. On approaches without a pedestrian crossing, the gate was positioned between the main entry gate that is most upstream on the approach and the middle gate near the Yield Sign on the pavement. Figure 12 shows typical positions for these three gates.

Figure 12. Photo. Typical position of approach monitoring gates used to capture vehicle attributes as drivers modify driving to enter the roundabout.

In addition, the researchers placed a third set of gates to capture vehicle attribute information within the circular path. These "circulating vehicle" gates are called neutral gates because they are neither for exiting nor entry vehicles. These gates were positioned at three locations:

- At the top right corner of the splitter island and with a direction that is normal to the circular path.
- At the middle of each splitter island and with a direction that is normal to the circular path.
- At the midpoint location between any two approaches and with a direction that is normal to the circular path.

Figure 13 shows the typical positions of the neutral gates used in capturing vehicle information within the circular path.

Figure 13. Photo. Position of circulating vehicle gates (blue lines) used to record vehicle attributes in the circular path.

Finally, the researchers used “action regions” to detect the presence of vehicles within certain areas of the pavement that are likely to conflict with the approaching vehicle at the stop line. These “conflict area” regions are defined for each approach and their attributes contain the information related to the positions and speeds of the potential conflicting vehicles at different times. For any particular approach, its action region was defined as:

- The part of the circular pavement stretching from the right corner of its splitter island to the immediate upstream approach.
- The part of the circular pavement stretching from the right corner of its splitter island up to the left corner of the splitter island that is two approaches downstream.

Figure 14 shows a typical action region detector.

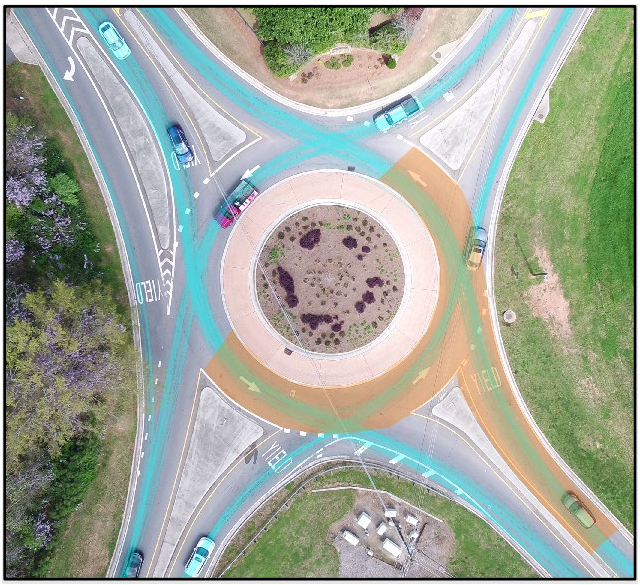

Figure 14. Photo. An action region detector for top right approach of roundabout.

Once all the detectors had been set and defined, the DataFromSky™ Viewer software was used to generate different vehicle time stamps associated with observed gate crossings within the video. These data were exported for further analysis as four comma-separated value (.csv) text files, as follows:

- **Action Regions Alert Events File**: Contains vehicle and trajectory attributes including region_id, trajectory_track_id, entry_time, exit_time, average_speed, and average_acceleration for events within the active regions.
- **Trajectories File**: Contains vehicle and trajectory attributes for all vehicles within the image including trajectory_track_id, vehicle_type, entry_gate, entry_time, exit_gate, exit_time, traveled_distance, average_speed, latitude, longitude, speed, tangential_acceleration, lateral_acceleration, and time. The trajectory time stamps have a resolution of 1/30 second (i.e., a single frame from the video).
- **Gate Crossing Events File**: Contains vehicle and trajectory attributes including gate_id, trajectory_track_id, vehicle_type, time, speed, headway (time), and headway (distance) for all gate crossing events.
- **OD File**: Provides the entering and exiting times and locations for all vehicles entering and leaving the roundabout.

GAP EXTRACTION

Extraction of the accepted and rejected gaps for vehicles entering the roundabout were obtained semi-automatically (i.e., some analyst intervention was required to complete the

analysis) using the vehicle trajectory information. This method uses the .csv files described in the previous section (except for the OD File) to identify when a vehicle approaches the roundabout and then locates the positions of all potential conflicting vehicles. It continues to monitor the location of conflicting vehicles until the approaching vehicle enters the roundabout. The shortest gap to a conflicting vehicle when the approaching vehicle begins to enter the roundabout circle is taken as the "accepted gap" and all conflicting vehicle gaps that did not result in the approaching vehicle entering the roundabout circle were recorded as "rejected gaps." The research team designed an algorithm that could automatically detect the accepted or rejected gaps of each arriving vehicle in the minor approach and compute the gap time and gap distance accordingly. The major steps in the extraction of these gap-acceptance data are illustrated in Figure 15 and discussed below.

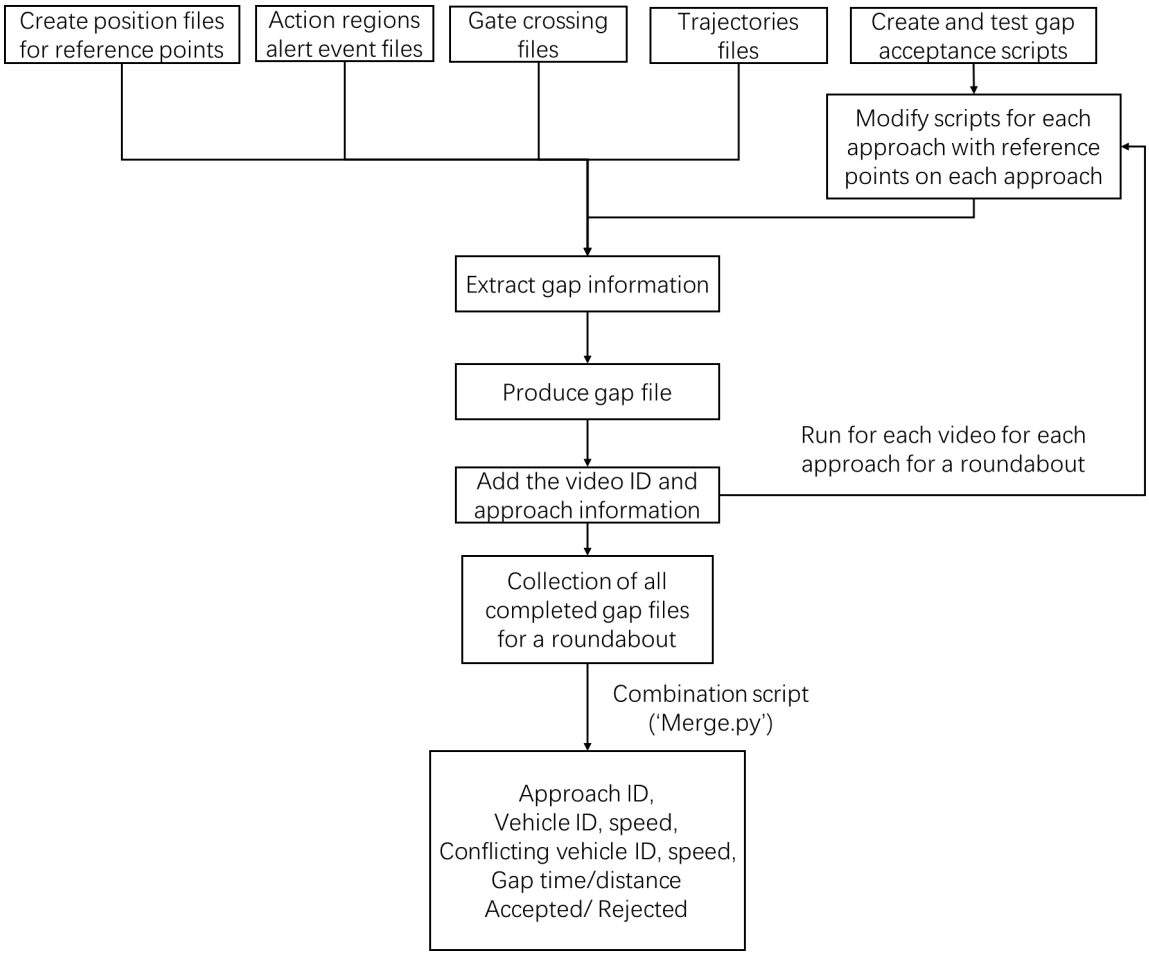

Figure 15. Diagram. Flowchart of gap extraction process.

To illustrate this process, consider the analysis on the east approach of the roundabout at the intersection of New Providence Rd and SR 372 (Roundabout ID#8) as an example. In figure 16 and figure 17, the east approach is located in the upper right corner of the photograph. For this roundabout and approach, the gates and action regions are set as described in the previous section. In these figures, gate 10 detects when a vehicle arrives on the minor approach, gate 9 is used to indicate whether this approaching vehicle is about to enter the roundabout, and gate 12 is set at the location that is considered to be the initial potential conflict point between the circulating and approaching vehicles.

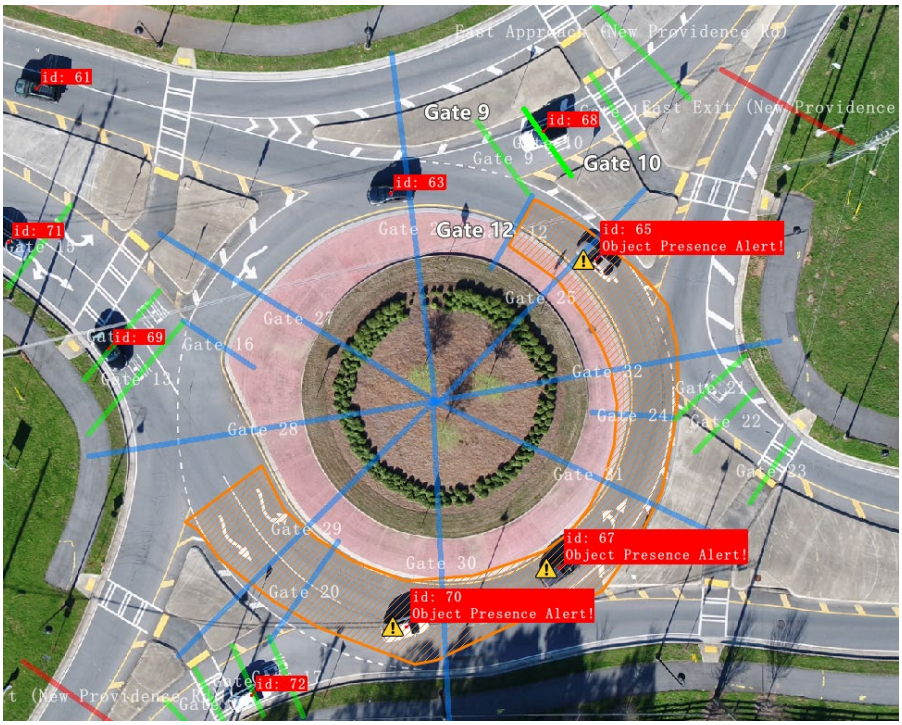

Figure 16. Photo. Gates in the east approach annotation of roundabout New Providence Rd / SR 372 (Roundabout ID#8).

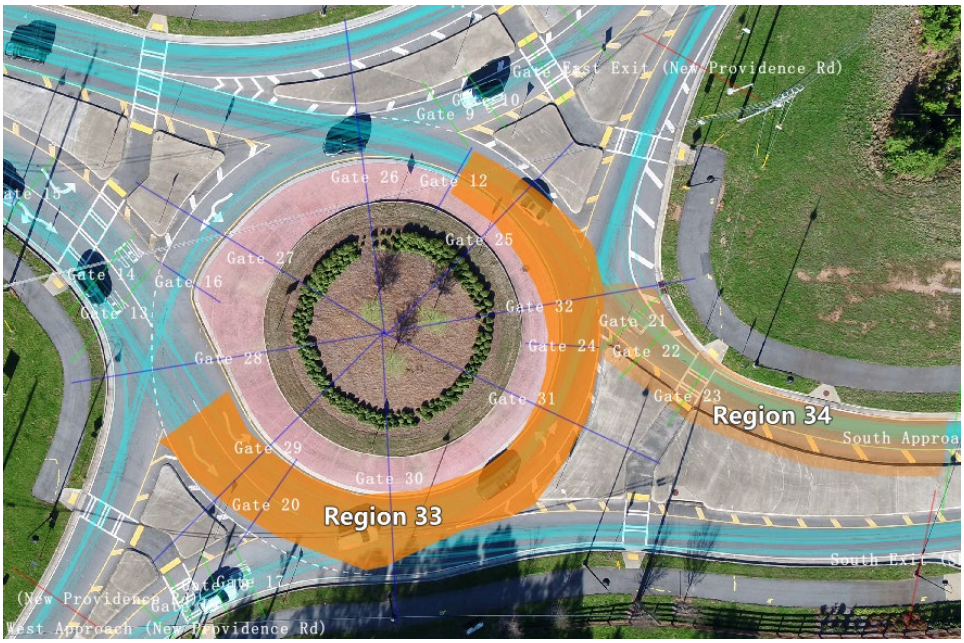

Figure 17. Photo. Circular region 33 and upstream region 34 set in the east approach annotation of roundabout New Providence Rd / SR 372 (Roundabout ID#8).

When processing a video, the algorithm initially identifies all of the vehicles that have crossed the trigger gate (gate 10 in figure 16) and entered the roundabout from the minor approach. Then, for each of these vehicles the following steps are used to extract the gap data:

- For each approaching vehicle, obtain the time t_0 when it travels past the trigger gate (from Gate Crossing Events File).
- For time t_0, identify any vehicle records from the Action Regions Alert Events File that satisfy the conditions: (1) the 'Action Region ID' of the record is either from the corresponding circular region ID 33 (the orange region in figure 17) or the upstream approach region ID 34, and (2) t_0 is within the time interval between the record's entry and exit time with respect to either region 33 or 34.
- If such records exist, the 'Track ID' in the action region datasets indicates the vehicle ID of the potentially conflicting vehicles, and this ID is used to obtain the speed v_c and position (latitude and longitude) of this conflicting vehicle at time t_0 from the trajectories file.
- Once the information of conflicting vehicles has been acquired, the algorithm computes the distance d_c from the conflicting vehicle's current position to the potential conflict points, and the gap time is calculated using $t_g = d_c/v_c$. If multiple conflicting vehicles exist at time t_0, the one with the minimum gap time t_{g_min} is considered first.
- The algorithm then determines whether this gap is accepted or rejected by comparing the time t_e when the approaching vehicle enters the roundabout (i.e.,

crosses gate 9 in figure 16) and the time t_1 when the conflicting vehicle has arrived at the particular conflict point (gate 12 in figure 16). Both of the times are obtained from the gate crossing events file. If $t_e \leq t_1$, that indicates the approaching vehicle has arrived at gate 9 first and the gap is considered an accepted gap; otherwise, the gap is considered as rejected.

- The above process is repeated for each approaching vehicle to get all the gap records for this east approach.

This gap extraction algorithm was implemented in Python 3.7 and the corresponding scripts are attached in appendix E. All the trajectories files exported from DataFromSky™ are in terms of each roundabout approach; thus, the scripts were also created in an approach level with modifications on the imported .csv file names as well as the gate IDs and action region IDs.

QUALITY ASSURANCE

During the gap extraction process, if there are no potential conflicting vehicles present within the action regions when an approaching vehicle arrives at the stop line (i.e., crosses the trigger gate), then the algorithm would consider this gap time to be infinite. In total, 5750 gap records were extracted from the video data, and 1814 of them were identified as “infinite” gaps. For purposes of critical gap estimation, these “infinite” gaps were not considered.

Additionally, in the quality assurance review of the gap-acceptance results, the team identified 4 out of 5750 records with rejected gaps larger than 10 seconds. Upon further

investigation, we found that these large rejected gaps occurred either because the DataFromSky Viewer™ would occasionally identify a vehicle towing another as two vehicles, or the presence of bicycles within the roundabout would cause approaching vehicles to wait longer without being recognized by the software. These gap records were also excluded from further analysis.

METADATA

A metadata file containing all the approach-level information on the roundabouts was created as a Microsoft Excel® spreadsheet. These metadata consisted of both identifying information such as Roundabout_ID, intersecting road names, latitude and longitude, date of data collection, and video_ID, as well as geometric design and observed operational data related to the roundabout.

Most of the geometric data were populated by using images from Google Maps® and Google Earth® to collect additional information relating to geometry (including lane width, splitter width, and inscribed circle diameter), design (including presence of truck apron, yield sign, warning sign, and posted speed), and the year that the roundabout was opened to traffic.

The metadata related to observed operational characteristics of the roundabouts (based on analysis of the drone videos) were populated using the data exported from the DataFromSky™ Viewer to estimate these other variables (including probability of right turns, circulating volume, average approach speeds, and heavy vehicle percentage).

In all, the final metadata contained 50 variables (columns) relating to the roundabouts with each variable having approach-level resolution (159 rows). Appendix D in this report contains a description of these variables and the project supplemental information for the full metadata spreadsheet.

CHAPTER 6. GAP ANALYSIS

To describe drivers' gap-acceptance behaviors at roundabout approaches, critical headway is often used as a representative variable and it is also one of the key components of roundabout capacity models. As mentioned in chapter 2, since the critical headways cannot be measured directly from the field, various methods (e.g., Raff 1950, Siegloch 1973, Troutbeck 1992) have been proposed for its estimation. While the maximum likelihood method is often considered to be the most reliable and is considered as a standard reference (Vasconcelos et al. 2013), it uses an iterative process to estimate the mean and variance of critical headway distributions rather than directly modeling the gap-acceptance behaviors within the roundabouts.

In practice, the rejected/accepted gaps observed in most roundabout approaches tend to follow a standard sigmoidal (logistic) curve. Since the main goal of this project is to determine how various factors influence these gap-acceptance curves, the team chose to use the logistic regression method, which was also adopted in the previous GDOT local calibration studies (Barry 2012 and Schmitt 2013), to estimate the probability that a gap will be accepted, and further to determine the critical headways for each roundabout approach.

LOGISTIC REGRESSION

During the gap extraction process, the variable "gap type" was created to indicate whether this certain gap was accepted (gap type = 1) or rejected (gap type = 0). To

predict the probability of accepting a gap, gap type is treated as the dependent variable, while gap time (seconds) is considered as the only explanatory variable. Since the dependent variable is categorical with only two possible outcomes and the explanatory variable gap time is continuous, a binary logistic regression model was used for the analysis of gap time against gap decisions (i.e., gap type) based on both the accepted and rejected gaps. The general form of the logistic model is:

$$p(x) = \frac{1}{1+e^{-t}} = \frac{1}{1+e^{-(\beta_0+\beta_1 x)}} \quad (25)$$

Where, t is assumed to be a linear function of explanatory variable gap time; β_0 and β_1 are the intercept and coefficient of the linear function, respectively, and $p(x)$ is the probability of accepting the gap when the gap size is x seconds.

The logistic regression was implemented in Python 3.7 through the built-in module 'Statsmodels', which provides various functions for estimating different statistical models and performing statistical tests. After being fitted to the gap data, a gap-acceptance curve was obtained for each roundabout approach, and the critical headway was also determined at the point where the probability of accepting the gap is 50 percent (i.e., logistic inflection point). The plotted results from these regressions are shown in appendix C and the Python™ script used for the calculation can be found in appendix F.

For quality assurance purposes, these regression results were also compared with those obtained via the "Solver" add-in to Microsoft Excel®, as well as from the "R" statistical package. No discrepancies in the results were observed for any of these methods.

ANALYSIS RESULTS

Due to the limited observations of rejected gaps in some roundabout approaches (6 out of 46 approaches), the gap data distribution can be seen as achieving a complete or quasi-complete separation, which would cause the maximum likelihood algorithm to fail to converge; therefore, the maximum likelihood estimates for these cases are undefined (Allison 2008). Under these circumstances, the coefficient and intercept of the logistic model was set to 0 and the critical gap, which was normally estimated at the point with 50 percent of probability, would also be considered as less than the smallest gaps observed in that approach. The regression results with respect to the model parameters and the critical headway are presented in table 5.

Table 5. Logistic regression results for each roundabout approach.

ID	Approach	Intercept β_0	Coeff. β_1	Gap_time@ 50	Sample Size
2	East	−0.591	0.870	0.680	36
2	North	−3.865	1.184	3.264	13
2	South	0	0	less than 0.882	2
2	West	−6.461	2.328	2.776	42
4	East	1.737	0.466	less than 2.010	131
4	North	−3.021	1.476	2.047	115
4	South(Melody)	0	0	less than 3.909	3
4	South	−1.192	0.743	1.604	123
4	West	0.275	0.561	less than 1.583	281
3	East	−4.136	2.346	1.763	174
3	South	−3.840	1.304	2.944	60
3	West	−10.387	5.919	1.755	236
1	East	−3.140	1.016	3.091	80
1	North	−1.739	0.599	2.901	128
1	South	−6.586	1.982	3.323	96
1	West	−3.461	0.713	4.856	67

ID	Approach	Intercept β_0	Coeff. β_1	Gap_time@ 50	Sample Size
7	East	−4.283	1.258	3.406	77
7	North	−2.885	1.130	2.552	103
7	South	−1.811	0.781	2.319	95
7	West	−3.215	0.785	4.096	74
9	East	−2.355	0.770	3.060	112
9	South	−3.366	1.133	2.970	178
9	West	−3.507	1.200	2.923	80
9	North	−3.028	1.039	2.915	114
15	North	−12.334	4.696	2.627	39
15	South	−9.055	3.290	2.752	49
15	West	−14.644	4.727	3.098	41
16	North	−11.424	4.345	2.629	141
16	South	−3.616	1.512	2.392	81
16	West	−1.038	1.139	0.911	42
5	East	−4.156	1.242	3.347	69
5	North	−2.311	0.928	2.490	52
5	South	−0.025	0.400	0.063	30
5	West	−0.226	0.485	0.467	65
8	East	−1.645	0.557	2.953	49
8	North	−0.772	0.422	1.829	115
8	South	−1.429	0.709	2.016	98
8	West	−2.927	0.585	5.005	85
17	West	−6.095	1.872	3.256	91
17	East	−4.503	1.730	2.604	24
17	North	0	0	less than 5.064	5
17	South	0	0	less than 6.732	2
14	East	−3.090	0.898	3.441	166
14	North	−3.115	0.634	4.913	134
14	South	−3.491	0.862	4.049	52
14	West	−5.427	1.348	4.025	82

After excluding the six roundabout approaches with convergence failure in logistic regression, the mean value of the estimated critical headways (logistical method) is 2.75 s with the standard deviation being 1.106 s. A histogram of the critical headways estimated

in each roundabout approach is shown in figure 18. Please note that these headways are not directly comparable on an "absolute" basis with those determined by the maximum likelihood method due to different probability bases (i.e., 50 percent acceptance probability for the logistic regression versus 95 percent for the MLM).

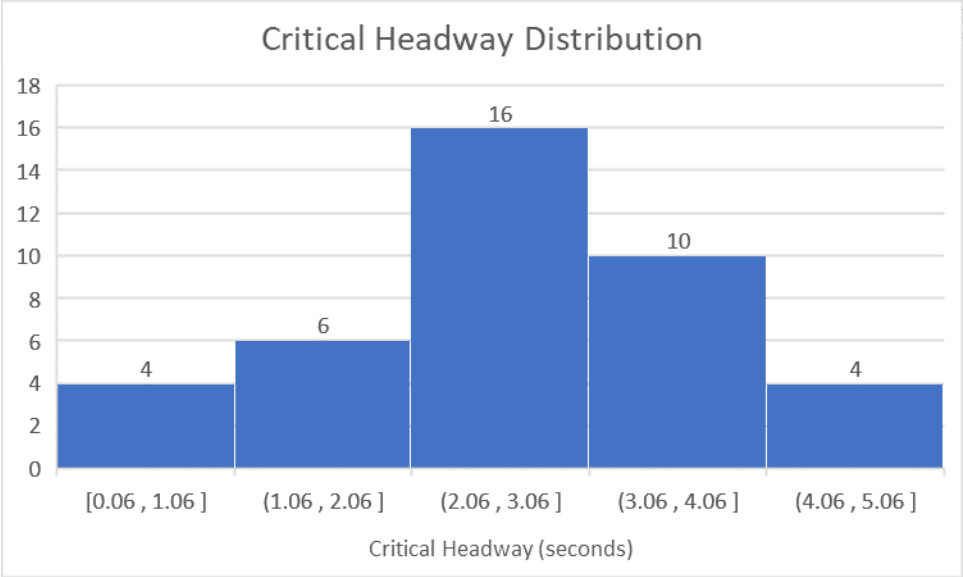

Figure 18. Chart. Estimated critical headway distributions of roundabout approaches.

These critical headway predictions were merged with the metadata file discussed in chapter 5 to create the project database used for the model development discussed in chapter 7.

CHAPTER 7. MODEL DEVELOPMENT

This chapter describes the development of a model to predict the influence of various geometric and operational parameters of roundabouts on gap acceptance for Georgia roundabouts based on the drone video observations described in the previous chapters. These steps can be broadly described as:

- Development of a linear regression model to predict the critical gap at the roundabouts. The critical gap in this study is represented by the 50th percentile gap (*Gap_time@50*) from the fitted logistic regression curves fitted to the roundabout approaches discussed in chapter 6.
- Developing an arrival headway distribution model to provide a common dataset to conduct a sensitivity analysis of how this model may influence observed roundabout capacity.

LINEAR REGRESSION MODELING OF CRITICAL HEADWAYS

Selection of Variables

The first step in building a linear regression model to predict gap acceptance was to select the most influential variables. The project data and metadata contained 52 variables with attribute data at the resolution level of a roundabout approach. Table 6 gives a list of the available variables and their brief descriptions.

Table 6. List of variables and brief descriptions.

Variable Name	Brief Description
Roundabout_ID	Roundabout identification number.
Lat	GPS latitude of the roundabout center.
Lon	GPS longitude of the roundabout center.
No. Legs of Rndabt	Number of legs of roundabout.
Dia of Central Island. (ft)	Diameter of the roundabout's central island in feet.
No_Lanes	Number of lanes marked on a roundabout approach.
Road Names	The names of the crossroads roads at the roundabout.
Date	The date of drone video collection.
Flight #	Identification number of drone's flight at roundabout.
Video_ID_text	An alphanumeric identifier for every video file.
Video_ID_Num	A numeric identifier for every video file.
Approach	Assigned east, north, west, or south direction of leg.
Opening Year	The year the roundabout was opened to traffic.
Visual Angle to Ups App.	The angle between visual lines of sight from approach to upstream approach.
No. Cir Lanes Xing App	The no. of circulating lanes at approach.
Inscribed Cir Dia. (ft)	Inscribed diameter of circle in feet.
Width of Splitter Island (ft)	The width of the splitter island in feet.
Lane Width (ft)	Lane width on leg.
Presence of Left Offset on App?	Presence of a left offset on an approach.
Presence of Truck Apron?	Presence of a truck apron.
Ups App on State Route?	Is upstream approach on a state route?
App on State Route?	Is approach on a state route?
Posted Speed at Entry on App	Posted speed on approach near entry point.
Rabt Ahead Sign?	Roundabout ahead warning sign upstream?
Presence of Yield	Yield sign near the roundabout entrance?
Ped Xing on App	Pedestrian crossing on approach?
Ped Xing on Ups App	Pedestrian crossing on the upstream approach?
Prob_right_turn	Probability turning right turn from an approach.
Entry_count	Count of entering vehicles at approach.
Entry_volume(pce/h)	Entry volume in hourly rate.
Circulating_count	Count of circulating vehicles.
Circulating_volume(pce/h)	Volume of circulating vehicles in hourly rate.
Exiting_count	Count of vehicles exiting at approach.
Exiting_volume(pce/h)	Exiting volume at approach.
Exiting_prob	Probability of exiting at approach.
Video_length (msec)	Video length in milliseconds.

Variable Name	Brief Description
Video_length (h)	Video length in hours.
Avg_approach_speed (mph)	Average speed on approach in miles per hour.
Avg_conflict_speed (mph)	Average speed in the circulating lanes in miles per hour.
Heavy_vehicle_count	Count of heavy vehicles.
Bus_count	Count of buses.
Total_vehicle_count	Count of all entering vehicles.
Total_vehicle_volume(pce/h)	Entering vehicle volume in hourly rate.
Med_and_small	Count of cars and light trucks.
Heavy_vehicle_percentage	Percentage of heavy vehicles.
Bus_percentage	Percentage of buses.
Intercept	Intercept of logistic curve.
Coefficient	Coefficient from logistic curve.
Gap_time@50	50th percentile gap time on the logistic curve.
No. of datapoints	Number of data points used to estimate gap time.
Entry_Angle	Entry angle on approach.
Angle_to_Ups_App	Angle between approach and upstream approach.

Dropping Initial Variables

To identify the most influential variable for the regression model(s), the variables that did not have any meaningful relationship with *Gap_time@50* or did not show any variability among the observed roundabouts were filtered out first. The 16 variables, along with Gap_time@50, removed by this process are provided in table 7.

Table 7. List of metadata variables without a meaningful relationship with observed gaps at roundabouts.

Variable Name
Roundabout_ID
Lat.
Long.
Road Names
Date
Flight #
Video_ID_text
Video_ID_Num
Approach
Rabt Ahead Sign?
Presence of Yield Sign?
Video_length (msec)
Video_length (h)
Intercept
Coefficient
Presence of Truck Apron?

Correlation Analysis

The remaining variables were evaluated using a nonparametric correlation analysis to estimate the strength, direction, and significance of the pairwise relationship between *Gap_time@50* and the remaining variables. This correlation analysis was conducted using the 35 variables remaining from the previous step along with four additional

variables, bringing the total to 39 variables for the correlation analysis. These additional variables were *Op_Years* that gives the number of years the roundabout has been in operation (transformed from *Opening Year*); *State_route* that connected the variables "Ups App on State Route?" and "App on State Route?" in a logical "or" relationship, and two other variables, *SmallDia* and *LargeDia* representing roundabouts with an inscribed circle less than or equal to 125 ft and greater than or equal to 145 ft, respectively. Thus, there were 39 variables available in the correlation analysis.

The results of this nonparametric Spearman correlation analysis are shown in table 8. The variables meeting the selection criteria of a significance value less than or equal to 0.05 were selected and further analyzed for potential collinearity issues. These values are highlighted in table 8.

Table 8. Nonparametric correlation results of Gap_time@50 with other variables.

Variable 2	Spearman (ρ)	
	ρ	Prob>|ρ|
Angle_to_Ups_App	−0.3689	<.0001
No. Legs of Rndabt	0.0013	0.9874
Dia of Central Island. (ft)	−0.2865	0.0006
No_Lanes	−0.0091	0.9147
Opening Year	−0.2570	0.0021
Visual Angle to Ups App.	0.3471	<.0001
No. Cir Lanes Xsing App	0.3658	<.0001
Inscribed Cir Dia. (ft)	−0.2089	0.0129
Width of Splitter Island (ft)	−0.2258	0.0071
Lane Width (ft)	0.2418	0.0039
Presence of Left Offset on App?	−0.1246	0.1411
Ups App on State Route?	0.5515	<.0001
App on State Route?	−0.2381	0.0045

Variable 2	Spearman (ρ)	
	ρ	Prob>|ρ|
Posted Speed at Entry on App	0.0038	0.9645
Ped Xing on App	−0.0137	0.872
Ped Xing on Ups App	−0.1552	0.0661
Prob_right_turn	0.2624	0.0017
Entry_count	−0.2292	0.0063
Entry_volume(pce/h)	−0.2744	0.001
Circulating_count	0.0280	0.7421
Circulating_volume(pce/h)	−0.0432	0.6111
Exiting_count	−0.2048	0.0148
Exiting_volume(pce/h)	−0.2469	0.0032
Exiting_prob	−0.2029	0.0158
Avg_approach_speed (mph)	−0.4848	<.0001
Avg_conflict_speed (mph)	−0.1489	0.0813
Heavy_vehicle_count	0.1509	0.0741
Bus_count	0.1084	0.2009
Total_vehicle_count	0.1530	0.0702
Total_vehicle_volume(pce/h)	0.0904	0.2861
Med_and_small	0.1349	0.1107
Heavy_vehicle_percentage	0.1546	0.0671
Bus_percentage	0.0898	0.2895
Op_Years	0.2570	0.0021
State_route	0.2446	0.0035
SmallDia	0.3170	0.0001
LargeDia	−0.1090	0.1982

Collinearity Analysis

Due to the possibility of high collinearity within the selected variables, the researchers also analyzed for correlation between these variables. The detailed results of this correlation analysis are provided in appendix G.

For any two variables showing high correlation, the one with a lower significance estimate was removed (see table 8). Where the significance estimates are the same, the

one with a lower magnitude was removed. In all, 12 variables (see table 9) were retained as the first reduced variable set (LR1) for use in regression modeling.

Table 9. LR1 variable set.

No.	Variable Name
1	Angle_to_Ups_App
2	SmallDia (LR2)
3	Op_Years
4	No. Cir Lanes Xsing App (LR2)
5	Width of Splitter Island
6	Lane Width
7	Ups App on State Route (LR2)
8	App on State Route?
9	Prob_right_turn
10	Entry_volume
11	Exiting_volume
12	Avg_approach_speed (LR2)

A second variable set (LR2) using a stepwise algorithm to select the best of these 12 variables was also constructed. These variables are identified in table 9 by the (LR2) designation after the variable name.

Variable Clustering Analysis

A third reduced variable set (LR3) was also constructed by performing a variable clustering analysis in order to formulate a linear regression model with lower dimensionality. Variable clustering analysis attempts to group a set of variables into non-overlapping clusters containing similar variables. Each cluster can subsequently be represented by the single most representative variable or a component variable that is a linear combination of all variables in the cluster. The variable clustering analysis was

performed on the 12 variables that were identified in the previous section. The analysis was performed with JMP® Pro version 15.

This analysis yielded three clusters as shown in table 10. The overall proportion of variance explained by the clustering is 0.526.

Table 10. Cluster member summary.

Variable Name	Cluster	R^2 within Own Cluster
Width of Splitter Island (ft)	1	0.681
Op_Years	1	0.582
SmallDia	1	0.576
Avg_approach_speed (mph)	1	0.449
Entry_volume(pce/h)	2	0.757
Exiting_volume(pce/h)	2	0.699
Ups App on State Route?	2	0.321
Angle_to_Ups_App	2	0.36
Prob_right_turn	2	0.232
Lane Width (ft)	3	0.706
App on State Route?	3	0.572
No. Cir Lanes Xsing App	3	0.381
The proportion of variation explained by clustering is 0.526		

The researchers used the representative variables in each cluster (based on R^2 values) to construct a third variable set (LR3). Table 11 shows the variables selected for LR3.

Table 11. Third linear regression variables (LR3).

No.	Variable name
1	Width of Splitter Island (ft)
2	Entry_volume(pce/h)
3	Lane Width (ft)

Formulated Linear Regression Models

A total of five linear regression models were evaluated in this study. All models attempt to predict critical gap based on different independent variable formulations. Variable sets LR1, LR2, and LR3 were used along with two more comprehensive variable sets described below to create "best fit" models.

First Linear Regression Model (LR 1)

Model LR 1 was constructed using the 12 LR1 variables to estimate a standard linear least-squares model of the critical gaps (*Gap_time@50*) determined by logistic regression of the gap-acceptance data determined from the drone videos. The overall fit of the model shows an adjusted R-squared (R^2) of 0.62 with a root means square error of 0.67. Table 12 presents the parameter estimates and summary of fit for model LR 1, and Figure 19 presents a plot of actual versus predicted critical gaps for model LR 1.

Table 12. Parameter estimates and summary of fit for model LR 1.

Parameter	Estimate	Std Error	t Ratio	Prob>|t|
Intercept	1.743	0.510	3.41	0.0009
Angle_to_Ups_App	0.0028	0.0034	0.82	0.4132
No. Cir Lanes Xing App	1.016	0.224	4.53	<.0001
Width of Splitter Island (ft)	−0.0225	0.0097	−2.31	0.0227
Lane Width (ft)	0.0130	0.0159	0.82	0.4159
Ups App on State Route?	1.614	0.210	7.69	<.0001
App on State Route?	0.351	0.198	1.77	0.0793
Prob_right_turn	0.2602	0.2895	0.9	0.3704
Entry_volume(pce/h)	0.0014	0.0006	2.33	0.0215
Exiting_volume(pce/h)	−0.0011	0.0005	−2.06	0.0419
Avg_approach_speed (mph)	−0.0611	0.0237	−2.58	0.0109
Op_Years	0.0330	0.0266	1.24	0.2175
SmallDia	0.9522	0.1750	5.44	<.0001
R^2 = 0.6502 Adjusted R^2 = 0.6166 RMSE = 0.6727				

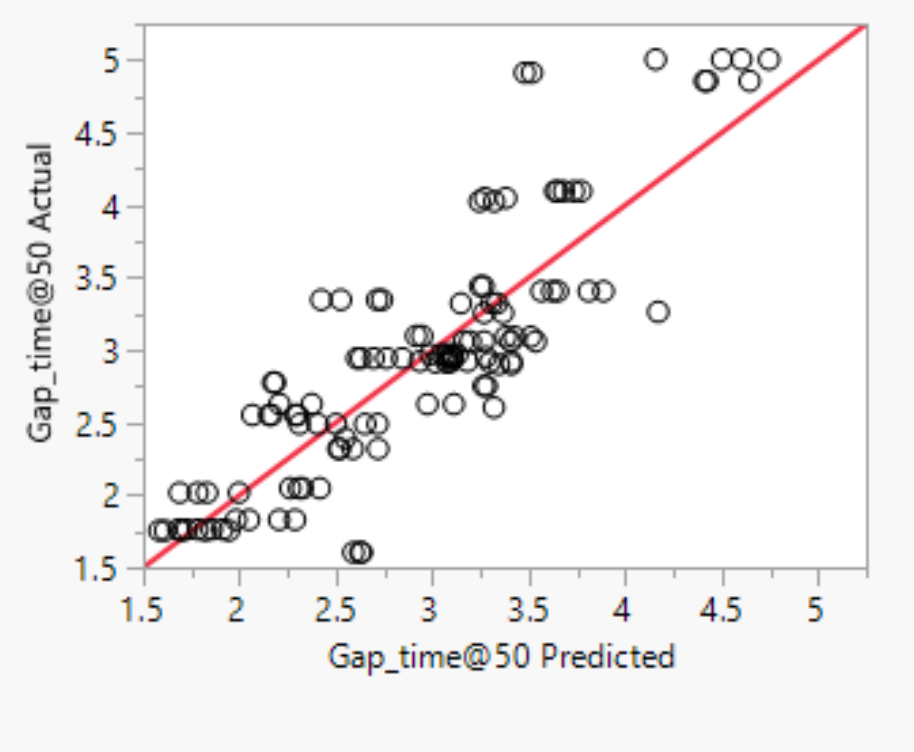

Figure 19. Chart. Actual versus predicted critical gaps for model LR 1.

Second Linear Regression Model (LR 2)

Model LR 2 included all 12 variables used in LR 1; however, unlike LR 1, LR 2 was developed with a stepwise regression, which facilitates searching and selecting the best variables for the least-squares algorithm. Variable inclusion in the model was based on a minimum Bayesian information criterion (BIC). Out of the starting 12 variables, only 4 were retained in this approach. The overall fit of LR 2 shows an adjusted R^2 value of 0.60 with an RMSE of 0.69. Table 13 presents the parameter estimates and summary of the goodness of fit for model LR 2, and Figure 20 presents a plot of actual versus predicted critical gaps for model LR 2.

Table 13 Parameter estimates and summary of fit for model LR 2.

Term	Estimate	Std Error	t Ratio	Prob>|t|
Intercept	2.023	0.376	5.38	<.0001
No. Cir Lanes Xsing App	1.099	0.206	5.34	<.0001
Ups App on State Route?	1.307	0.173	7.57	<.0001
Avg_approach_speed (mph)	−0.0848	0.0207	−4.09	<.0001
SmallDia	1.023	0.151	6.76	<.0001
R^2 = 0.6026 Adjusted R^2 = 0.5907 RMSE = 0.6951				

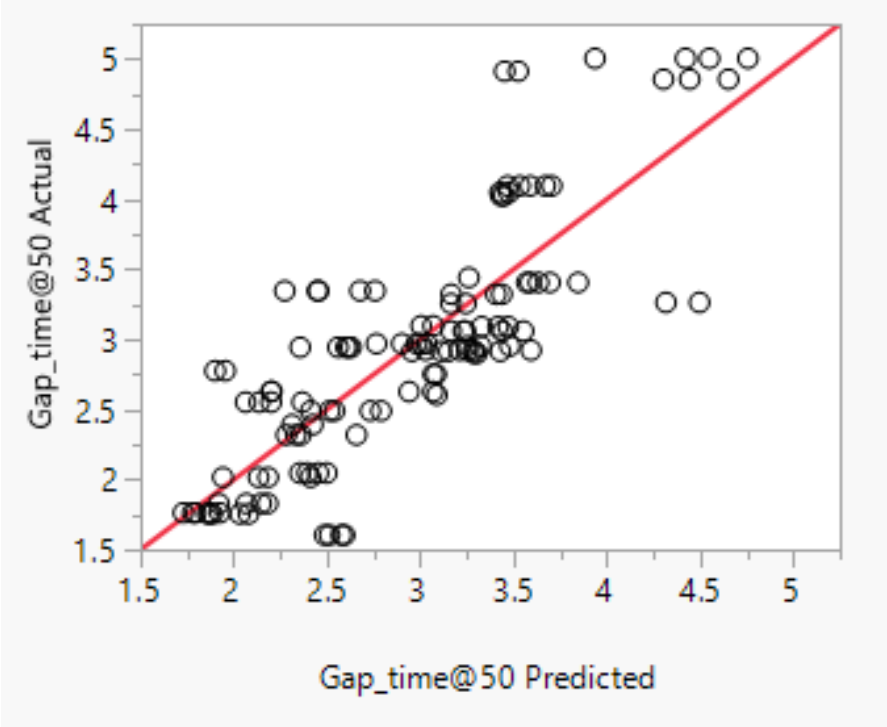

Figure 20. Chart. Actual versus predicted critical gaps for model LR 2.

Third Linear Regression Model (LR 3)

Model LR 3 was constructed with the three representative variables from the clusters. The overall fit of the model shows an adjusted R^2 of 0.0658 with a RMSE of 1.0608. Due to these low predictive values, this model was not considered further.

Fourth Linear Regression Model

The LR4A variable list included 33 of the 38 potential variables. The count variables were omitted in favor of their corresponding volume equivalents and Opening Year was omitted as it was perfectly collinear with the transformed variable Op_year. This model was developed in a stepwise regression, as for model LR 2, and coefficients for nine variables were found to be significant. The overall goodness of fit estimate shows an adjusted R^2 of 0.73 with an RMSE of 0.44. Table 14 presents the summary parameter

estimates and goodness of fit from model LR 4A, and Figure 21 presents a plot of actual versus predicted for model LR 4A

Table 14. Parameter estimates and summary of fit for model LR 4A.

Parameter	Estimate	Std Error	t Ratio	Prob>|t|
Intercept	4.117	0.580	7.1	<.0001
Angle_to_Ups_App	−0.0080	0.0023	−3.45	0.0008
No. Legs of Rndabt	−0.4252	0.0980	−4.34	<.0001
No. Cir Lanes Xsing App	0.9325	0.1410	6.61	<.0001
Ups App on State Route?	0.8951	0.1169	7.66	<.0001
Ped Xing on App	0.2877	0.1288	2.23	0.0275
Avg_approach_speed (mph)	−0.0615	0.0147	−4.18	<.0001
SmallDia	1.075	0.120	8.97	<.0001
LargeDia	0.3295	0.1112	2.96	0.0037
$R^2 = 0.7416$ Adjusted $R^2 = 0.7286$ RMSE = 0.4397				

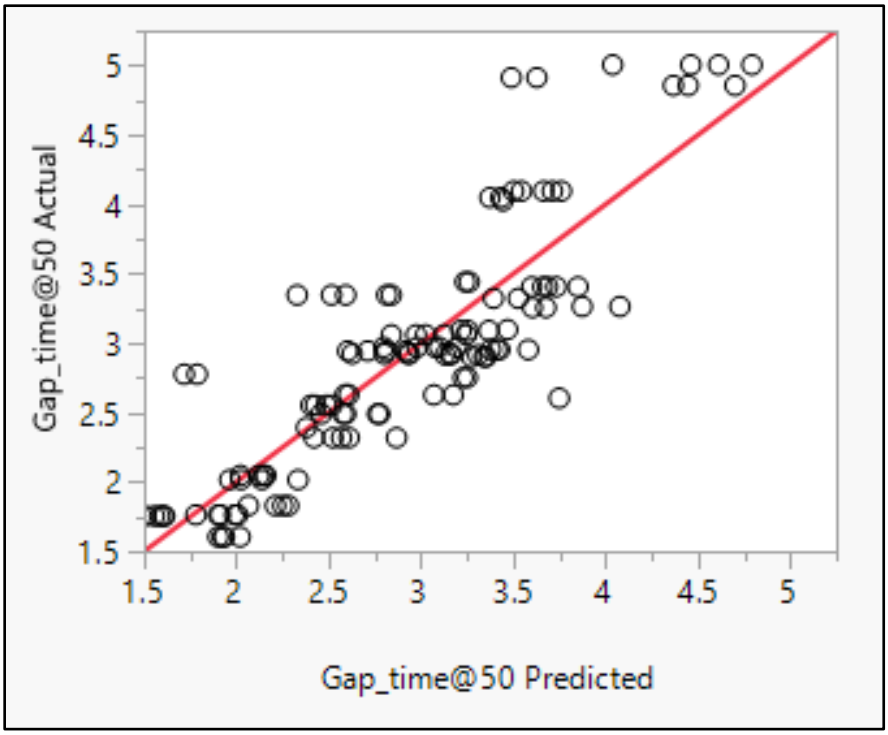

Figure 21. Chart. Actual vs predicted critical gaps for model LR 4A.

Model LR 4A was the best model obtained. However, the definition of the variables can make it inconvenient to interpret the results. Therefore, in order to make the interpretation from the model clearer, the researchers modified the definition of some variables for clarity. These revised definitions are shown in table 15. This final model was called LR 4B. It is essentially the same model as LR 4A (same parameter estimates and goodness of fit estimates) but with a different intercept due to the new variable definitions. Table 16 presents the parameter and goodness of fit estimates for model LR 4B.

Table 15. Modified variable names for model LR 4B.

Variable Name	Modified Variable Name
Angle_to_Ups_App	Angle to Ups App minus 90 degrees
No. Legs of Rndabt	No Legs minus 4
No. Cir Lanes Xsing App	Additional Crossing Lanes at App
Ups App on State Route?	Ups App on State Route?
Ped Xing on App	Ped Xing on App
Avg_approach_speed (mph)	App Speed minus 20
SmallDia	SmallDia
LargeDia	LargeDia

Table 16. Parameter estimates and summary of fit for model LR 4B.

Term	Estimate	Std Error	t Ratio	Prob>|t|
Intercept	1.402	0.165	8.47	<.0001
Angle to Ups App minus 90 degrees	−0.0080	0.0023	−3.45	0.0008
No Legs minus 4	−0.4252	0.0980	−4.34	<.0001
Additional Crossing Lanes at App	0.9325	0.1410	6.61	<.0001
Ups App on State Route?	0.8951	0.1169	7.66	<.0001
Ped Xing on App	0.2877	0.1288	2.23	0.0275
App Speed minus 20	−0.0614	0.0147	−4.18	<.0001
SmallDia	1.075	0.120	8.97	<.0001
LargeDia	0.3295	0.1112	2.96	0.0037
$R^2 = 0.7461$ Adjusted $R^2 = 0.7285$ RMSE = 0.4397				

CAPACITY MODEL SENSITIVITY ANALYSIS

To understand how the parameters identified in the linear regression models of critical headways would impact the estimated capacity of a particular roundabout approach, a derivative-based sensitivity analysis was conducted on the model predictions. To make the linkage between critical headway (and follow-up headway taken to be 0.6 times the observed critical headway) and capacity, a gap distribution for critical headways must be selected. Both the HCM 2010 model and HCM 6 model use the same general form (M1 distribution) to describe the conflicting gap distribution resulting in an estimation of roundabout capacity given by:

$$c = A \cdot \exp(-B \cdot v_c) \tag{26}$$

Where, c is the approach capacity in passenger car equivalents per hour (pce/h); $A = 3600/t_f$, $B = (t_c - 0.5\ t_f)/3600$, where t_c is the critical headway in seconds and t_f is the follow-up headway also in seconds; and v_c is the conflicting flow rate (pce/h).

Since a constant ratio of 0.6 was assumed to exist between the follow-up headways and critical headways in this project, the above equation can be simplified through substituting t_f with $0.6\ t_c$:

$$c = \frac{3600}{t_f} exp[-v_c \frac{(t_c - 0.5\ t_f)}{3600}] = \frac{6000}{t_c} exp(-\frac{0.7 v_c t_c}{3600}) \quad (27)$$

Then, by taking the partial derivative of the model output capacity c with respect to the input variable critical headway t_c, the sensitivity function is obtained:

$$\frac{\partial c}{\partial t_c} = -(\frac{6000}{{t_c}^2} + \frac{7 v_c}{6 t_c}) \cdot exp(-\frac{7 v_c t_c}{36000}) \quad (28)$$

The conflicting flow rate is another input variable in the capacity models, so to account for its potential effects, the model sensitivity was analyzed under three situations with different conflicting flow rates.

- Conflicting flow rate $\mathrm{v_c} = 400$ pce/h

$$\frac{\partial c}{\partial t_c} = -(\frac{6000}{{t_c}^2} + \frac{1400}{3 t_c}) \cdot exp(-\frac{7 t_c}{90}) \quad (29)$$

- Conflicting flow rate $v_c = 800\ pce/h$

$$\frac{\partial c}{\partial t_c} = -(\frac{6000}{{t_c}^2} + \frac{2800}{3t_c}) \cdot exp(-\frac{7t_c}{45}) \quad (30)$$

- Conflicting flow rate $v_c = 1200\ pce/h$

$$\frac{\partial c}{\partial t_c} = -(\frac{6000}{{t_c}^2} + \frac{1400}{t_c}) \cdot exp(-\frac{7t_c}{30}) \quad (31)$$

Assuming the capacity model sensitivity with respect to the critical headways is analyzed at the mean value $\bar{t_c} = 2.75s$, then if the mean critical headway is increased by 0.1 s, the capacity estimated by the HCM model would decrease by 77.76 pce/h, 73.85 pce/h, and 68.56 pce/h, respectively, under the above three flow rate conditions.

CHAPTER 8. DISCUSSION

MODEL RESULTS

The linear regression models explored in this study collectively tested the influence of 33 roundabout variables on driver's gap-acceptance behavior, specifically on the observed value of the logistic "critical gap/critical headway." The results indicate that 21 of the variables had no measurable influence on the observed critical gap time. Of these 21 variables, 16 were never included in any of the tested linear regression model formulations, whereas the 5 variables that were included in any of the model analyses never showed a statistically significant coefficient for predicting Gap_time@50.

Based on the results of the preferred model LR 4B, the intercept suggests that for a certain approach within a 4-legged single-lane roundabout with the inscribed circle diameter between 125 ft and 145 ft, if the upstream of this approach is not on the state route and there is no pedestrian crossing present, then the critical headway of drivers on this approach is expected to be about 1.40 seconds for a 20 mph average approach speed. These conditions will be considered as the "base case" in our discussion. While this critical headway is relatively somewhat lower than the national average, the model indicates that most approaches could be expected to have higher critical headways than this base condition. Likewise, driver behaviors reflected by this critical gap are found to be generally consistent with previous studies.

The eight model parameters in model LR 4B can be classified as geometric, environmental and operation variables. To analyze the importance of each of these

identified variables and understand their impacts on the critical headway, the one-at-a-time (OAT) technique will be used in the following discussions.

GEOMETRIC VARIABLES

The influence of two geometric variables *Angles to the upstream approach* and *Number of roundabout legs* on the critical headways can often be viewed as a combination since they interact with each other. For a three-legged, evenly spaced approach roundabout with the other attributes set to the same as in the base case, the critical headway on the approach is estimated to increase by 0.19 seconds relative to the base value. While for a five-legged, evenly spaced roundabout, the corresponding gap would decrease by 0.28 seconds. While the variable *Number of roundabout legs* alone is not highly correlated with critical headway from the correlation analysis results (0.0013 with a p-value of 0.987), the stepwise linear regression process included this variable largely due to the interactions with the variable *Angles to the upstream approach.* Therefore, focusing on the effects of the variable *Number of roundabout legs* alone may not be a controlling factor in roundabout gap behavior but rather may influence such behavior by impacting the angular separation of the approaches.

Another two geometric variables *SmallDia* and *LargeDia* were defined as a pair of categorical variables to depict roundabout size and to supplement several size related quantitative parameters used in the analysis including the diameter of the inscribed circle, the diameter of the center island, presence of a truck apron, and lane width. The results of

the stepwise regression showed that these categorical variables did a better job of predicting gap-acceptance behavior than any of the quantitative variables.

The regression coefficients for these categorical variables suggest that "medium-sized" roundabouts (i.e., between 125 and 145 ft inscribed circles) produced shorter accepted gaps than either their larger or smaller counterparts. For large roundabouts (>145 ft) the critical headways were indicated to be about one-third of a second longer (0.33 s) than for medium roundabouts. Likewise, for small roundabouts (< 125 ft) the critical headway was found to be more than one second longer (1.07 s) than for their medium counterparts.

Why might this be the case? There are a number of reasonable hypotheses to explain this somewhat counterintuitive result. For example, it is likely that large roundabouts are, in general, more complicated in their geometric and operational characteristics than their smaller counterparts. That is, these roundabouts are large normally due to the incorporation of additional lanes on certain approaches, slip or bypass lanes or other features into their designs and the observed increase in gap-acceptance time may reflect the additional processing time that drivers need to process the surrounding environment.

This hypothesis, of course, would not explain the significant increase in gap-acceptance time (+1.07 s) on smaller roundabouts. One hypothesis for this increase is that gap distance may play a more important role than gap time during drivers' decision-making process for small roundabouts. When dealing with the same circulating rate (degrees/sec), drivers in the minor approach would perceive a much closer gap distance within small roundabouts than for their larger counterparts. This effect might make them inclined to

believe that an equivalent gap time is less safe than for a larger roundabout and thus require a larger gap.

To examine this possibility, the observed relationship between circulating speed and inscribed circle diameter is shown in figure 22, the average speeds of the circulating stream would increase with the inscribed circle diameter.

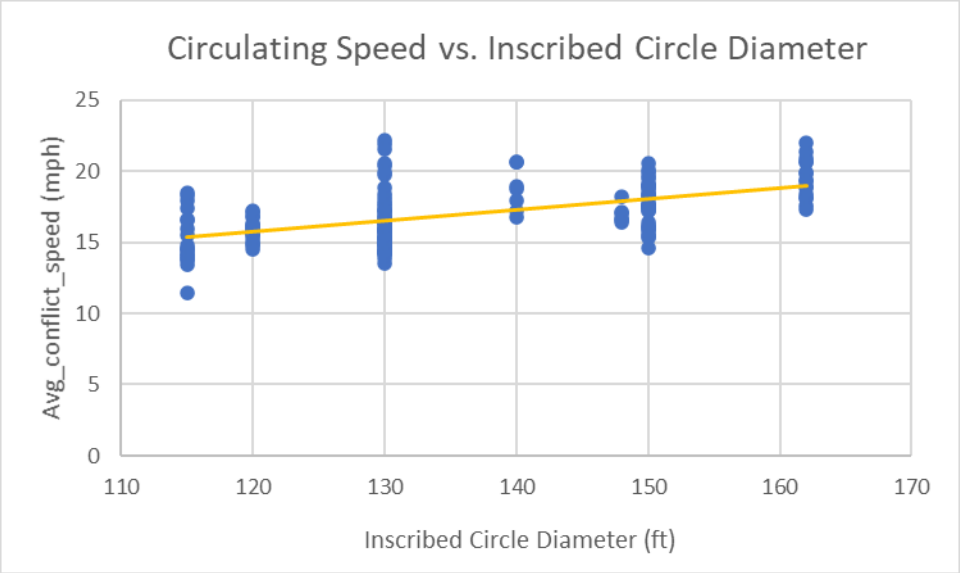

Figure 22. Chart. Observed relationship between inscribed circle diameter and circulating speed.

Based on this trend line, when a driver in the minor approach is faced with the same gap distance, as the circulating speeds in small roundabouts are relatively lower than the large ones, though the differences in speed may not be as direct as in distance, it would eventually take more time for the driver to wait for those conflicting vehicles to arrive at the conflict point, and thus resulting in larger rejected gaps.

This is, of course, not the only possible explanation for these observed differences. For example, the smaller roundabouts in the data are, on average, more than two years older than their larger counterparts. Changes in design policy or increased experience of designers could also result in designs that result in lower accepted gaps in more modern designs. The existing data is not sufficient to choose between these, or other, hypotheses for these differences in gap-acceptance time.

ENVIRONMENTAL VARIABLES

In addition to the geometric factors, the regression model also indicates that for vehicles in the minor approach, having an upstream approach that is a state route has a significant influence on drivers' gap-acceptance behavior. In the reference model (model LR 4B), having the immediate upstream approach as a state route leads to an increase in the observed critical headway by 0.9 s.

None of the roundabouts studied in this project is at the intersection of two state routes, so if the value of variable *Ups App on State Route* is 1, it can be deduced that the analyzed approach is not on the state route. As a result, one can hypothesize that drivers in a minor approach that is crossed by a state route tend to be more cautious and conservative when merging into the circulating stream, as they may expect a heavier traffic volume traveling at higher speeds. Although previous studies have not identified this variable as affecting the critical headway on an approach, its impact is found to be consistent through all the models tested based on the field data collected in this project.

Apart from the influence of a state route on the upstream approach, the variable *Additional circulating lanes* also shows a strong correlation with the critical headway for an approach. As predicated by the model, the addition of an additional circulating lane opposing an approach leads to an increase of 0.93 s in the gap time accepted by drivers in the minor stream. This is not surprising as the additional lane would typically result in more potential conflicting vehicles and more complex driving situations that, similar to the effect suggested for larger roundabouts, would require drivers to expend more time in the gap-acceptance decision process.

Similar to the effects of additional circulating lanes, the placement of pedestrian crosswalks in an approach was found to add an extra 0.29 s to the critical headway for that approach. When arriving vehicles are approaching crosswalks, the drivers are likely to spend additional time scanning for potential pedestrian activities and preparing to yield at any time. These activities require both time and attention from drivers and, thus, might be expected to add to gap-acceptance times.

OPERATIONAL VARIABLES

The only operational variable identified in the model is *Approach speed*. Interpreted from the model coefficient, if the average approaching speed of the minor stream exceeds 20 mph in the base case by 5 mph, then the estimated critical headway would go down by 0.31 s and vice versa for lower speeds. This observation is likely due to the adoption of merging behaviors by local drivers in Atlanta. If the approaching vehicle can perceive and understand the circulation within roundabouts from a distance and decides to take the

gap, then the driver would be able to adjust his or her speed to match with the navigating speeds in advance. This will not only reduce the lost time caused by deceleration and acceleration maneuvers, but also make the driver feel safer to take a smaller gap to merge into the conflicting flow. It should be noted that this observation would likely only apply to approaches with good sight lines and no queuing vehicles present at the approach.

CHAPTER 9. CONCLUSIONS AND RECOMMENDATIONS

PROJECT SUMMARY

This project focused on determining the potential impacts of various geometric and operational parameters on gap-acceptance behavior for approaches to roundabouts in the metro-Atlanta area. These roundabouts were selected to provide a range of different conditions in terms of number of legs, number of circulating lanes, conflicting volumes, presence of pedestrian crossings, etc. The primary data collection method was collection of high-resolution videos shot from a remotely operated drone equipped with video stabilization controls to provide, to the extent possible, a fixed field of view of the roundabout and its approaches from a sufficient altitude (just less than 400 ft) to encompass the complete facility within a single frame.

The resulting videos were processed using commercial machine vision systems supplemented by additional computer-assisted analysis to determine vehicle trajectories, spacings, and potential conflicts on a frame-by-frame basis. These data, in turn, were used to establish gap-acceptance behavior of each roundabout approach and, through the use of logistic regression on the data, to establish critical headways for each approach.

The variation in these observed headways was then modeled against known parameters of both the roundabout and the specific approach to develop a predictive model as to how critical headways and gap-acceptance behavior were impacted by these factors. The major findings of this model were that several factors were observed to have significant impacts on critical headways, including geometric (size category of the roundabout,

number of legs, and visual angle to the upstream approach), environmental (presence of a state route on the upstream approach, presence of additional conflicting lanes, presence of a pedestrian crosswalk on the approach), and operational (approach speeds) factors.

DATA COLLECTION

Despite a variety of early operational problems with the drone and drone camera system that led to significant delays in the data collection phase, the drone data collection would have to be viewed as a major success for the project. The superior field of view and near-nadir camera orientation greatly reduced the required labor, time, and complexity of the data collection and analysis process compared to traditional methods.

While a direct comparison with earlier methods is difficult to make, it is likely that data collection and analysis at a roundabout or a similar intersection for the parameters measured in this study using older methods would cost at least five times as much as the drone approach. ***Given the results from this project, it would be difficult to recommend that fixed near-surface cameras be used for any analytical work that can be achieved with drone systems.*** This recommendation obviously does not apply to continuous monitoring for which fixed-camera systems excel but rather for the short-term types of studies represented by this project.

DATA ANALYSIS

Similar to the conclusions regarding data collection, the rapidity by which the field data could be reduced to usable vehicle trajectories and the sheer volume of information that

could be achieved by the simultaneous tracking of all vehicles in the field of view greatly exceeded that which could be achieved by traditional methods.

Although the need for experienced and qualified data analysts is similar for both the current and more traditional approaches, the time and labor spent on support personnel (e.g., those involved in manual or semi-automated data extraction from videos) is greatly reduced. Perhaps more importantly, ***the data collected by the trajectory analysis approach represents a resource that could be of enormous value in the future. These georeferenced vehicle trajectories represent a resource that can be used in the future to examine how subtle changes in the operations of facilities can occur over extended periods. GDOT should consider standards for the archival of vehicle trajectory data for use in future operational, safety, and evaluation studies.***

GAP ACCEPTANCE AT ROUNDABOUTS

Despite the small number of roundabouts involved in the study (i.e., 12) the resulting data were remarkably consistent and many of the conclusions were significant at a very high statistical level. That, of course, does not imply that these conclusions are universal or that our interpretations of their underlying roots are correct, but they do provide a first glimpse into some important factors.

First, it appears that many of the factors are related to the ***visual complexity*** of the roundabout scene. For example, the presence of a pedestrian crossing in the approach, along with the presence of a second circulating lane conflicting with the approach in a large (>145-ft inscribed circle) roundabout is predicted to add more than 2 seconds to the

critical gap time for a typical driver relative to a 130-ft diameter roundabout with a single circulating lane and no pedestrian accommodations.

Second, some of the variables imply that drivers increase their desired gap-acceptance times when confronted with conditions that they may view as representing ***elevated risk***. For example, the presence of a state route on the upstream approach, a visual angle to that approach of less than 90 degrees, and smaller (<125-ft diameter) roundabouts were all shown to increase critical headway time.

These are, obviously, conclusions based on a limited sample of observations, but they do represent the result of observing driver behavior over a wide range of conditions. ***These results should help designers and planners evaluate how these factors may impact "real world" performance of an individual roundabout rather than using national or Georgia-specific conditions.*** To assist in this effort, a spreadsheet tool for evaluating individual roundabouts has been provided in the supplemental materials for this project.

APPENDIX A. ROUNDABOUTS USED FOR DATA COLLECTION

ROUNDABOUT ID: #1

Road Names: Houze Rd / Hembree Rd
Latitude: 34.06127
Longitude: -84.3462
Opening Year: 2017
No. Legs: 4
Diameter of Central Island (ft): 100
Inscribed Circle Diameter (ft): 150
Presence of Truck Apron: Yes

Approach	Width of Splitter Island (ft)	Lane Width	No. of Lanes on Approach	No. of Circulating Lanes Crossing Approach	Pedestrian Crossing Present?	State Route?	Posted Speed at Entry (mph)	Roundabout Ahead Sign?	Yield Sign?
East	48	25	2	1	Yes	No	25	Yes	Yes
North	40	25	2	2	Yes	Yes	25	Yes	Yes
West	50	25	2	2	Yes	No	25	Yes	Yes
South	47	16	1	2	Yes	Yes	25	Yes	Yes

ROUNDABOUT ID: #2

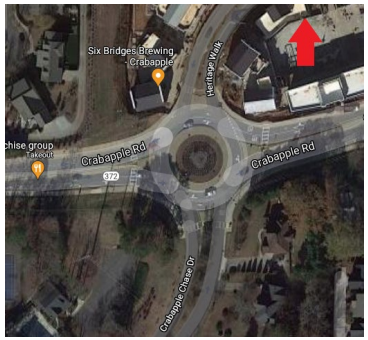

Road Names: Crabapple Rd / Crabapple Chase Dr / Heritage Walk
Latitude: 34.08884
Longitude: -84.3445
Opening Year: 2018
No. Legs: 4
Diameter of Central Island (ft): 110
Inscribed Circle Diameter (ft): 140
Presence of Truck Apron: Yes

Approach	Width of Splitter Island (ft)	Lane Width	No. of Lanes on Approach	No. of Circulating Lanes Crossing Approach	Pedestrian Crossing Present?	State Route?	Posted Speed at Entry (mph)	Roundabout Ahead Sign?	Yield Sign?
East	44	28	2	1	Yes	Yes	25	Yes	Yes
North	42	11	1	2	Yes	No	25	Yes	Yes
West	42	28	2	1	Yes	Yes	25	Yes	Yes
South	33	19	1	2	Yes	No	25	Yes	Yes

ROUNDABOUT ID: #3

Road Names: Hardscrabble Rd / Chaffin Rd
Latitude: 34.06921
Longitude: -84.3739
Opening Year: 2018
No. Legs: 3
Diameter of Central Island (ft): 100
Inscribed Circle Diameter (ft): 130
Presence of Truck Apron: Yes

Approach	Width of Splitter Island (ft)	Lane Width	No. of Lanes on Approach	No. of Circulating Lanes Crossing Approach	Pedestrian Crossing Present?	State Route?	Posted Speed at Entry (mph)	Roundabout Ahead Sign?	Yield Sign?
East	50	12	1	1	Yes	No	25	Yes	Yes
West	47	11	1	1	Yes	No	25	Yes	Yes
South	27	12	1	1	Yes	No	25	Yes	Yes

ROUNDABOUT ID: #4

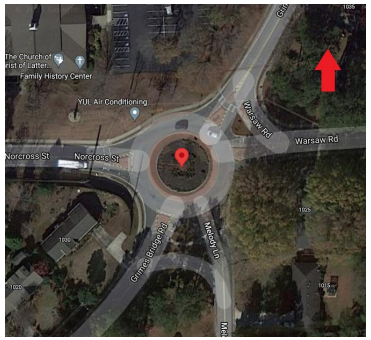

Road Names: Norcross St / Warsaw Rd / Grimes Bridge Rd / Melody Ln
Latitude: 34.02621
Longitude: -84.3447
Opening Year: 2011
No. Legs: 5
Diameter of Central Island (ft): 90
Inscribed Circle Diameter (ft): 130
Presence of Truck Apron: Yes

Approach	Width of Splitter Island (ft)	Lane Width	No. of Lanes on Approach	No. of Circulating Lanes Crossing Approach	Pedestrian Crossing Present?	State Route?	Posted Speed at Entry (mph)	Roundabout Ahead Sign?	Yield Sign?
East	24	11	1	1	Yes	No	15	Yes	Yes
North	24	11	1	1	Yes	No	15	Yes	Yes
West	26	11	1	1	Yes	No	15	Yes	Yes
Southeast	24	11	1	1	Yes	No	15	Yes	Yes
South	25	11	1	1	Yes	No	15	Yes	Yes

ROUNDABOUT ID: #5

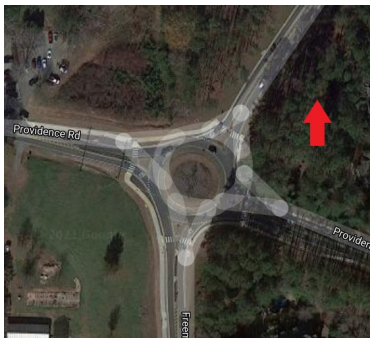

Road Names: Providence Rd / Freemanville Rd
Latitude: 34.11962
Longitude: -84.3301
Opening Year: 2019
No. Legs: 4
Diameter of Central Island (ft): 115
Inscribed Circle Diameter (ft): 150
Presence of Truck Apron: Yes

Approach	Width of Splitter Island (ft)	Lane Width	No. of Lanes on Approach	No. of Circulating Lanes Crossing Approach	Pedestrian Crossing Present?	State Route?	Posted Speed at Entry (mph)	Roundabout Ahead Sign?	Yield Sign?
East	33	12	1	1	Yes	No	25	Yes	Yes
North	33	12	1	1	Yes	No	25	Yes	Yes
West	39	12	1	1	Yes	No	25	Yes	Yes
South	40	12	1	1	Yes	No	25	Yes	Yes

ROUNDABOUT ID: #7

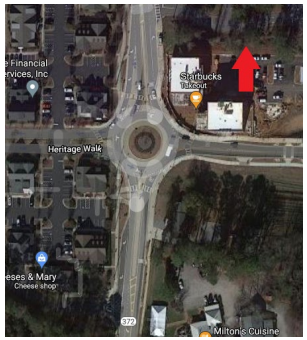

Road Names: Heritage Walk / SR 372
Latitude: 34.0918
Longitude: -84.3395
Opening Year: 2018
No. Legs: 4
Diameter of Central Island (ft): 100
Inscribed Circle Diameter (ft): 130
Presence of Truck Apron: Yes

Approach	Width of Splitter Island (ft)	Lane Width	No. of Lanes on Approach	No. of Circulating Lanes Crossing Approach	Pedestrian Crossing Present?	State Route?	Posted Speed at Entry (mph)	Roundabout Ahead Sign?	Yield Sign?
East	28	12	1	1	Yes	No	25	Yes	Yes
North	32	13	1	1	Yes	Yes	25	Yes	Yes
West	34	14	1	1	Yes	No	25	Yes	Yes
South	32	12	1	1	Yes	Yes	25	Yes	Yes

ROUNDABOUT ID: #8

Road Names: New Providence Rd / SR 372 / Providence Rd
Latitude: 34.11946
Longitude: -84.3425
Opening Year: 2015
No. Legs: 4
Diameter of Central Island (ft): 124
Inscribed Circle Diameter (ft): 162
Presence of Truck Apron: Yes

Approach	Width of Splitter Island (ft)	Lane Width	No. of Lanes on Approach	No. of Circulating Lanes Crossing Approach	Pedestrian Crossing Present?	State Route?	Posted Speed at Entry (mph)	Roundabout Ahead Sign?	Yield Sign?
East	44	14	1	1	Yes	No	25	Yes	Yes
North	39	31	2	1	Yes	Yes	25	Yes	Yes
West	36	16	1	2	Yes	No	25	Yes	Yes
South	62	11	1	1	Yes	Yes	25	Yes	Yes

ROUNDABOUT ID: #9

Road Names: Hopewell Rd / Cogburn Rd / Francis Rd
Latitude: 34.13777
Longitude: -84.2845
Opening Year: 2015
No. Legs: 4
Diameter of Central Island (ft): 83
Inscribed Circle Diameter (ft): 120
Presence of Truck Apron: Yes

Approach	Width of Splitter Island (ft)	Lane Width	No. of Lanes on Approach	No. of Circulating Lanes Crossing Approach	Pedestrian Crossing Present?	State Route?	Posted Speed at Entry (mph)	Roundabout Ahead Sign?	Yield Sign?
East	27	12	1	1	Yes	No	25	Yes	Yes
North	24	12	1	1	Yes	No	25	Yes	Yes
West	39	11	1	1	Yes	No	25	Yes	Yes
South	27	11	1	1	Yes	No	25	Yes	Yes

ROUNDABOUT ID: #14

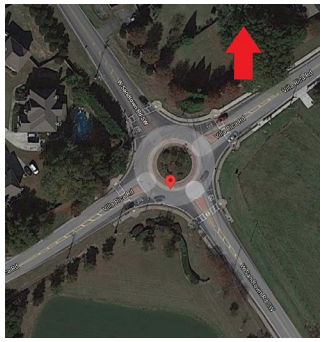

Road Names: Villa Rica Rd / W Sandtown Rd SW
Latitude: 33.92694
Longitude: -84.6378
Opening Year: 2009
No. Legs: 4
Diameter of Central Island (ft): 77
Inscribed Circle Diameter (ft): 115
Presence of Truck Apron: Yes

Approach	Width of Splitter Island (ft)	Lane Width	No. of Lanes	No. of Circulating Lanes Crossing Approach	Pedestrian Crossing Present?	State Route?	Posted Speed at Entry (mph)	Roundabout Ahead Sign?	Yield Sign?
East	21	13	1	1	Yes	No	15	Yes	Yes
North	21	12	1	1	Yes	No	15	Yes	Yes
West	23	12	1	1	Yes	No	15	Yes	Yes
South	23	13	1	1	Yes	No	15	Yes	Yes

ROUNDABOUT ID: #15

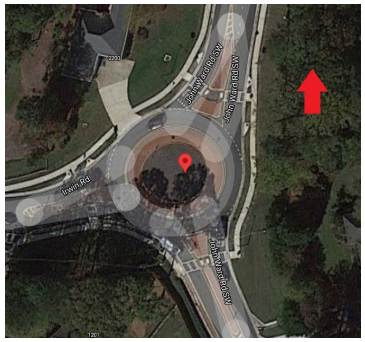

Road Names: Irwin Rd / John Ward Rd SW
Latitude: 33.91969
Longitude: -84.6201
Opening Year: 2018
No. Legs: 3
Diameter of Central Island (ft): 93
Inscribed Circle Diameter (ft): 115
Presence of Truck Apron: Yes

Approach	Width of Splitter Island (ft)	Lane Width	No. of Lanes on Approach	No. of Circulating Lanes Crossing Approach	Pedestrian Crossing Present?	State Route?	Posted Speed at Entry (mph)	Roundabout Ahead Sign?	Yield Sign?
North	36	14	1	1	Yes	No	20	Yes	Yes
West	32	14	1	1	Yes	No	20	Yes	Yes
South	31	13	1	1	Yes	No	20	Yes	Yes

ROUNDABOUT ID: #16

Road Names: John Ward Rd SW / Cheatham Hill Rd
Latitude: 33.93735
Longitude: -84.6063
Opening Year: 2016
No. Legs: 3
Diameter of Central Island (ft): 118
Inscribed Circle Diameter (ft): 148
Presence of Truck Apron: Yes

Approach	Width of Splitter Island (ft)	Lane Width	No. of Lanes on Approach	No. of Circulating Lanes Crossing Approach	Pedestrian Crossing Present?	State Route?	Posted Speed at Entry (mph)	Roundabout Ahead Sign?	Yield Sign?
North	27	14	1	1	Yes	No	15	Yes	Yes
West	26	15	1	1	Yes	No	15	Yes	Yes
South	33	14	1	1	Yes	No	15	Yes	Yes

ROUNDABOUT ID: #17

Road Names: Oxford Rd NE / N Decatur Rd / Dowman Dr
Latitude: 33.78833
Longitude: -84.3258
Opening Year: 2011
No. Legs: 4* (northernmost leg is currently blocked)
Diameter of Central Island (ft): 84
Inscribed Circle Diameter (ft): 115
Presence of Truck Apron: Yes

Approach	Width of Splitter Island (ft)	Lane Width	No. of Lanes on Approach	No. of Circulating Lanes Crossing Approach	Pedestrian Crossing Present?	State Route?	Posted Speed at Entry (mph)	Roundabout Ahead Sign?	Yield Sign?
East	14	11	1	1	Yes	No	15	No	Yes
North	12	14	1	1	Yes	No	15	Yes	Yes
West	15	11	1	1	Yes	No	15	Yes	Yes
South	12	11	1	1	Yes	No	15	Yes	Yes

APPENDIX B. DRONE VIDEO STANDARD OPERATING PROCEDURE

The following standard operating procedures were used by the data collection team for video data collection.

Before Departure to the Field

- Ensure that there is no event near the roundabout location that will generate large crowds because drones must not be flown over a large crowd.
- Check for Notice to Airmen (NOTAM) for the vicinity of the roundabout and local weather forecast. Field trips should proceed only if no rain is forecast, temperatures are in the range of −4 to 104°F and wind speeds do not exceed 15 MPH. For best results, wind speeds should not exceed 8 MPH.
- Check the FAA's B4UFLYapp to ensure that the planned location is not in a restricted air space or has not been designated as a temporary no fly zone.
- Ensure that all batteries for the remote controller and the Intelligent Flight Batteries are fully charged.
- Ensure that no member of the team is under the influence of alcohol or drugs.
- Any team member who is fatigued or impacted by emotional or psychological stress must not go into the field.
- Ensure the DJI GO 4 app or DJI GS PRO app and the aircraft's firmware have been upgraded to the latest version.
- Ensure that the gimbal is detached from the drone during travel to and from the site.

Preflight

- Ensure that all propellers are in good condition and securely tightened.
- Rotate each propeller to ensure that it moves freely without touching any part of the drone.
- Check to ensure that the gimbal can rotate freely before powering it on.
- Ensure that the lens cover is off, and the lens is clean and free of stains.

- Ensure that the memory card has at least 10 GB of available data space (when using 1920 × 1080p Resolution).
- Ensure that the camera settings match specifications for flight. The standard specifications are:

Standard Zenmuse X5S Specifications for Roundabout Video Recording	
Parameters	**Labeled Settings**
Camera Mode	Auto (400 ft)
Resolution	1920 × 1080p
Exposure Value	+ 0.5
ISO Setting	300
White Balance	Default
Auto Focus	Enabled
Shooting Mode	Single Shot (enabled)
Shutter Speed	Auto
Aperture	Auto
Color Mode	Color (RGB)
Video Card	64GB minimum

- All field personnel must stay clear of the rotating propellers. The aircraft must only be touched by hand while the power is off.
- Observe the surroundings and develop an emergency landing plan in case drone cannot be returned to the takeoff point.
- Ensure that the drone's takeoff and landing positions are clear of overhead power lines and/or tree branches.
- Ensure that Wi-Fi on any mobile device is turned off to avoid causing interference to the remote controller.

During Flight

- Drone's altitude should never be allowed to exceed 400 ft AGL.
- Drone's altitude should be in the range of 390 ± 5 ft.
- Drone should be flown such that it hovers directly above the central island as much as possible.

- In case of a necessary emergency landing or loss of power that causes a free-fall crash of the drone, ***do not attempt to catch the drone. The rotating propellers can cause significant body harm*.**
- The pilot and observer(s) must maintain visual line of sight to the drone at all times.
- The pilot must not answer any incoming phone calls or use the features of their mobile device while controlling the drone.
- In the instance of low battery warning or dangerous wind speed warning, land the drone immediately at a safe location.
- Do not remove the micro SD card while the drone is powered on.

Post Flight

- The aircraft must only be picked up while the power is off.
- Detach the gimbal from the drone and put both in secure travel mode before departing to base or to another measurement location.
- Do not connect the aircraft system to any USB interface that is older than version 2.0.
- Download the recorded videos from the SD card onto an external storage device or laptop.

APPENDIX C. OBSERVED GAP TIMES AT THE ROUNDABOUTS

ROUNDABOUT ID: #1

Hembree Road/Houze Road

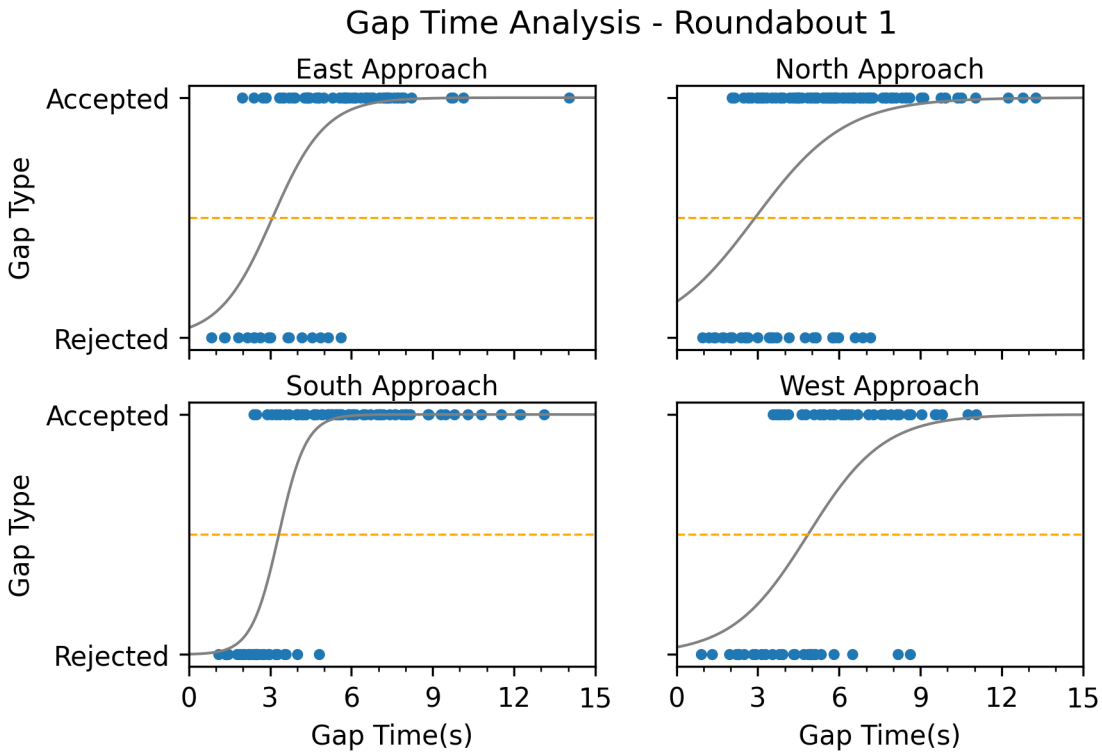

ROUNDABOUT ID: #2

Crabapple Road/Crabapple Chase Drive

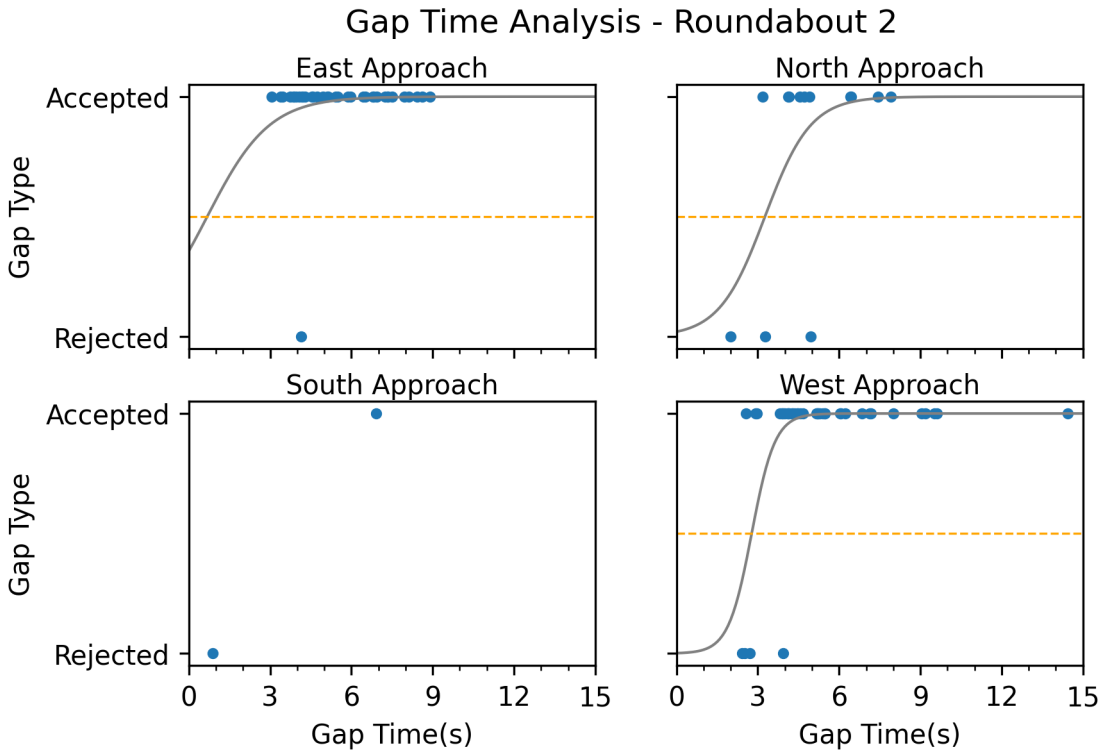

ROUNDABOUT ID: #3

Hardscrabble Road/Chaffin Road

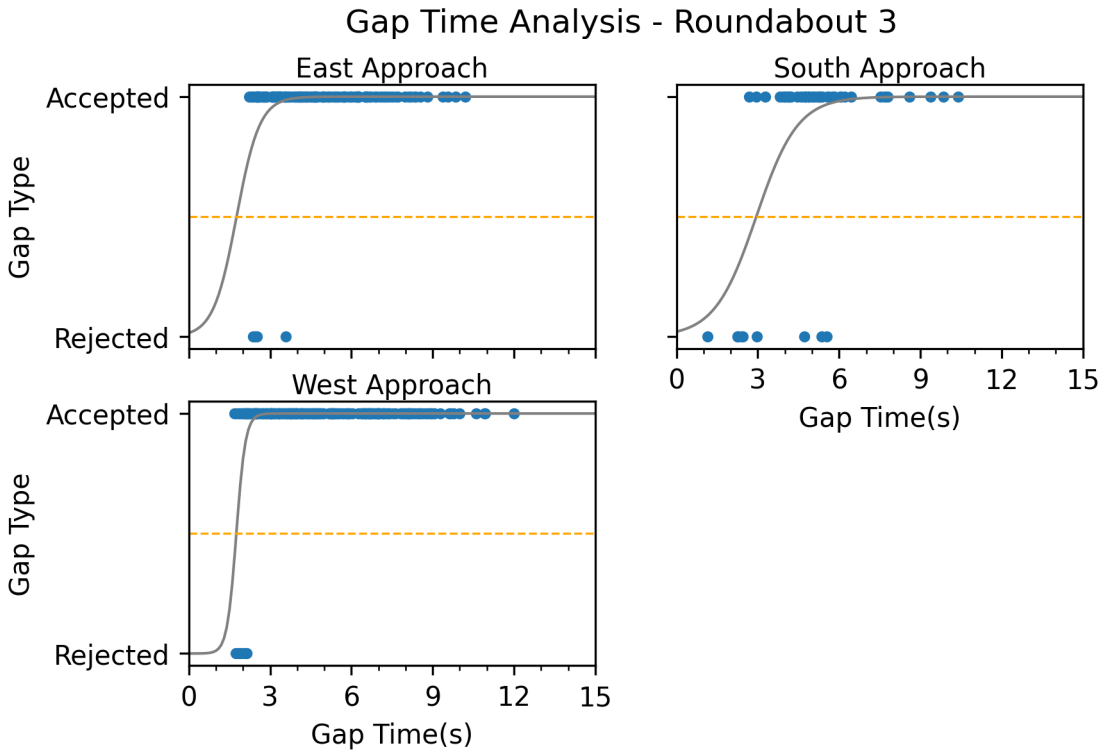

ROUNDABOUT ID: #4

Norcross Street/Warsaw Road/Grimes Bridge Road/ Melody Lane

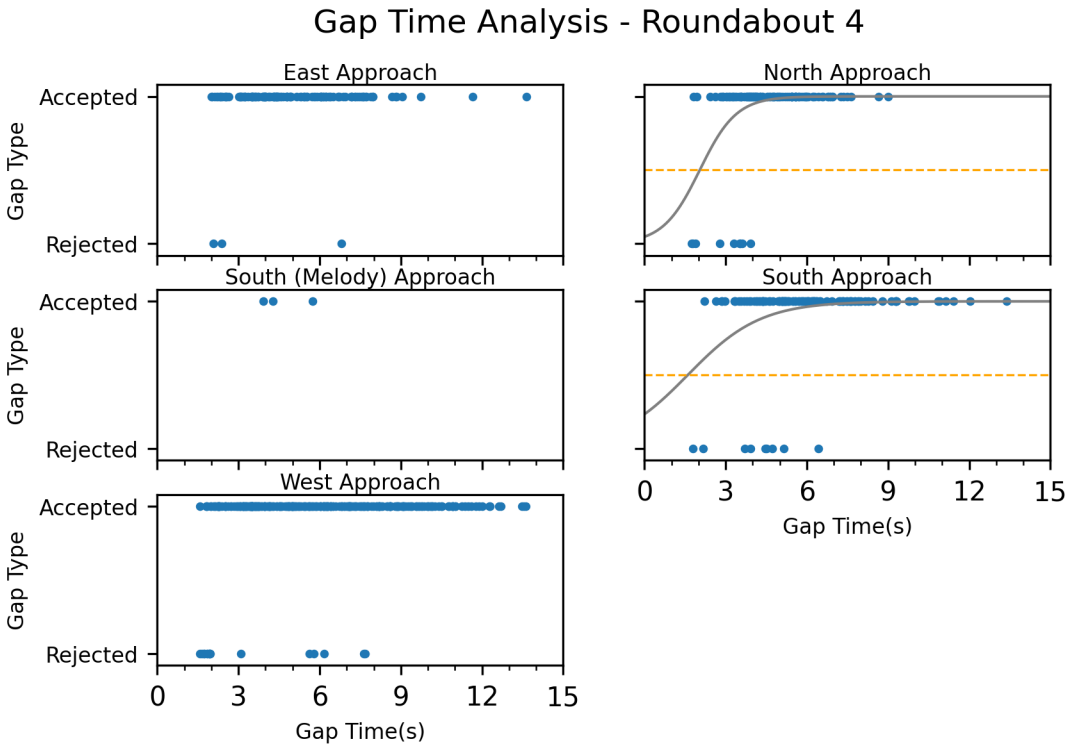

ROUNDABOUT ID: #5

Providence Road/Freemanville Road

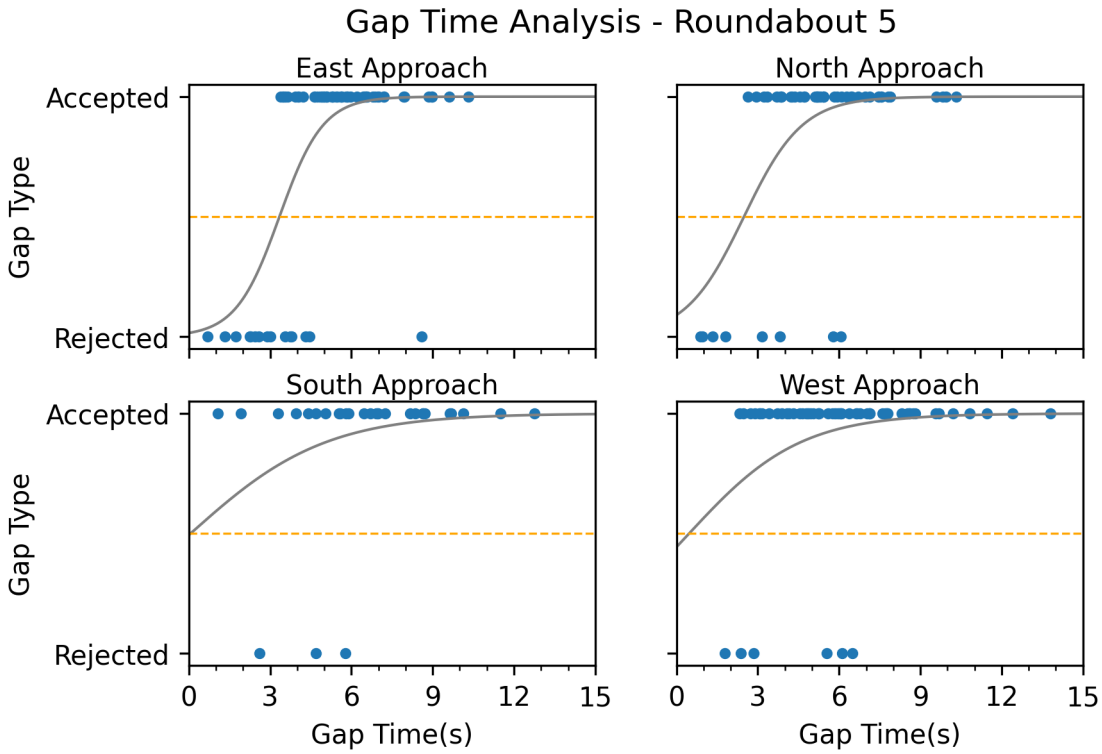

ROUNDABOUT ID: #7

Heritage Walk/SR 372

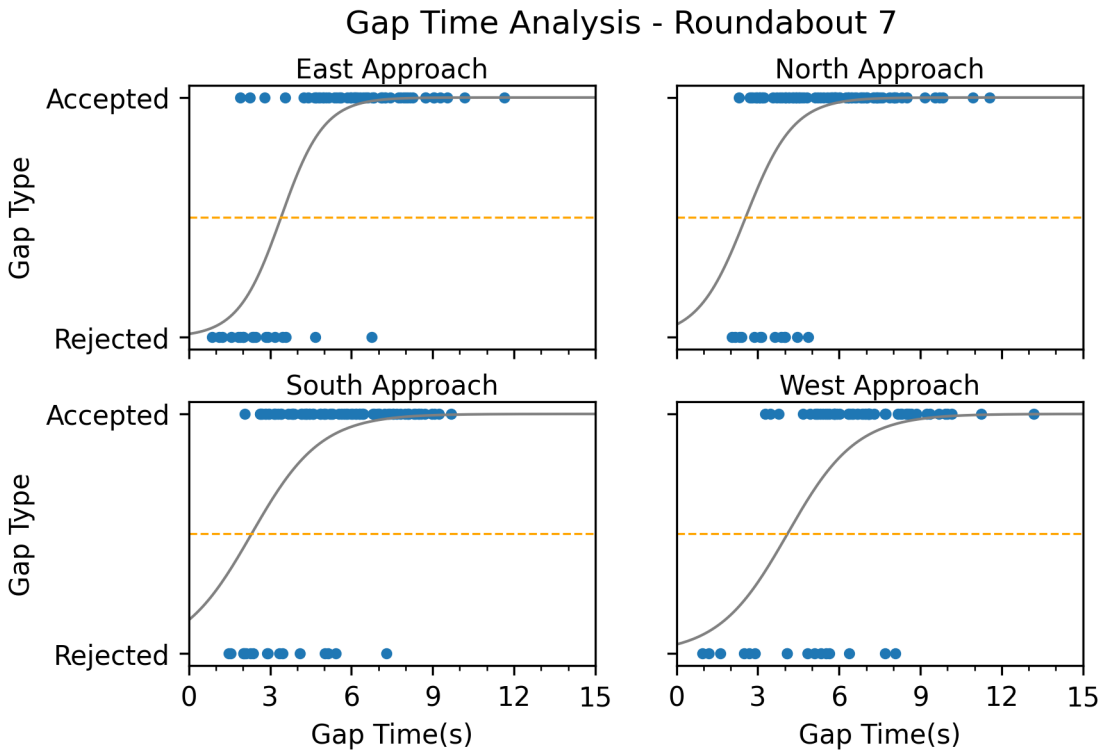

ROUNDABOUT ID: #8

New Providence Road/SR 372

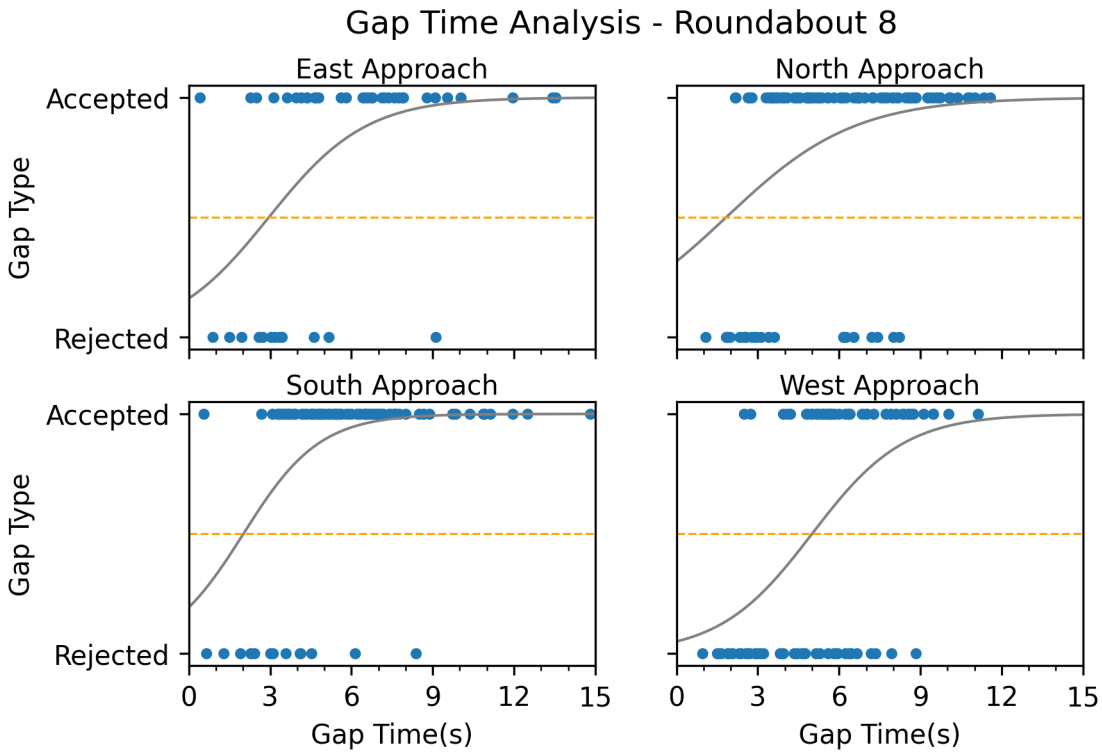

ROUNDABOUT ID: #9

Hopewell Road/Columbia Road/Francis Road

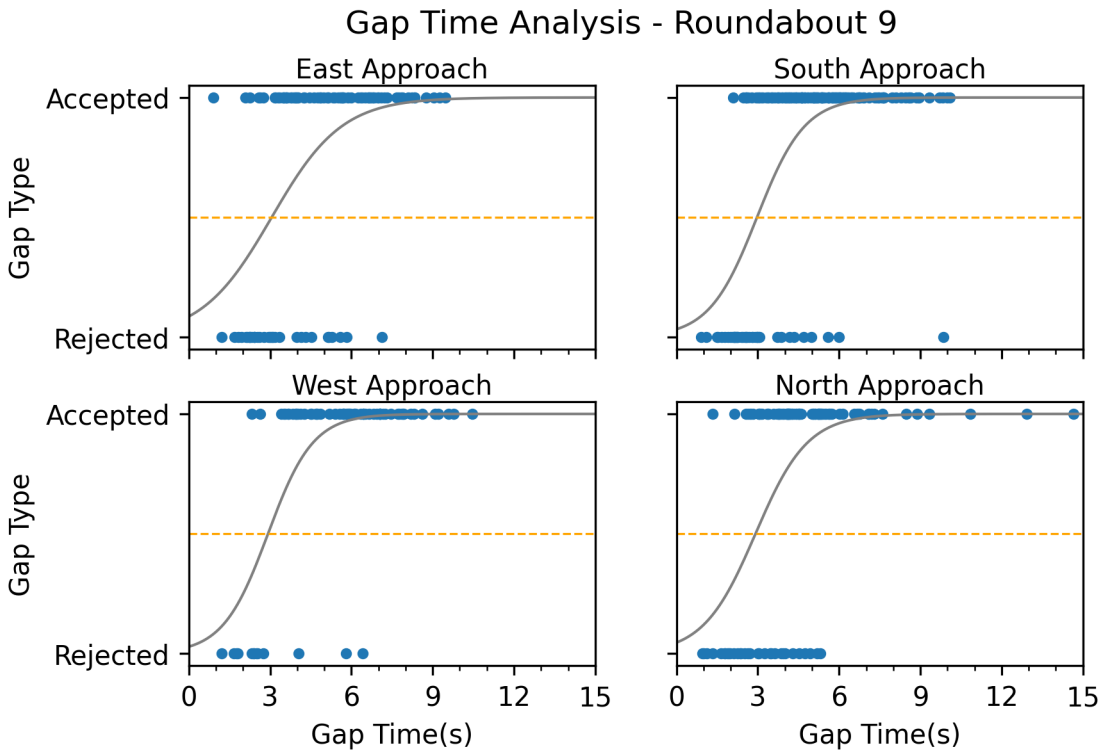

ROUNDABOUT ID: #14

Villa Rica Road/West Sandtown Road SW

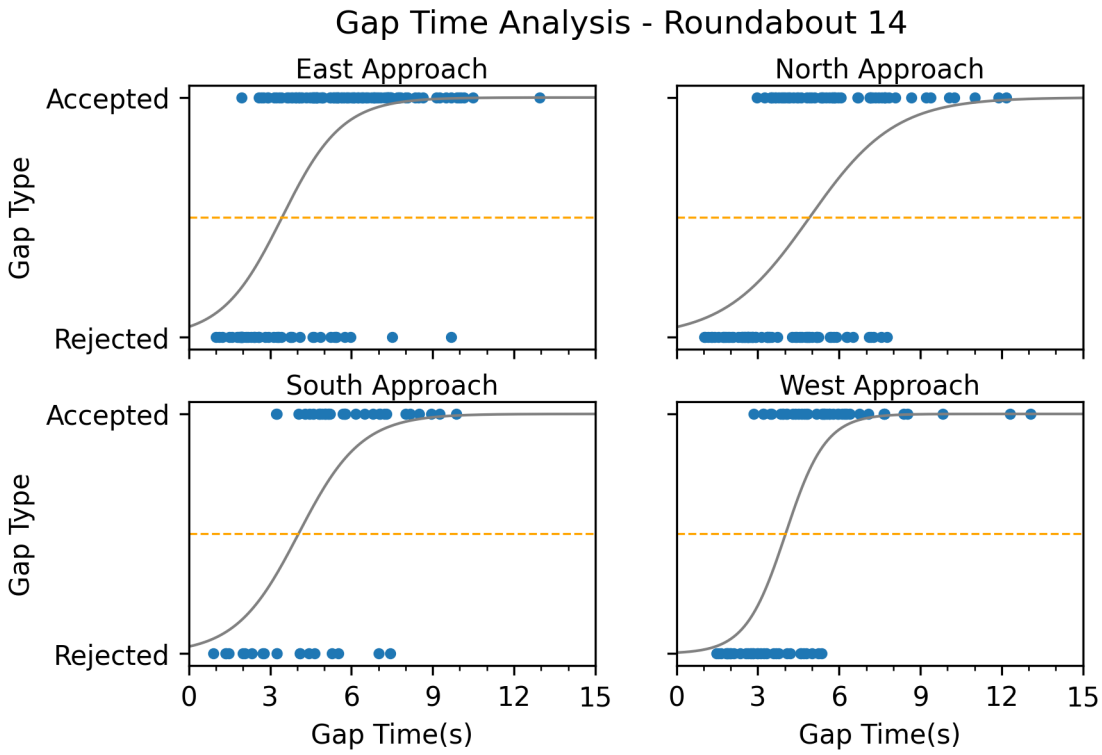

ROUNDABOUT ID: #15

Irwin Road/John Ward Road SW

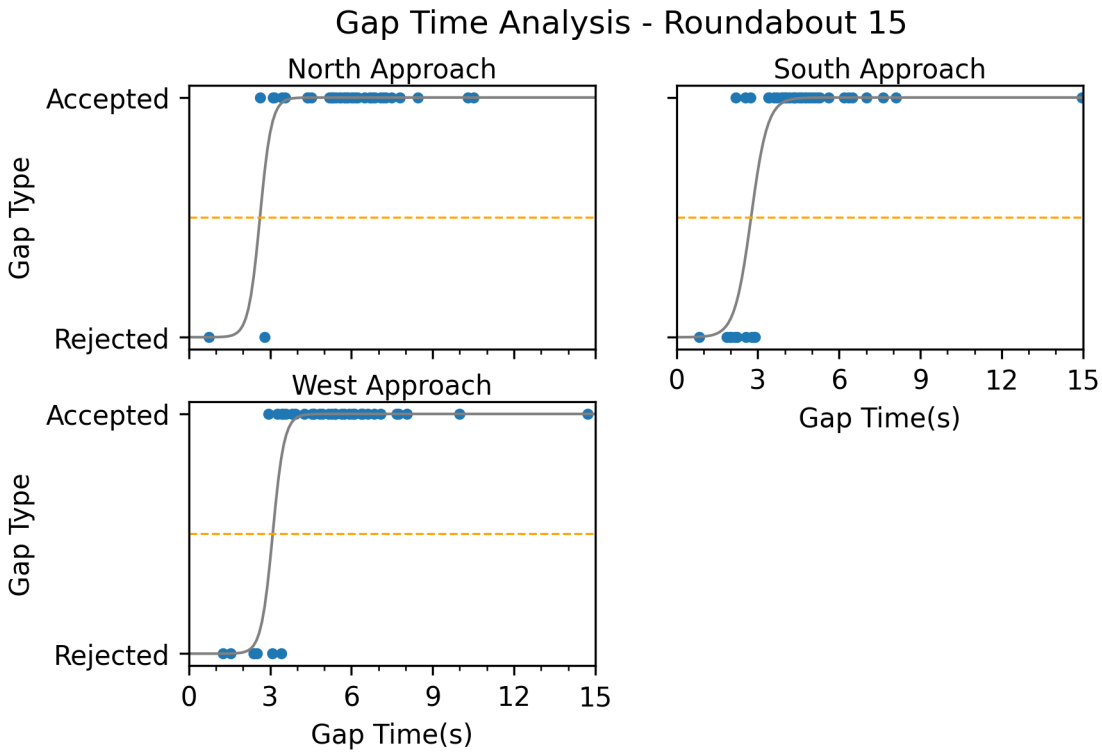

ROUNDABOUT ID: #16

John Ward Road SW/Cheatham Hill Road

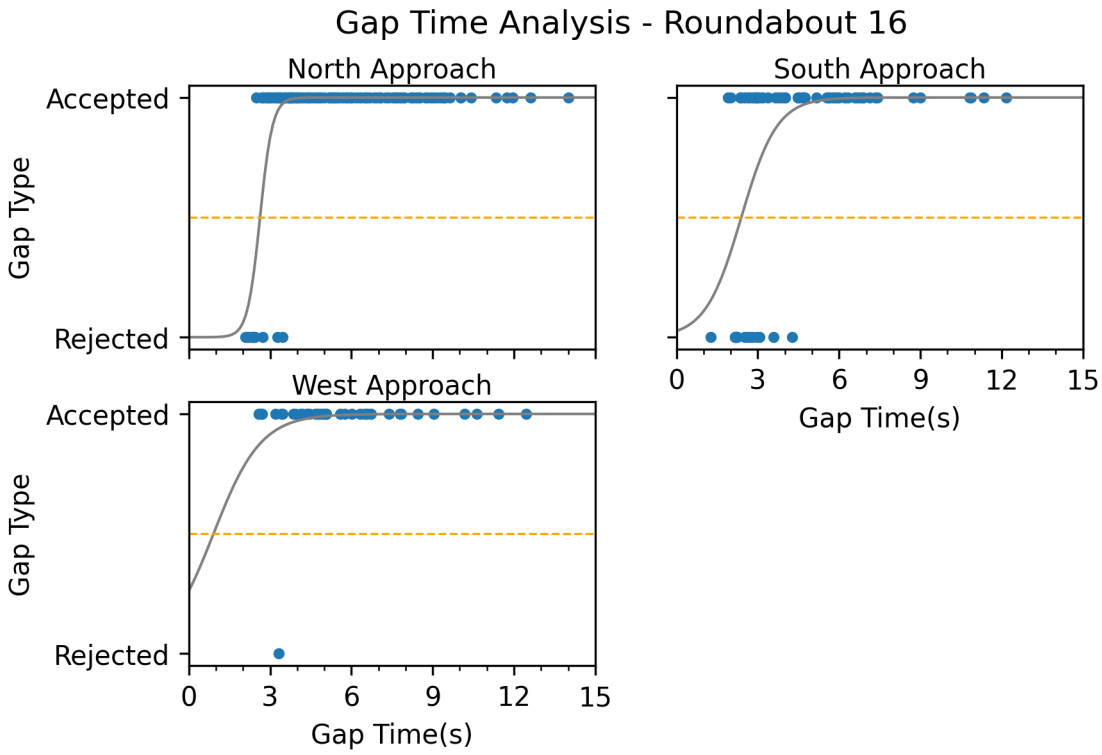

ROUNDABOUT ID: #17

Oxford Road NE/North Decatur Road

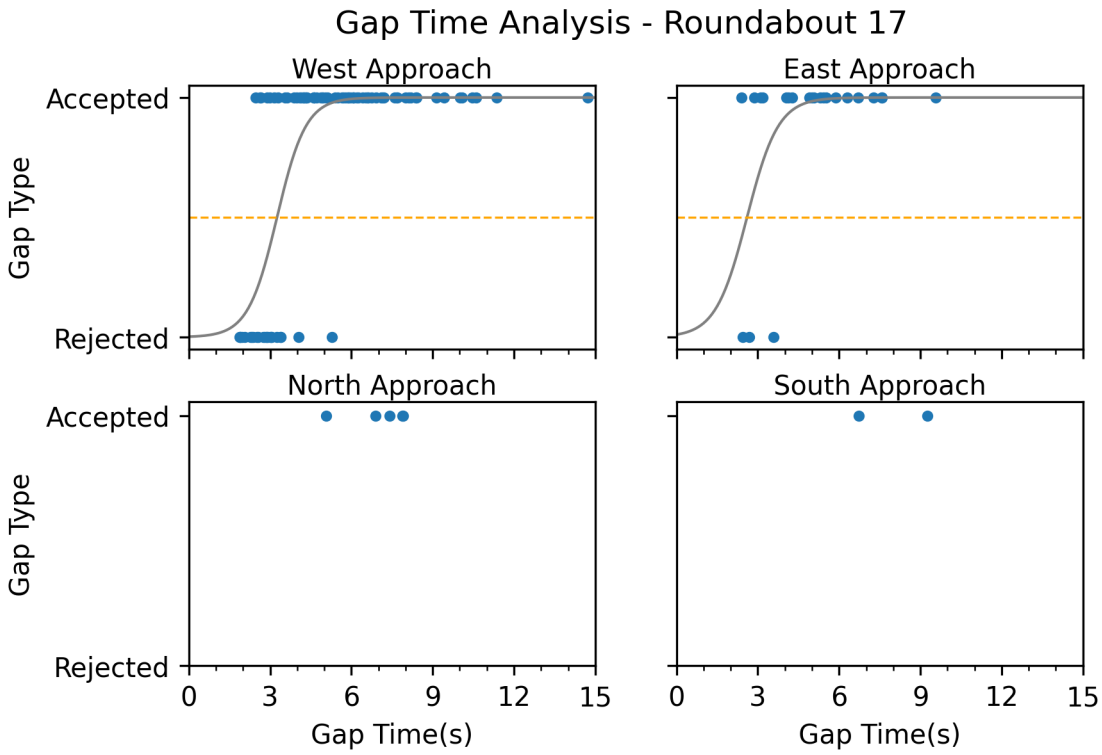

APPENDIX D DATABASE FILE WITH VARIABLE DICTIONARY

The complete electronic database file is provided as an electronic supplement to this report. The data dictionary for the variables within this database are provided in this appendix.

GDOT Research Project No. 18-25
FACTORS INFLUENCING ROUNDABOUT PERFORMANCE

DATABASE ON ROUNDABOUTS INCLUDED IN THE STUDY

This data dictionary provides the meaning of variables included in the datafile for the project roundabouts

Variable Name	Meaning
Roundabout_ID	A unique number assigned to each roundabout as a unique identifier
Lat	Latitude coordinate of the roundabout center given in decimal degrees format
Lon	Longitude coordinate of the roundabout center given in decimal degree format
No. Legs of Rndabt	The total number of legs (approaches) of a roundabout
Dia of Central Island. (ft)	Diameter of the roundabout's central island in feet
No_Lanes	Number of marked lanes on a roundabout approach
Road Names	The names of roads intersecting at the roundabout
Date	The date of video collection with the drone
Flight #	A number of value 1 or 2 used to indicate the first and second flights at a roundabout location. A value of 1 means that estimated data on that row of the metadata was obtained from video 1
Video_ID_text	An alpha-numeric identifier for every video file
Video_ID_Num	A numeric identifier for every video file

Approach	An assigned direction name for the roundabout leg. The direction value is usually East, North, West, or South. In cases where a pair of legs all seem to fall into one of these directions, the road names can be appended to distinguish between the two
Opening Year	The year the roundabout was opened to traffic
Visual Angle to Ups App.	The angle through which a driver's line of sight will have to turn counterclockwise at the yield line in order to see a vehicle on the yield line of the upstream approach
No. Cir Lanes Xsing App	The number of circulating lanes immediately left of an approach
inscribed Cir Dia. (ft)	Diameter of the roundabout's inscribed circle in feet
Width of Splitter Island (ft)	The width of the splitter island on an approach in feet
Lane Width (ft)	Width of the lane on an approach just before the flare point
Presence of Left Offset on App?	A binary value (Yes or No) used to indicate the presence of a left offset on an approach
Presence of Truck Apron?	A binary value (Yes or No) used to indicate the presence of a truck apron
Ups App on State Route?	A binary value (Yes or No) used to indicate if the upstream approach is on a state route
App on State Route?	A binary value (Yes or No) used to indicate if an approach is on a state route
Posted Speed at Entry on App	The value of the posted speed limit for entry into the roundabout
Rabt Ahead Sign?	A binary value (Yes or No) used to indicate the presence of a roundabout ahead warning sign upstream on an approach
Presence of Yield	A binary value (Yes or No) used to indicate the presence of a yield sign near the roundabout entrance on an approach
Ped Xing on App	A binary value (Yes or No) used to indicate the presence of a pedestrian crossing on an approach
Ped Xing on Ups App	A binary value (Yes or No) used to indicate the presence of a pedestrian crossing on the upstream approach
Prob_right_turn	An estimate of the probability that a vehicle will make a right turn from an approach
Entry_count	Total number of vehicles that entered the roundabout from an approach during the data recording period
Entry_volume(pce/h)	An hourly estimate of the total number of entering vehicles from an approach during data collection period. This estimate is made after accounting for the passenger car equivalence of heavy vehicles and buses
Circulating_count	Total number of vehicles entering the roundabout that did not make a right turn from the approach during the data collection period. These vehicles entered the circulating lane
Circulating_volume(pce/h)	An hourly estimate of the total number of circulating vehicles during the data collection period. This estimate is made after accounting for the passenger car equivalence of heavy vehicles and buses
Exiting_count	Total number of vehicles exiting the roundabout at an approach

Exiting_volume(pce/h)	An hourly estimate of the total number of exiting vehicles at an approach during the data collection period. This estimate is made after adjusting for passenger car equivalence of heavy vehicles and buses
Exiting_prob	An estimate of the probability that a conflicting vehicle will exit at an approach
Video_length (msec)	Duration of video in milliseconds
Video_length (h)	Duration of video in hours
Avg_approach_speed (mph)	Average speed of vehicles on an approach in miles per hour
Avg_conflict_speed (mph)	Average speed of vehicles in the circulating lanes in miles per hour
Heavy_vehicle_count	Total number of heavy vehicles entering the roundabout during the data collection period
Bus_count	Total number of buses entering the roundabout during the data collection period
Total_vehicle_count	Total number of vehicles that entered the roundabout during the data collection period
Total_vehicle_volume(pce/h)	An hourly estimate of the total number of vehicles entering the roundabout during the data collection period. This estimate is made after adjusting for passenger car equivalence of heavy vehicles and buses
Med_and_small	Total number of vehicles other than buses and heavy vehicles that entered the roundabout during the data collection period
Heavy_vehicle_percentage	Percentage of heavy vehicles that entered the roundabout during the data collection period
Bus_percentage	Percentage of buses that entered the roundabout during the data collection period
Intercept	Estimated intercept of the logistic curve fitting the rejected and accepted gaps at an approach
Coefficient	Estimated coefficient of the logistic curve fitting the rejected and accepted gaps at an approach
Gap_time@50	An estimate of the gap coinciding with the 50th percentile on the logistic curve
No. of datapoints	Total number of data points used to estimate Gap_time@50 for the approach
Entry_Angle	The designed entry angle for an approach. It is the angle between the approach and the circular path at the entry point
Angle_to_Ups_App	This is the angle between the approach and the upstream approach. This is also a geometric design variable

APPENDIX E. GAP EXTRACTION ALGORITHM – PYTHON SCRIPT

The script is attached in the open document text below. To view the script, simply double-click on the following text. It is also available in the electronic supplements.

```
# New Providence Rd SR 372 DJI 0036 East approach
# Changes needed: initialize_setting()-bypass gate, get_distance_circular, get_distance_adjacent

import numpy as np
import pandas as pd
import math
import geopy.distance
from collections import defaultdict
from Trajectories import Trajectory

#Read the gate crossing, action region alert event and trajectories data file and create the corresponding dataframe
extract = pd.read_excel (r'.\Gap_extraction - New Providence Rd SR 372 DJI
0036.xlsx', sheet_name= r'East Approach')
gatecross = pd.read_csv(r'.\Gatecrossing - New Providence Rd SR 372 DJI 0036 East
Approach.csv')
traject = pd.read_csv(r'.\Trajectories - New Providence Rd SR 372 DJI 0036 East Ap-
proach.csv')
actions = pd.read_csv(r'.\Actionregion - New Providence Rd SR 372 DJI 0036 East Ap-
proach.csv')
action = actions.set_index('Alert_ID')

# Use the get_trajectories function defined in the Trajectory class to generate a dictionary named 'trajectories' based on
the original trajectory dataset
# Dictionary 'trajectories' (key: track_ID, values: a dict of trajectories related information at each image ID)
traj = Trajectory(traject)
trajectories = traj.get_trajectories()

# Return a dataframe containing the information of approaching vehicle from the gate crossing dataset
def get_events(trigger_gate_id):
    # extract events that any vehicles have crossed the trigger_gate 10
    event = gatecross.iloc[:,0:6]
    alert = event.loc[(event['Gate_ID']== trigger_gate_id)]
    alert = alert.set_index('Track_ID')     # set 'Track_ID' as the index
    return alert

# Initialze all the ID of check gates and action regions based on the values extracted from the 'Gap_extraction' excel file
# Return the values of each gate or action region ID
def initialize_setting():
    circular_region_id = extract.iloc[1,1]
    adjacent_region_id = extract.iloc[1,2]
    ped_gate_id = extract.iloc[1,3]
    trigger_gate_id = extract.iloc[1,4]
    check_gate_id = extract.iloc[1,5]
    exit_gate_id = extract.iloc[1,6]
    bypass_gate = 1
    circular_check = 26

    return circular_region_id, adjacent_region_id, ped_gate_id, trigger_gate_id,
check_gate_id, exit_gate_id, bypass_gate, circular_check
```

APPENDIX F. LOGISTIC REGRESSION ANALYSIS - PYTHON SCRIPT

The script is attached in the open document text below. To view the script, simply double-click on the following text. It's also available in the electronic supplements.

```
"""
Logistic regression
"""

import os
import csv
import pandas as pd
import matplotlib.pyplot as plt
import numpy as np
from sklearn.linear_model import LogisticRegression
import statsmodels.api as sm
import statsmodels.tools as st

# read the gap dataset file
df = pd.read_csv('.\Dataset_gap_updated.csv')

# get a list of roundabout ID
roundabout = df['Roundabout_ID'].unique()

#exclude records with rejected gaps>10s
del_ind = df.index[(df['Gap_time(s)']>=10) & (df['Gap_type']==0)].tolist()
df = df.drop(df.index[del_ind])

# Use statsmodels to run the logistic regression
with open('Roundabout_Approach_gap_analysis_stats_updated.csv', 'w', newline='') as
file:
    writer = csv.writer(file)
    writer.writerow(["Roundabout_ID", "Approach", "Intercept", "Coefficient",
"Gap_time@50", r"No. of datapoints"])

# for each roundabout
for r in roundabout:
    # get a table of gap records without infinity gaps of the corresponding roundabout r
    dr = df.loc[(df['Roundabout_ID'] == r) & (df['Gap_distance(m)'] !=
float('inf'))]
    appr = dr['Approach'].unique()

# for each approach run the logistic regression
    for a in appr:
        dra = dr.loc[dr['Approach'] == a]
        dra['intercept'] = 1
        nodata = dra.shape[0]
        # define the independent and dependent variables
        x= dra[[r'Gap_time(s)', 'intercept']]
        y = dra[['Gap_type']]

        # if the model doesn't converge, then let the coefficient and intercept to be 0
        try:
            logit_model=sm.Logit(y,x)
```

APPENDIX G.CORRELATION MATRIX OF CANDIDATE VARIABLES

Estimated correlations greater than or equal to 0.6 are shown highlighted in red cells and with red font.

	Dia of Central Island. (ft)	Opening Year	Op_Years	Angle to Ups App.	No. Cir Lanes Xsing App	inscribed Cir Dia. (ft)	Width of Splitter Island (ft)	Lane Width (ft)	Ups App on State Route?	App on State Route?	Prob_right_turn	Entry_count	Entry_volume(pcu/h)	Exiting_count	Exiting_volume(pcu/h)	Exiting_prob	Avg_approach_speed (mph)	State_route
Dia of Central Island. (ft)	1.000	0.516	-0.516	-0.132	0.164	0.913	0.545	0.301	0.240	0.256	0.015	-0.110	-0.073	-0.138	-0.050	-0.007	0.357	0.402
Opening Year	0.516	1.000	-1.000	-0.378	0.062	0.353	0.473	0.105	0.127	0.147	0.082	-0.124	-0.020	-0.238	-0.091	-0.002	0.316	0.222
Op_Years	-0.516	-1.000	1.000	0.378	-0.062	-0.353	-0.473	-0.105	-0.127	-0.147	-0.082	0.124	0.020	0.238	0.091	0.002	-0.316	-0.222
Angle to Ups App.	-0.132	-0.378	0.378	1.000	0.080	-0.001	-0.445	-0.013	0.175	-0.068	-0.025	-0.359	-0.255	-0.388	-0.290	-0.315	-0.351	0.084
No. Cir Lanes Xsing App	0.164	0.062	-0.062	0.080	1.000	0.359	0.276	0.328	0.370	0.174	-0.031	-0.021	-0.082	-0.091	-0.145	-0.235	-0.063	0.438
inscribed Cir Dia. (ft)	0.913	0.353	-0.353	-0.001	0.359	1.000	0.595	0.430	0.288	0.289	-0.063	-0.135	-0.111	-0.129	-0.061	-0.088	0.261	0.466
Width of Splitter Island (ft)	0.545	0.473	-0.473	-0.445	0.276	0.595	1.000	0.320	0.196	0.334	-0.187	0.081	0.162	-0.011	0.089	-0.020	0.492	0.430
Lane Width (ft)	0.301	0.105	-0.105	-0.013	0.328	0.430	0.320	1.000	0.196	0.465	-0.205	0.045	0.069	0.227	0.293	0.239	0.250	0.538
Ups App on State Route?	0.240	0.127	-0.127	0.175	0.370	0.288	0.196	0.196	1.000	-0.237	0.209	-0.384	-0.362	-0.309	-0.270	-0.328	-0.169	0.604
App on State Route?	0.256	0.147	-0.147	-0.068	0.174	0.289	0.334	0.465	-0.237	1.000	-0.167	0.163	0.323	0.141	0.301	0.291	0.256	0.632
Prob_right_turn	0.015	0.082	-0.082	-0.025	-0.031	-0.063	-0.187	-0.205	0.209	-0.167	1.000	-0.199	-0.239	-0.220	-0.262	-0.167	-0.161	0.030
Entry_count	-0.110	-0.124	0.124	-0.359	-0.021	-0.135	0.081	0.045	-0.384	0.163	-0.199	1.000	0.746	0.774	0.553	0.403	0.230	-0.173
Entry_volume(pcu/h)	-0.073	-0.020	0.020	-0.255	-0.082	-0.111	0.162	0.069	-0.362	0.323	-0.239	0.746	1.000	0.531	0.769	0.417	0.273	-0.024
Exiting_count	-0.138	-0.238	0.238	-0.388	-0.091	-0.129	-0.011	0.227	-0.309	0.141	-0.220	0.774	0.531	1.000	0.765	0.722	0.211	-0.131
Exiting_volume(pcu/h)	-0.050	-0.091	0.091	-0.290	-0.145	-0.061	0.089	0.293	-0.270	0.301	-0.262	0.553	0.769	0.765	1.000	0.756	0.264	0.032
Exiting_prob	-0.007	-0.002	0.002	-0.315	-0.235	-0.088	-0.020	0.239	-0.328	0.291	-0.167	0.403	0.417	0.722	0.756	1.000	0.281	-0.023
Avg_approach_speed (mph)	0.357	0.316	-0.316	-0.351	-0.063	0.261	0.492	0.250	-0.169	0.256	-0.161	0.230	0.273	0.211	0.264	0.281	1.000	0.075
State_route	0.402	0.222	-0.222	0.084	0.438	0.466	0.430	0.538	0.604	0.632	0.030	-0.173	-0.024	-0.131	0.032	-0.023	0.075	1.000

APPENDIX H. CRITICAL HEADWAY DATA FLOW

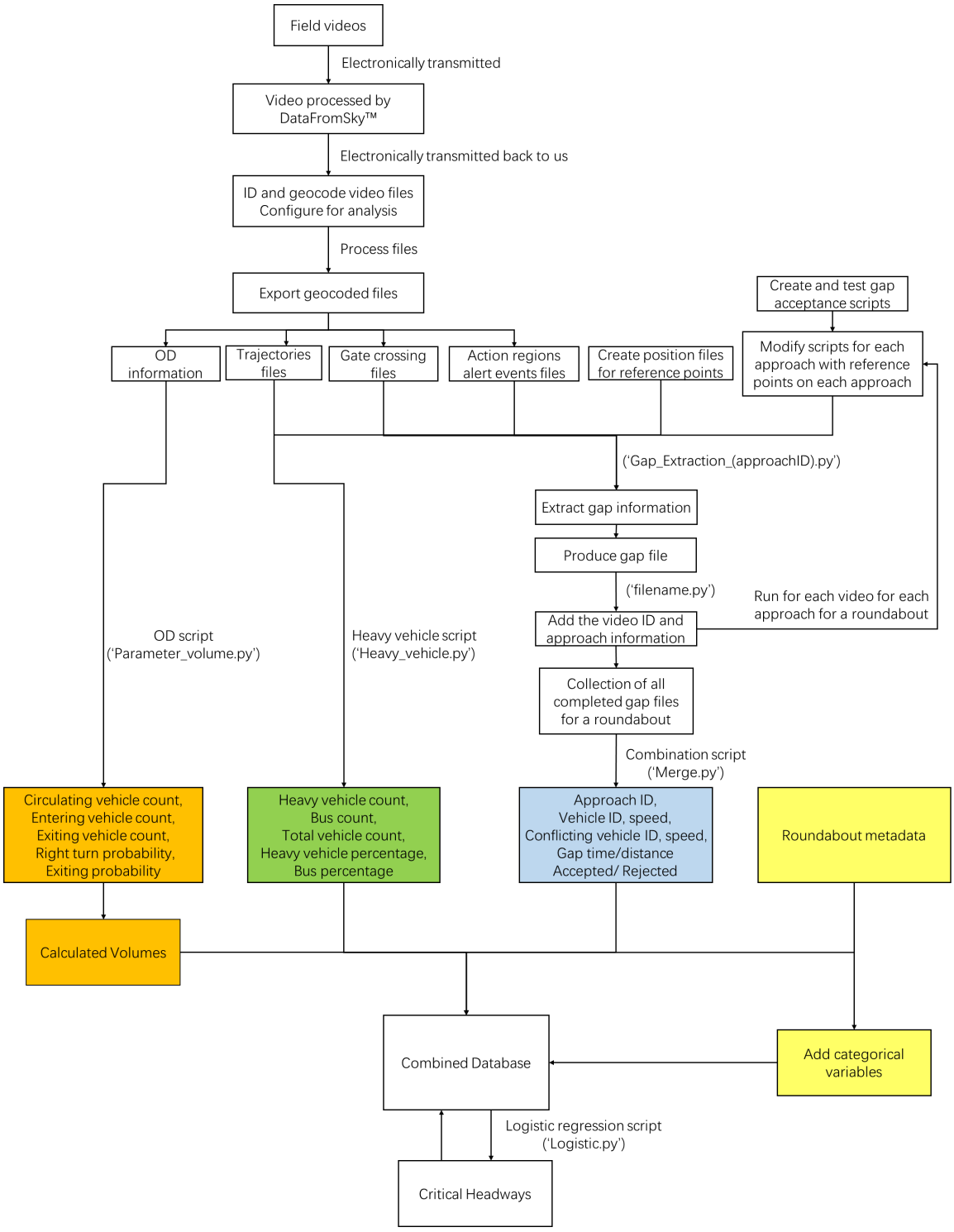

REFERENCES

Akçelik, R. (1994). "Gap-acceptance Modelling by Traffic Signal Analogy." *Traffic Engineering & Control*, *35*(9), pp. 498–501.

Akçelik, R. (2003). "Speed-flow and Bunching Relationships for Uninterrupted Flows." Presented at 25th Conference of Australian Institutes of Transportation Research (CAITR 2003), University of South Australia, Adelaide, Australia.

Akçelik, R. (2004). "Roundabouts with Unbalanced Flow Patterns." Presented at ITE 2004 Annual Meeting, Lake Buena Vista, FL, USA.

Akçelik, R. (2006). "Speed-flow and Bunching Models for Uninterrupted Flows." Presented at Transportation Research Board 5th International Symposium on Highway Capacity and Quality of Service, Yokohama, Japan. Available online: https://www.researchgate.net/publication/241746496_Speed-Flow_and_Bunching_Relationships_for_Uninterrupted_Flows

Akçelik, R. (2007). "A Review of Gap-acceptance Capacity Models." Presented at The 29th Conference of Australian Institutes of Transport Research (CAITR 2007), University of South Australia, Adelaide, Australia

Akçelik, R. (2011). "An Assessment of the Highway Capacity Manual 2010 Roundabout Capacity Model." Presented at TRB International Roundabout Conference, Carmel, IN, USA.

Akçelik, R. (2017). "An Assessment of the Highway Capacity Manual Edition 6 Roundabout Capacity Model." Presented at 5th International Roundabout Conference, Green Bay, WI, USA.

Akçelik, R. and Besley, M. (2005). "Differences Between the AUSTROADS Roundabout Guide and AUSIDRA Roundabout Analysis Methods." *Road & Transport Research Journal*, *14*(1), pp. 44–64.

Al-Omari, B., Al-Masaeid, H., and Al-Shawabkah, Y. (2004). "Development of a Delay Model for Roundabouts in Jordan." *Journal of Transportation Engineering*, *130*(1), pp. 76–82.

Allison, P.D. (2008). "Convergence Failures in Logistic Regression." SAS Global Forum, San Antonio, TX, USA.

Alphand, F., Noelle, U., and Guichet, B. (1991). "Evolution of Design Rules for Urban Roundabouts in France." In *Intersections Without Traffic Signals II*, Springer, pp. 126–140.

Armitage, D. and McDonald, M. (1974). "Roundabout Capacity." *Traffic Engineering & Control*, *15*(18).

Ashworth, R. (1968). "A Note on the Selection of Gap Acceptance Criteria for Traffic Simulation Studies." *Transportation Research*, *2*(2), pp. 171–175. Available online: https://doi.org/https://doi.org/10.1016/0041-1647(68)90060-9.

AUSTROADS (1988). *Guide to Traffic Engineering Practice, Part 2: Roadway Capacity* (0-85588-223-9). Association of Australian State Road and Transport Authorities. https://trid.trb.org/view/1197737

AUSTROADS. (1993). *Guide to Traffic Engineering Practice, Part 6: Roundabouts (Second Edition)* (0-85588-425-8). Association of Australian State Road and Transport Authorities. https://trid.trb.org/view/374119

Bared, J.G. and Afshar, A M. (2009). "Using Simulation to Plan Capacity Models by Lane for Two-and Three-Lane Roundabouts." *Transportation Research Record: Journal of the Transportation Research Board*, *2096*(1), pp. 8–15.

Bared, J. and Edara, P.K. (2005). "Simulated Capacity of Roundabouts and Impact of Roundabout within a Progressed Signalized Road." Presented at National Roundabout Conference, Vail, CO, USA.

Barry, C.D. (2012). *Calibration of the HCM 2010 Roundabout Capacity Equations for Georgia Conditions*. Georgia Institute of Technology, Atlanta, GA, USA. Available online: https://smartech.gatech.edu/handle/1853/44887.

Brilon, W. (1988). "Recent Developments in Calculation Methods for Unsignalized Intersections in West Germany." In: Brilon W. (eds), *Intersections without Traffic Signals*. Springer, Berlin, Heidelberg. Available online: https://doi.org/10.1007/978-3-642-83373-1_8.

Brilon, W. (2005). "Roundabouts: A State of the Art in Germany." Presented at National Roundabout Conference, Vail, CO, USA.

Brilon, W., Koenig, R., and Troutbeck, R.J. (1999). "Useful Estimation Procedures for Critical Gaps." *Transportation Research Part A: Policy and Practice*, *33*(3–4), pp. 161–186.

Brilon, W. and Wu, N. (2001). "Capacity at Unsignalized Intersections Derived by Conflict Technique." *Transportation Research Record: Journal of the Transportation Research Board*, *1776*(1), pp. 82–90.

Chen, R. (2018). *Microscopic Simulation and Evaluation of the Roundabout Capacity Model in Highway Capacity Manual*. M.S. thesis, Retrieved from the University of Minnesota Digital Conservancy, Minneapolis, MN, USA. Available online: https://hdl.handle.net/11299/194661.

Codjoe, J., Thapa, R., Ayernor, S. M. A., Loker, M., Center, L. T. R., Transportation, L. D. o., & Development. (2021). *Determining Louisiana's Roundabout Capacity*. Louisiana Transportation Research Center. https://books.google.com/books?id=745uzgEACAAJ

Cowan, R.J. (1975). "Useful Headway Models." *Transportation Research*, *9*(6), pp. 371–375.

Federal Highway Administration (FHWA). (2020). *Types of Traffic Analysis Tools*. U.S. Department of Transportation. Available online: https://academic.oup.com/biomet/article-abstract/54/3-4/657/230952. Retrieved June 3, 2021.

Gleue, A.W. (1972). "Vereinfachtes Verfahren zur Berechnung Signalgeregelter Knotenpunkte." *Forschung Strassenbau und Strassenverkehrstechnik*, *136*, Bonn.

Guichet, B. (1997). "Roundabouts in France: Development, Safety, Design, and Capacity." Presented at Third International Symposium on Intersections Without Traffic Signals, Transportation Research Board, Federal Highway Administration, National Center for Advanced Transportation Technology, University of Idaho, Transportation Northwest, University of Washington.

Harders, J. (1968). "Die Leistungsfähigkeit Nicht Signalgeregelter Städtischer Verkehrsknoten." *Strassenbau und Strassenverkehrstechnik*, *76*.

Jacobs, F. (1979). *Capacity Calculations for Unsignalized Intersections*. (Technical report in German) Institute fur Starßrenßau und Verkehrswesen, University Stuttgart.

Kang, N. and Nakamura, H. (2015). "Estimation of Roundabout Entry Capacity that Considers Conflict with Pedestrians." *Transportation Research Record: Journal of the Transportation Research Board*, *2517*(1), pp. 61–70.

Kimber, R.M. (1980). *The Traffic Capacity of Roundabouts*. Transport and Road Research Laboratory (TRRL), 43 pp. Available online: https://trid.trb.org/view/157408.

Kittelson & Associates, Inc. (2010). *Roundabout Evaluation and Design Guidelines*. City of Bend, OR, USA, April. Available online: https://www.bendoregon.gov/Home/ShowDocument?id=2512.

Macioszek, E. and Akçelik, R. (2017). "A Comparison of Two Roundabout Capacity Models." Presented at 5th International Roundabout Conference, Green Bay, WI, USA.

Mensah, S., Eshragh, S., and Faghri, A. (2010). "A Critical Gap Analysis of Modern Roundabouts." Presented at Transportation Research Board Annual Meeting, Washington, DC, USA.

Mereszczak, Y., Dixon, M.P., Kyte, M., Rodegerdts, L., and Blogg, M. (2005). *Incorporating Exiting Vehicles in Capacity Estimation at Single-Lane U.S. Roundabouts*. Transportation Research Circular, Issue E-C083, 25 pp. Available online: https://trid.trb.org/view/775543.

Oketch, T., Delsey, M., and Robertson, D. (2004). "Evaluation of Performance of Modern Roundabouts Using Paramics Micro-simulation Model." Transportation Association of Canada (TAC) Annual Conference and Exhibition, Quebec, Ontario, Canada.

Patnaik, A.K., Chaulia, S., and Bhuyan, P.K. (2021). "Roundabout Entry Capacity Models: Genetic Programming Approach." *Proceedings of the Institution of Civil Engineers – Transport*, *174*(3), pp. 182–196. Available online: https://doi.org/10.1680/jtran.17.00089.

Patnaik, A.K., Krishna, Y., Rao, S., and Bhuyan, P.K. (2017). "Development of Roundabout Entry Capacity Model Using INAGA Method for Heterogeneous Traffic Flow Conditions." *Arabian Journal for Science and Engineering*, *42*(9), pp. 4181–4199.

Patnaik, A.K., Ranjan, A.R., and Bhuyan, P.K. (2018). "Investigating Entry Capacity Models of Roundabouts Under Heterogeneous Traffic Conditions." *Transportation Research Record: Journal of the Transportation Research Board*, *2672*(15), pp. 35–43.

Patnaik, A.K., Rao, S., Krishna, Y., and Bhuyan, P. (2017). "Empirical Capacity Model for Roundabouts under Heterogeneous Traffic Flow Conditions." *Transportation Letters*, *9*(3), pp. 152–165.

Raff, M.S. (1950). *A Volume Warrant for Urban Stop Signs*. Eno Foundation for Highway Traffic Control, Washington, DC, USA. Available online: https://trid.trb.org/view/118780.

Robinson, B.W., Rodegerdts, L., Scarborough, W., Kittelson, W., Troutbeck, R., Brilon, W., et al. (2000). *Roundabouts: An Informational Guide.* Publication No. FHWA-RD-00-067, Project 2425, Federal Highway Administration, Washington, DC, USA.

Rodegerdts, L., Bansen, J., Tiesler, C., Knudsen, J., Myers, E., Johnson, M., Moule, M., Persaud, B., Lyon, C., and Hallmark, S. (2010). *Roundabouts: An Informational Guide*. NCHRP Report 672, Transportation Research Board, Washington, DC, USA.

Rodegerdts, L., Blogg, M., Wemple, E., Myers, E., Kyte, M., Dixon, M., List, G., Flannery, A., Troutbeck, R., and Brilon, W. (2007a). Appendixes to NCHRP Report 572: *Roundabouts in the United States*. NCHRP Web-Only Document. Available online: https://www.nap.edu/catalog/21999/appendixes-to-nchrp-report-572-roundabouts-in-the-united-states.

Rodegerdts, L., Blogg, M., Wemple, E., Myers, E., Kyte, M., Dixon, M., List, G., Flannery, A., Troutbeck, R., and Brilon, W. (2007b). *Roundabouts in the United States*. NCHRP Report 572, Transportation Research Board, Washington, DC, USA.

Rodegerdts, L.A., Malinge, A., Marnell, P., Beaird, S., Kittelson, M.J., and Mereszczak, Y.S. (2015). *Accelerating Roundabout Implementation in the United States: Volume II of VII: Assessment of Roundabout Capacity Models for the Highway Capacity Manual*. Report No. FHWA-SA-15-070, Kittelson & Associates, Inc. for Federal Highway Administration, Washington, DC, USA.

Rossi, R., Gastaldi, M., and Meneguzzer, C. (2018). "Headway Distribution Effect on Gap-acceptance Behavior at Roundabouts: Driving Simulator Experiments in a Case Study." *Advances in Transportation Studies*, *46*.

Ruhazwe, E., Moses, R., Kadeha, C., and Ozguven, E.E. (2019). "Field Determination of Gap Acceptance Parameters for Florida Roundabouts." Presented at Transportation Research Board 98th Annual Meeting, Washington, DC, USA. Available online: https://trid.trb.org/view/1680024.

Schmitt, L.E. (2013). *Calibration of the HCM 2010 Single-lane Roundabout Capacity Equations for Georgia Conditions (Phase 2)*. Georgia Institute of Technology, Atlanta, GA, USA. Available online: https://smartech.gatech.edu/handle/1853/50413.

Siegloch, K.P. (1973). Die Leistungsermittlung an Knotenpunkten ohne Lichtsignalsteuerung (Capacity estimation at unsignalized intersections). Straßenbau und Straßenverkehrstechnik, Heft 154. Hrsg.: Bundesminister für Verkehr, Abt. Straßenbau, Bonn.

Stanek, D. and Milam, R.T. (2005). *High-Capacity Roundabout Intersection Analysis: Going Around in Circles*. Transportation Research Circular, Issue E-C083. Available online: https://trid.trb.org/view/775448.

Stuwe, B. and Springer, V. (1991). "Capacity and Safety of Roundabouts – German Results." Presented at Intersections without Traffic Signals II. Proceedings of an International Workshop, Springer Verlag, 1991, pp. 1–12. Available online: https://trid.trb.org/view/376365.

Tanner, J.C. (1962). "A Theoretical Analysis of Delays at an Uncontrolled Intersection." *Biometrika*, *49*(1/2), pp. 163–170. Available online: https://doi.org/10.2307/2333477.

Tanner, J.C. (1967). "The Capacity of an Uncontrolled Intersection." *Biometrika*, *54*(3–4), pp. 657–658.

Tian, Z., Troutbeck, R., Kyte, M., Brilon, W., Vandehey, M., Kittelson, W., and Robinson, B. (2000). "A Further Investigation on Critical Gap and Follow-up Time." In *Proceedings of the 4th International Symposium on Highway Capacity, Maui/Hawaii,* Transportation Research Circular E-C018, pp. 409–421.

Transportation Research Board (TRB). (2016). "The Highway Capacity Manual 6th Edition: A Guide for Multimodal Mobility Analysis." Elefteriadou, L. (ed). *ITE Journal*, *86*(4), pp 14–18. Available online: https://trid.trb.org/view/1403977.

Troutbeck, R. J. (1986). Average Delay at an Unsignalized Intersection with Two Major Streams Each Having a Dichotomized Headway Distribution. Transportation Science, 20(4), pp. 272-286.

Troutbeck, R.J. (1989). *Evaluating the Performance of a Roundabout*. SR No. 5, Australian Road Research, ARRB, Melbourne, Australia. Available online: https://trid.trb.org/view/306235.

Troutbeck, R. (1992). *Estimating the Critical Assessment Gap from Traffic Movements*. Research Report, Queensland University of Technology, Issue 92-5, 23 p. Available online: https://trid.trb.org/view/377243.

Troutbeck, R.J. (2014). "Estimating the Mean Critical Gap." *Transportation Research Record: Journal of the Transportation Research Board*, *2461*, pp. 76–84. https://doi.org/10.3141/2461-10. Available online: https://trid.trb.org/view/1287480.

Troutbeck, R. and Brilon, W. (1997) "Unsignalized Intersection Theory." *Traffic Flow Theory: A State-of-the-Art Report*, N. Gartner, H. Mahmassani, C.J. Messer, H. Lieu, R. Cunard, and A.K. Rathi (eds), Transportation Research Board, London, pp 8.1–8.47.

Troutbeck, R.J. and Kako, S. (1999). "Limited Priority Merge at Unsignalized Intersections." *Transportation Research Part A: Policy and Practice*, *33A*(3/4), pp. 291–304. Available online: https://trid.trb.org/view/1163403.

Vaiana, R., Gallelli, V., and Iuele, T. (2013). "Sensitivity Analysis in Traffic Microscopic Simulation Model for Roundabouts." *Baltic Journal of Road and Bridge Engineering*, *8*(3), pp. 174–183. https://doi.org/10.3846/bjrbe.2013.22. Available online: https://trid.trb.org/view/1267207.

Vasconcelos, A.L.P., Seco, A.J.M., and Silva, A.M.C.B. (2013). "Comparison of Procedures to Estimate Critical Headways at Roundabouts." *PROMET-Traffic & Transportation*, *25*(1), pp. 43–53. Available online: https://doi.org/10.7307/ptt.v25i1.1246.

Wei, T. and Grenard, J.L. (2012). "Calibration and Validation of Highway Capacity Manual 2010 Capacity Model for Single-Lane Roundabouts." *Transportation Research Record: Journal of the Transportation Research Board*, 2286, pp. 105–110. https://doi.org/10.3141/2286-12. Available online: https://trid.trb.org/view/1130352.

Wei, T., Grenard, J.L., and Shah, H.R. (2011). "Developing Capacity Models for Local Roundabouts: Streamlined Process." *Transportation Research Record: Journal of the Transportation Research Board*, *2257*, pp. 1–9. Available online: https://doi.org/10.3141/2257-01.

Wu, N. (2001). "A Universal Procedure for Capacity Determination at Unsignalized (Priority-controlled) Intersections. *Transportation Research Part B: Methodological*, *35*(6), pp. 593–623.

Wu, N. (2006). "A New Model for Estimating Critical Gap and Its Distribution at Unsignalized Intersections Based on the Equilibrium of Probabilities." 5th International Symposium on Highway Capacity and Quality of Service, Japan Society of Traffic Engineers, pp. 517–526. Available online: https://trid.trb.org/view/792789.

Wu, N. and Brilon, W. (2018). "Total Capacity of Roundabouts Analyzed by a Conflict Technique." *Transportation Research Record: Journal of the Transportation Research Board*, *2672*(15), pp. 9–22. https://doi.org/10.1177/0361198118788171. Available online: https://trid.trb.org/view/1494604.

Xu, F. and Tian, Z.Z. (2008). "Driver Behavior and Gap-Acceptance Characteristics at Roundabouts in California." *Transportation Research Record: Journal of the Transportation Research Board*, *2071*(1), pp. 117–124. Available online: https://doi.org/10.3141/2071-14.

Yap, Y.H., Gibson, H.M., and Waterson, B.J. (2013). "An International Review of Roundabout Capacity Modelling." *Transport Reviews*, *33*(5), pp. 593–616. https://doi.org/10.1080/01441647.2013.830160. Available online: https://trid.trb.org/view/1264287.

Zheng, D., Chitturi, M.V., Bill, A.R., and Noyce, D. (2012). "Critical Gaps and Follow-up Headways at Congested Roundabouts." Transportation Research Board Annual Meeting, Washington, DC, USA. Available online: http://pages.cs.wisc.edu/~dongxi/shared/TRB2012.pdf.

.

.